

On Optimal Scaling of Additive Transformation Based Markov Chain Monte Carlo

Kushal Kr. Dey¹ and Sourabh Bhattacharya²

¹Department of Statistics, University of Chicago, USA

²Indian Statistical Institute, Kolkata. Corresponding e-mail: bhsourabh@gmail.com

Abstract

Study of diffusion limits of the Metropolis-Hastings algorithm in high dimensions yields useful quantification of the scaling of the underlying proposal distribution in terms of dimensionality. Here we consider the recently introduced Transformation-based Markov Chain Monte Carlo (TMCMC) ([Dutta and Bhattacharya \(2014\)](#)), a methodology that is designed to update all the parameters simultaneously using some simple deterministic transformation of a one-dimensional random variable drawn from some arbitrary distribution on a relevant support. The additive transformation based TMCMC is similar in spirit to random walk Metropolis, except the fact that unlike the latter, additive TMCMC uses a single draw from a one-dimensional proposal distribution to update the high-dimensional parameter.

In this paper, we study the diffusion limits of additive TMCMC under various set-ups ranging from the product structure of the target density to the case where the target is absolutely continuous with respect to a Gaussian measure; we also consider the additive TMCMC within Gibbs approach for all the above set-ups. These investigations lead to appropriate scaling of the one-dimensional proposal density. We also show that the optimal acceptance rate of additive TMCMC is 0.439 under all the aforementioned set-ups, in contrast with the well-established 0.234 acceptance rate associated with optimal random walk Metropolis algorithms under the same set-ups. We also elucidate the ramifications of our results and clear advantages of additive TMCMC over random walk Metropolis with ample simulation studies and Bayesian analysis of a real, spatial dataset with which 160 unknowns are associated.

Keywords: *Additive Transformation; Diffusion Limit; High Dimension; Optimal Scaling; Random Walk; Transformation-based Markov Chain Monte Carlo.*

Contents

Contents	1
1 Introduction	2
2 A brief overview of TMCMC	4
2.1 Detailed balance	5
2.2 Discussion on the independence of the acceptance probability of the proposal density q	6
2.3 Relationship of TMCMC with the MH methodology	6
2.3.1 Additive TMCMC	7
2.3.2 Contrast of additive TMCMC with RWM	7
2.4 Contrast of TMCMC with deterministic transformation based generalized Gibbs/MH approaches	7
2.5 Contrast of the TMCMC idea with reversible jump Markov chain Monte Carlo (RJMCMC)	8
2.6 Discussion of extension of TMCMC to variable dimensional problems	8
3 Optimal scaling of additive TMCMC when the target density is a product based on <i>iid</i> random variables	8
3.1 TMCMC within Gibbs for <i>iid</i> product densities	10
4 Diffusion approximation for independent but non-identical random variables	11
4.1 TMCMC within Gibbs for independent but non-identical random variables . . .	13
5 Diffusion approximation for a more general dependent family of distributions	14
5.1 Representation of the additive TMCMC algorithm in the dependent set-up . . .	15
5.2 Formal statement of our main result in the general dependent set-up	16
5.2.1 Assumptions	17
5.3 TMCMC within Gibbs for the dependent family of distributions	18
6 Comparison with RWM	19
6.1 Comparison in the <i>iid</i> set-up	19
6.1.1 Within Gibbs comparison in the <i>iid</i> set-up	20
6.2 Comparison in the independent but non-identical set-up	21
6.2.1 Within Gibbs comparison in the independent but non-identical set-up . .	21
6.3 Dependent case	21
6.3.1 Within Gibbs comparison in the dependent set-up	23
7 Simulation Experiments	23
7.1 Comparison of additive TMCMC and RWM in the <i>iid</i> case	23
7.1.1 Average Kolmogorov-Smirnov distance for comparing convergence of TM-CMC and RWM	24
7.1.2 Observations regarding the results presented in Table 1	24
7.1.3 Visualizing the rate of convergence of TMCMC and RWM to the stationary distribution using Kolmogorov-Smirnov distance	25
7.2 Comparisons between additive TMCMC and RWM in the independent, but non-identical set-up	28
7.3 Comparisons between additive TMCMC and RWM in the dependent set-up . .	28
7.4 Discussion on simulation studies with multivariate Cauchy and multivariate t as target densities	29

8	Comparison of additive TMCMC and RWM in the case of a real, spatial data set	30
8.1	Model and prior specification	30
8.2	Optimal scaling	30
8.2.1	Pilot TMCMC for facilitating approximate optimal scaling	32
8.2.2	Approximately optimal acceptance rates of additive TMCMC and RWM using the stored eigenvalues	32
8.3	Results of comparison	33
9	Conclusion	33
S-1	Computational efficiency of TMCMC	38
S-2	Details on the need for optimal scaling of additive TMCMC	38
S-3	Discussion on consequences of non-robustness of RWM with respect to scale choices	42
S-4	Discussion on possible advantages of additive TMCMC for relatively more robust behaviour with respect to scale choices	42
S-5	Discussion on adaptive versions of RWM and additive TMCMC for enforcing optimal acceptance rates in complex, high-dimensional problems	43
S-6	Proofs of optimal scaling results of additive TMCMC	43
S-6.1	Proof of Theorem 3.1 of DB	43
S-6.2	Proof of Theorem 3.2 of DB	48
S-6.3	Proof of Theorem 4.1 of DB	49
S-7	Calculations related to the dependent set-up	52
S-7.1	Verification of the conditions of Lyapunov's central limit theorem	52
S-7.2	Expected drift	52
S-7.3	Expected diffusion coefficient	54
	Bibliography	56

1 Introduction

Markov Chain Monte Carlo (MCMC) methods have revolutionized Bayesian computation – this pleasing truth, however, is often hard to appreciate in the face of the challenges posed by computational complexities and convergence issues of traditional MCMC. Indeed, exploration of very high-dimensional posterior distributions using MCMC can be both computationally very expensive and troublesome convergence-wise. The random walk Metropolis (RWM) algorithm is a popular MCMC algorithm because of its simplicity and ease in implementation, but unless great care is taken to properly scale the proposal distribution the algorithm can have poor convergence properties. For instance, if the variance of the proposal density is small, then the jumps will be small in magnitude, implying that the Markov chain will require a large number of iterations to explore the entire state-space. On the other hand, large variance of the proposal density causes too many rejections of the proposed moves, again considerably slowing down convergence of the underlying Markov chain. The need for an optimal choice of the proposal variance is thus inherent in the RWM algorithms. The pioneering approach towards obtaining an optimal scaling of the RWM proposal is due to [Roberts *et al.* \(1997\)](#) in the case of target densities associated with independent and identical (*iid*) random variables; generalization of this

work to more general set-ups are provided by [Bedard \(2007\)](#) (target density associated with independent but non-identical random variables) and [Mattingly *et al.* \(2011\)](#) (target density absolutely continuous with respect to a Gaussian measure). The approach used in all these works is to study the diffusion approximation of the high-dimensional RWM algorithm, and maximization of the speed of convergence of the limiting diffusion. The optimal scaling, the optimal acceptance rate and the optimal speed of convergence of the limiting diffusion, along with the complexity of the algorithm are all obtained from this powerful approach.

In practice, a serious drawback of the RWM algorithm in high dimensions is that there is always a positive probability that a particular co-ordinate of the high-dimensional random variable is ill-proposed; in that case the acceptance ratio will tend to be extremely small, prompting rejection of the entire high-dimensional move. In general, unless the high-dimensional proposal distribution, which need not necessarily be a random walk proposal distribution, is designed with extreme care, such problem usually persists. Unfortunately, such carefully designed proposal density is rare in high dimensions. To combat these difficulties [Dutta and Bhattacharya \(2014\)](#) proposed an approach where the entire block of parameters can be updated simultaneously using some simple deterministic transformation of a scalar random variable sampled from some arbitrary distribution defined on some suitable support. The strategy effectively reduces the high-dimensional proposal distribution to a one-dimensional proposal, greatly improving the acceptance rate and computational speed in the process. This methodology is no longer Metropolis-Hastings for dimensions greater than one; the proposal density in more than one dimension becomes singular because it is induced by a one-dimensional random variable. However, in one-dimensional cases this coincides with Metropolis-Hastings with a specialized mixture proposal density; in particular, the additive transformation based TMCMC coincides with RWM in one-dimensional situations. [Dutta and Bhattacharya \(2014\)](#) refer to this new general methodology as Transformation-based MCMC (TMCMC). In their work the authors point out several advantages of the additive transformation in comparison with the other valid transformations. For instance, they show that additive TMCMC requires less number of ‘move-types’ compared to other valid transformations; moreover, the acceptance rate has a simple form for additive transformations since the Jacobian of additive transformations is 1.

In this work, our main goal is to investigate the diffusion limits of additive TMCMC in high-dimensional situations under various forms of the target density when the one-dimensional random variable used for the additive transformation is drawn from a left truncated zero-mean normal density. In particular, we consider situations when the target density corresponds to *iid* random variables, independent but non-identically distributed random variables; we also study the diffusion limit of additive TMCMC when the target is absolutely continuous with respect to a Gaussian measure. Since all these forms are considered in the MCMC literature related to diffusion limits and optimal scaling of RWM, comparisons of our additive TMCMC-based approaches can be made with the respective RWM-based approaches. Furthermore, in each of the aforementioned set-ups, we also consider additive TMCMC within Gibbs approach, where one or multiple components of the high-dimensional random variable are updated by additive TMCMC, conditioning on the remaining components. This we compare with the corresponding RWM within Gibbs approach under the same settings of the target densities.

Briefly, our investigations show that the optimal additive TMCMC acceptance rate in all the set-ups is 0.439, as opposed to 0.234 associated with RWM. Moreover, we point out that even though the optimal diffusion speed of RWM is slightly greater than that of additive TMCMC, the diffusion speed associated with additive TMCMC is more robust with respect to the choice of the scaling constant. In other words, if the optimal scaling constant for RWM is somewhat altered, this triggers a sharp fall in the diffusion speed, but in the case of additive TMCMC the rate of decrease of diffusion speed is much slower. Investigation of the consequences of this phenomenon with simulation studies reveal severe decline in the performance of RWM in

comparison with additive TCMC.

This non-robustness of RWM with respect to scale choices other than the optimal, presents quite important consequences for applied MCMC practitioners, which we elaborate with a real, spatial data analysis problem. In a nutshell, in the context of the spatial problem, we have provided a method, which appears to be generally applicable, for approximately achieving 44% and 23% acceptance rates for additive TCMC and RWM; however, achieving the desired acceptance rates in general problems where optimal scaling theories are yet lacking, does not guarantee that the achieved acceptance rates correspond to optimal scales, as there are usually very many scale choices corresponding to the same acceptance rate. Because of such sub-optimality, in the real spatial problem, RWM faces very serious performance problems. On the other hand, additive TCMC, because of its robustness with respect to the scales, performs quite reasonably.

Before we proceed with our optimal scaling theory, we first provide a brief tutorial on TCMC in Section 2 to facilitate accessibility. After the tutorial, we structure the rest of the article as follows. We develop the theory for optimal additive TCMC scaling in the *iid* set-up in Section 3; in the same section (Section 3.1) we also develop the corresponding theory for additive TCMC within Gibbs in the *iid* situation. In Section 4 we extend the additive TCMC-based optimal scaling theory to the independent but non-identical set-up; in Section 4.1 we outline the corresponding TCMC within Gibbs case. We then further extend our additive TCMC based optimal scaling theory to the aforementioned dependent set-up in Section 5, presenting the formal result in Section 5.2; the corresponding TCMC within Gibbs case is considered in Section 5.3. In Section 6 we provide numerical comparisons between additive TCMC and RWM in terms of optimal acceptance rates and diffusion speeds; in Section 7 we illustrate our theoretical results and compare the performances of additive TCMC and RWM using simulation studies, illustrating that the former is a far more effective algorithm in comparison with the latter. In Section 8 we compare additive TCMC with RWM with respect to a 160-dimensional posterior density associated with a real, spatial dataset, vividly demonstrating the clear superiority of additive TCMC over RWM. Finally, we make concluding remarks in Section 9.

Apart from the main developments provided in this article, we provide additional details in our supplementary material Dey and Bhattacharya (2015d), whose sections and figures have the prefix “S-” when referred to in this article. Briefly, in Section S-1 we provide details on computational efficiency of TCMC. Specifically, we demonstrate with an experiment the superior computational speed of additive TCMC in comparison with RWM, particularly in high dimensions. In Section S-2 we discuss, with appropriate experiments, the necessity of optimal scaling in additive TCMC, while in Sections S-3 and S-4 we delve into the robustness issues associated with the scale choices of additive TCMC and RWM. In Section S-5 we include brief discussions of adaptive versions of RWM and TCMC. Moreover, the proofs of all our technical results are provided in Sections S-6 and S-7 of the supplement.

2 A brief overview of TCMC

Suppose that we are simulating from a d dimensional space (usually \mathbb{R}^d , where \mathbb{R} is the real line), and suppose we are currently at a point $x = (x_1, \dots, x_d)$. Let us define the d -dimensional random vector $b = (b_1, \dots, b_d)$, such that, for $i = 1, \dots, d$,

$$b_i = \begin{cases} +1 & \text{with probability } p_i; \\ 0 & \text{with probability } 1 - p_i - q_i; \\ -1 & \text{with probability } q_i, \end{cases} \quad (1)$$

where, for each i , $0 < p_i, q_i < 1$ such that $p_i + q_i \leq 1$. Let $\epsilon \sim \varrho(\epsilon) = \tilde{\varrho}(\epsilon)I_{\mathbb{S}}(\epsilon)$, where $\tilde{\varrho}(\cdot)$ is any arbitrary density supported on some suitable space \mathbb{S} ; here $I_{\mathbb{S}}(\cdot)$ denotes the indicator function of \mathbb{S} .

TMCMC uses moves of the following type:

$$(x_1, \dots, x_d) \rightarrow (T^{b_1}(x_1, \epsilon), \dots, T^{b_d}(x_d, \epsilon)), \quad (2)$$

where $T^{+1}(x_i, \epsilon)$, the forward transformation to co-ordinate x_i , and $T^{-1}(x_i, \epsilon)$, the backward transformation to x_i , are bijective for fixed ϵ and injective for fixed x_i , satisfying

$$T^{+1}(T^{-1}(x_i, \epsilon), \epsilon) = T^{-1}(T^{+1}(x_i, \epsilon), \epsilon) = x_i. \quad (3)$$

The transformation

$$T^0(x_i, \epsilon) \equiv x_i, \quad \forall \epsilon \in \mathbb{S}, \quad (4)$$

indicates no change to the co-ordinate x_i while updating the vector $x = (x_1, \dots, x_d)$ to $x^* = \mathcal{T}_b(x, \epsilon)$, where $\mathcal{T}_b(x, \epsilon)$ denotes the updated vector $(T^{b_1}(x_1, \epsilon), \dots, T^{b_d}(x_d, \epsilon))$. Assuming for simplicity of illustration that $p_i = q_i$ for $i = 1, \dots, d$, move (2) is to be accepted with probability

$$\alpha = \min \left\{ 1, \frac{\pi(x^*)}{\pi(x)} J^b(x, \epsilon) \right\}, \quad (5)$$

where $J^b(x, \epsilon) = \left| \frac{\partial(\mathcal{T}^b(x, \epsilon))}{\partial(x, \epsilon)} \right|$ is the Jacobian of the transformation associated with \mathcal{T}^b . For general (p_1, \dots, p_d) and (q_1, \dots, q_d) , the acceptance ratio depends upon these probabilities; see [Dutta and Bhattacharya \(2014\)](#).

2.1 Detailed balance

In the supplement to [Dutta and Bhattacharya \(2014\)](#) the proof of detailed balance has been provided, but here we re-furnish the proof with more details and with more intuitive discussion. For the purpose of detailed balance, we need the following definition of “conjugate” $b^c = (b_1^c, \dots, b_d^c)$ of the random vector d :

$$b_i^c = \begin{cases} +1 & \text{with probability } q_i; \\ 0 & \text{with probability } 1 - p_i - q_i; \\ -1 & \text{with probability } p_i, \end{cases} \quad (6)$$

This definition is needed for returning to x from x^* , so that moving from x to x^* using the transformation \mathcal{T}^b has, in essence, the same probability as returning from x^* to x using the transformation \mathcal{T}^{b^c} . Details are provided below; at this point we note that for the i -th co-ordinate x_i , the probability of making a forward move to x_i^* using $T^{+1}(x_i, \epsilon)$ is p_i , which is also the probability of returning from x_i^* to x_i using the backward move $T^{-1}(x_i^*, \epsilon) = T^{(+1)^c}(x_i^*, \epsilon)$.

Letting K denote the Markov transition kernel associated with TMCMC, note that for moving from x to x^* , the kernel satisfies

$$\begin{aligned} \pi(x)K(x \rightarrow x^*) &= \pi(x)P(b)\varrho(\epsilon) \min \left\{ 1, \frac{\pi(x^*)}{\pi(x)} J^b(x, \epsilon) \right\} \\ &= \min \left\{ \pi(x)P(b)\varrho(\epsilon), P(b)\varrho(\epsilon)\pi(x^*)J^b(x, \epsilon) \right\}, \end{aligned} \quad (7)$$

where $P(b)$ is the probability of b responsible for the movement of the underlying Markov chain

from x to x^* . For returning from x^* to x , the kernel satisfies

$$\begin{aligned}
\pi(x^*)K(x^* \rightarrow x) &= \pi(x^*)P(b^c)\varrho(\epsilon)J^b(x, \epsilon) \min \left\{ 1, \frac{\pi(x)}{\pi(x^*)}J^{b^c}(x^*, \epsilon) \right\} \\
&= \min \left\{ \pi(x^*)P(b^c)\varrho(\epsilon)J^b(x, \epsilon), \pi(x)P(b^c)\varrho(\epsilon)J^b(x, \epsilon) \times J^{b^c}(x^*, \epsilon) \right\}, \\
&= \min \left\{ \pi(x^*)P(b^c)\varrho(\epsilon)J^b(x, \epsilon), \pi(x)P(b^c)\varrho(\epsilon)J^b(x, \epsilon) \times J^{b^c}(x^*, \epsilon) \right\}.
\end{aligned} \tag{8}$$

It follows from (3) and (4) that $\mathcal{T}^{b^c}(\mathcal{T}^b(x, \epsilon)) = x$, so that

$$\begin{aligned}
&J^b(x, \epsilon) \times J^{b^c}(x^*, \epsilon) \\
&= \left| \frac{\partial(\mathcal{T}^b(x, \epsilon), \epsilon)}{\partial(x, \epsilon)} \right| \times \left| \frac{\partial(\mathcal{T}^{b^c}(\mathcal{T}^b(x, \epsilon)), \epsilon)}{\partial(\mathcal{T}^b(x, \epsilon), \epsilon)} \right| \\
&= \left| \frac{\partial(\mathcal{T}^b(x, \epsilon), \epsilon)}{\partial(x, \epsilon)} \right| \times \left| \frac{\partial(x, \epsilon)}{\partial(\mathcal{T}^b(x, \epsilon), \epsilon)} \right| \\
&= 1.
\end{aligned} \tag{9}$$

Substituting (9) in (8) we obtain

$$\pi(x^*)K(x^* \rightarrow x) = \min \left\{ \pi(x^*)P(b^c)g(\epsilon)J^b(x, \epsilon), \pi(x)P(b^c)g(\epsilon) \right\}. \tag{10}$$

If, for simplicity of illustration we assume $p_i = q_i$ for $i = 1, \dots, d$, it follows that $P(b) = P(b^c)$, so that (10) is equal to (7), proving detailed balance. Detailed balance of course holds for general probabilities (p_1, \dots, p_d) and (q_1, \dots, q_d) ; see the supplement of [Dutta and Bhattacharya \(2014\)](#).

2.2 Discussion on the independence of the acceptance probability of the proposal density ϱ

An important feature of the TMCMC acceptance probability distinguishing it from the acceptance probability of the Metropolis-Hastings algorithms is its independence of the proposal density ϱ , irrespective of whether or not it is symmetric, and for all valid transformations T^b . The reason for this is implicit in the above detailed balance arguments – the same ϵ is generated from the proposal density ϱ while moving forward from x to x^* as well as while returning to x from x^* . This is exactly the reason why $\varrho(\epsilon)$ features in both (7) and (8). Consequently, detailed balance is satisfied only if the acceptance ratio of TMCMC is independent of ϱ .

2.3 Relationship of TMCMC with the MH methodology

Note that, although in Section 2 we indicated a single random variable ϵ to be used in the transformations, it is permissible to use k random variables $\{\epsilon_1, \dots, \epsilon_k\}$, where $k \in \{1, \dots, d\}$. Here it is also important to remark that general TMCMC with $k = d$ does not reduce to general MH method for the very reason that the acceptance ratio of TMCMC is always independent of the proposal density, while in MH it is not. For dimension $d = 1$, however, TMCMC boils down to an MH algorithm with a specialized two-component mixture proposal density, where the mixture components correspond to the two available move types, forward and backward. See [Dutta and Bhattacharya \(2014\)](#) for the complete technical details.

In Sections 2.3.1 and 2.3.2 below we describe additive TMCMC, and show that RWM is its special case.

2.3.1 Additive TMCMC

The additive TMCMC, which is of our interest in this work, uses moves of the following type:

$$(x_1, \dots, x_d) \rightarrow (x_1 + b_1\epsilon, \dots, x_d + b_d\epsilon),$$

where $\epsilon \sim \varrho(\epsilon)$. Here $\varrho(\cdot)$ is an arbitrary density with support \mathbb{R}_+ , the positive part of the real line. In other words, we assume that $T^{b_i}(x_i, \epsilon) = x_i + b_i\epsilon$. In this work, we shall assume that $p_i = 1/2$ and $q_i = 1/2$ for $i = 1, \dots, d$, so that the probabilities of choosing $b_i = 0$ and $b_i^c = 0$ are zero. Indeed, as proved in [Dutta and Bhattacharya \(2014\)](#), this is a completely valid and efficient choice for additive transformations. For this work we set $\varrho(\epsilon)I_{\{\epsilon>0\}} \equiv N(0, \frac{\ell^2}{d})I_{\{\epsilon>0\}}$.

Note that, for each i , $b_i\epsilon \sim N(0, \frac{\ell^2}{d})$, but even though $b_i\epsilon$ are pairwise uncorrelated ($E(b_i\epsilon \times b_j\epsilon) = 0$ for $i \neq j$), they are not independent since all of them involve the same ϵ . Also observe that $b_i\epsilon + b_j\epsilon = 0$ with probability $1/2$ for $i \neq j$, showing that the linear combinations of $b_i\epsilon$ need not be normal. In other words, the joint distribution of $(b_1\epsilon, \dots, b_d\epsilon)$ is not normal, even though the marginal distributions are normal and the components are pairwise uncorrelated. This also shows that $b_i\epsilon$ are not independent, because independence would imply joint normality of the components.

Thus, a single ϵ is simulated from a truncated normal distribution, which is then either added to, or subtracted from each of the d co-ordinates of x with probability $1/2$. Assuming that the target distribution is proportional to π , the new move $x^* = (x_1 + b_1\epsilon, \dots, x_d + b_d\epsilon)$ is accepted with probability

$$\alpha = \min \left\{ 1, \frac{\pi(x^*)}{\pi(x)} \right\}. \quad (11)$$

2.3.2 Contrast of additive TMCMC with RWM

The RWM algorithm, on the other hand, proceeds by simulating $\epsilon_1, \dots, \epsilon_d$ independently from $N(0, \frac{\ell^2}{d})$, and then adding ϵ_i to the co-ordinate x_i , for each i . The new move is accepted with probability having the same form as (11). As discussed in Section 2.3 for TMCMC it is permissible to use k random variables $\{\epsilon_1, \dots, \epsilon_k\}$, where $k \in \{1, \dots, d\}$. Thus, with such a proposal, if $k = d$, additive TMCMC reduces to RWM, showing that the latter is a special case of the former.

Discussion of computational efficiency of TMCMC is already provided in [Dutta and Bhattacharya \(2014\)](#). In this article, we supplement the discussion by demonstrating with an experiment the substantial computational gains of additive TMCMC over RWM, particularly in high dimensions; see Section S-1.

2.4 Contrast of TMCMC with deterministic transformation based generalized Gibbs/MH approaches

TMCMC uses deterministic transformations to update the variables; however, deterministic transformations have also been considered by [Liu and Yu \(1999\)](#), [Liu and Sabatti \(2000\)](#), [Kou et al. \(2005\)](#) in an attempt to improve mixing behaviour of the underlying usual Gibbs or MH algorithm. In a nutshell, these authors apply suitable deterministic transformations, usually additive, as $(x_1, \dots, x_d) \rightarrow (x_1 + \epsilon, \dots, x_d + \epsilon)$, or multiplicative, $(x_1, \dots, x_d) \rightarrow (\eta x_1, \dots, \eta x_d)$, to the samples generated at each iteration of Gibbs or MH in a way that the stationarity of the target distribution is preserved, while mixing properties of chain after the transformation may perhaps be improved. To maintain stationarity, ϵ and η must be simulated from some appropriate distribution which is often impossible to generate from (see [Liu and Yu \(1999\)](#)). To alleviate the problem [Liu and Sabatti \(2000\)](#) (see also [Kou et al. \(2005\)](#)) suggest MH methods.

As pointed out in the supplement of [Dutta and Bhattacharya \(2014\)](#), the purpose of these generalized Gibbs/MH methods is only to attempt to improve mixing of the underlying MCMC,

which can be usefully employed in TMCMC as well to further improve its mixing, if necessary. These are not stand-alone methodologies which can converge to the target by themselves, unlike TMCMC. In fact, as shown in the supplement of [Dutta and Bhattacharya \(2014\)](#) the aforementioned additive and multiplicative transformations of generalized Gibbs/MH approaches are themselves not even irreducible, and are hence generally non-convergent. See the supplement of [Dutta and Bhattacharya \(2014\)](#) for detailed discussions regarding various issues pertaining to these approaches.

2.5 Contrast of the TMCMC idea with reversible jump Markov chain Monte Carlo (RJMCMC)

Interestingly, although both TMCMC and RJMCMC are based on deterministic transformations, the philosophy of TMCMC is in sharp contrast with that of RJMCMC. Firstly, TMCMC is designed for simulation from fixed-dimensional distributions while RJMCMC is meant for generating from variable-dimensional distributions. Secondly, the deterministic transformations in RJMCMC are not required for move-types that are not meant for changing dimensions, while in TMCMC none of the moves change dimensions, yet all of them are based on deterministic transformations. Thirdly, the acceptance rates of dimension changing moves of RJMCMC depend upon the proposal density because for moving from lower to higher dimension simulation of random variables is required but for returning to lower dimension from higher dimension no simulation is necessary. For instance, for moving from $x_1 \in \mathbb{R}$ to $(x_1^*, x_2^*) \in \mathbb{R}^2$, one may simulate $u \sim \varphi$, where φ is some density supported on \mathbb{R} , and then make the transformation $x_1^* = x_1 - u$ and $x_2^* = x_1 + u$. However, for returning from (x_1^*, x_2^*) to x_1 , one simply sets $x_1 = \frac{x_1^* + x_2^*}{2}$, without simulating any random variable. On the other hand, as discussed in Section 2.2, since ϵ is simulated from ϱ while moving forward and also for moving back, the detailed balance condition dictates that the acceptance ratio of TMCMC must always be independent of ϱ .

2.6 Discussion of extension of TMCMC to variable dimensional problems

[Das and Bhattacharya \(2014\)](#) extend TMCMC to accommodate variable-dimensional problems; they refer to the new variable dimensional methodology as Transdimensional Transformation based Markov chain Monte Carlo (TTMCMC). TTMCMC is designed to update the entire set of parameters, both fixed and variable dimensional, as well as the number of parameters, in a single block using simple deterministic transformations of some low-dimensional (often one-dimensional) random variable drawn from some fixed, but arbitrary distribution defined on some relevant support. Again, the acceptance probability is independent of the proposal density. The advantages of TMCMC over Metropolis-Hastings algorithms are clearly carried over to the advantages of TTMCMC over RJMCMC. In fact, since it is well-known that efficient implementation of RJMCMC is generally infeasible, TTMCMC offers huge advantages in this regard; see [Das and Bhattacharya \(2014\)](#) for details.

3 Optimal scaling of additive TMCMC when the target density is a product based on *iid* random variables

It must be emphasized that the proposal density for ϵ in TMCMC can be any distribution on the positive support. Similarly, the RWM algorithm also does not require the proposal to be normal. However, the optimal scaling results for RWM inherently assume normality, and for the sake of comparison, we have also restricted our focus on $\epsilon \sim N(0, \frac{\ell^2}{d})I_{\{\epsilon > 0\}}$ in the subsequent sections.

In this paper, we are primarily interested in choosing the parameters of the process judiciously so as to enhance the performance of the chain. Our method as stated above involves

only a single parameter – the proposal variance, or to be more precise, the scaling factor ℓ . Details on the need for optimal scaling of additive TMCMC with regard to the scaling factor ℓ are provided in Section S-2 of the supplement.

In this section we consider the problem of optimal scaling in the simplest case where the target density π is a product of *iid* marginals, given by

$$\pi(x) = \prod_{i=1}^d f(x_i). \quad (12)$$

Assuming that the TMCMC chain is started at stationarity, we shall show that for each component of X , the corresponding one-dimensional process converges to a diffusion process which is analytically tractable and whose diffusion and drift speeds may be numerically evaluated. It is important to remark that it is possible to relax the assumption of stationarity; see Jourdain *et al.* (2013) in the context of RWM, although we do not pursue this in our current work.

Let $X_t^d = (X_{t,1}, \dots, X_{t,d})$. We define $U_t^d = X_{[dt],1}$ ($[\cdot]$ denotes the integer part), the sped up first component of the actual additive TMCMC-induced Markov chain. Note that this process proposes a jump every $\frac{1}{d}$ time units. As $d \rightarrow \infty$, that is, as the dimension grows to ∞ , the process essentially becomes a continuous time diffusion process.

Before proceeding first let us introduce the notion of Skorohod topology (Skorohod (1956)). It is a topology generated by a class of functions from $[0, 1] \rightarrow \mathbb{R}$ for which the right hand and the left hand limits are well defined at each point (even though they may not be the same). It is an important tool for formulating Poisson process, Levy process and other stochastic point processes. As considered in Roberts *et al.* (1997) here we also consider the metric separable topology on the above class of functions as defined in Skorohod (1956). In other words, whenever we mention convergence of discrete time stochastic processes to diffusion process in this paper, we mean convergence with respect to this topology.

In what follows, we assume the following:

$$E_f \left(\frac{f'(X)}{f(X)} \right)^4 < \infty, \quad (13)$$

$$E_f \left(\frac{f''(X)}{f(X)} \right)^4 < \infty, \quad (14)$$

$$E_f \left(\frac{f'''(X)}{f(X)} \right)^4 < \infty. \quad (15)$$

$$E_f \left| \frac{f''''(X)}{f(X)} \right| < \infty. \quad (16)$$

These assumptions can also be somewhat relaxed, depending upon the order of the Taylor's series expansions used in the proofs. Following Roberts *et al.* (1997) let us denote weak convergence of processes in the Skorohod topology by \Rightarrow .

We next present our formal result in the *iid* situation, the proof of which is presented in Section S-6.1. Our proof differs from the previous approaches associated with RWM particularly because as already shown in Section 2, in additive TMCMC, the terms $b_i\epsilon$ are not jointly normally distributed unlike the RWM-based approaches. Thus, unlike the RWM-based approaches, in our case obtaining appropriate normal approximation to relevant quantities are not assured. To handle the difficulty, we had to apply Lyapunov's central limit theorem on sums associated with the discrete random variables $\{b_i; i = 2, \dots, d\}$, conditional on ϵ (and b_1). This required us to verify Lyapunov's condition (see, for example, Korolov and Sinai (2007)) before applying the central limit theorem. We then integrated over ϵ and b_1 . These issues make our proof substantially different from the previous approaches associated with RWM. It is important to

remark that, not only in this *iid* scenario, but in all the set-ups that we consider in this paper, application of Lyapunov's central limit theorem, conditionally on ϵ (and often b_1), is crucial, before finally integrating over the conditioned variables to obtain our results.

Theorem 3.1. *Assume that f is positive with at least three continuous derivatives and that the fourth derivative exists almost everywhere. Also assume that $(\log f)'$ is Lipschitz continuous, and that (13) – (16) hold. Let $X_0^d \sim \pi$, that is, the d -dimensional additive TMCMC chain is started at stationarity, and let the transition be given by $(x_1, \dots, x_d) \rightarrow (x_1 + b_1\epsilon, \dots, b_d\epsilon)$, where for $i = 1, \dots, d$, $b_i = \pm 1$ with equal probability and $\epsilon \equiv \frac{\ell}{\sqrt{d}}\epsilon^*$, where $\epsilon^* \sim N(0, 1)I_{\{\epsilon^* > 0\}}$. We then have*

$$\{U_t^d; t \geq 0\} \Rightarrow \{U_t; t \geq 0\},$$

where $U_0 \sim f$ and $\{U_t; t \geq 0\}$ satisfies the Langevin stochastic differential equation (SDE)

$$dU_t = g(\ell)^{1/2} dB_t + \frac{1}{2} g(\ell) (\log f(U_t))' dt, \quad (17)$$

with B_t denoting standard Brownian motion at time t ,

$$g(\ell) = 4\ell^2 \int_0^\infty u^2 \Phi\left(-\frac{u\ell\sqrt{\mathbb{I}}}{2}\right) \phi(u) du; \quad (18)$$

$\Phi(\cdot)$ and $\phi(\cdot)$ being the standard normal cumulative distribution function (cdf) and density, respectively, and

$$\mathbb{I} = E_f \left(\frac{f'(X)}{f(X)} \right)^2. \quad (19)$$

In connection with our diffusion equation (see Equation (18) in connection with the proof of Theorem 3.1 in Section S-6.1), we note that our SDE is also Langevin like the usual RWM approach. But, we have a different *speed* and it is interesting to compare how the two *speed* functions of our method is related to that of RWM and also, how it alters the optimal expected acceptance rate of the process. In what follows, we use the terms *speed* and *diffusion speed* of the process, given by $g(\ell)$ as in (18) interchangeably.

Corollary 3.1. *The diffusion speed $g(\ell)$ is maximized by*

$$\ell_{opt} = \frac{2.426}{\sqrt{\mathbb{I}}}, \quad (20)$$

and the optimal acceptance rate is given by

$$\alpha_{opt} = 4 \int_0^\infty \Phi\left(-\frac{u\ell_{opt}\sqrt{\mathbb{I}}}{2}\right) \phi(u) du = 0.439 \quad (\text{up to three decimal places}). \quad (21)$$

3.1 TMCMC within Gibbs for *iid* product densities

The main notion of Gibbs sampling is to update one or multiple components of a multidimensional random vector conditional on the remaining components. In TMCMC within Gibbs, we update only a fixed proportion c_d of the d co-ordinates, where c_d is a function of d and we assume that as $d \rightarrow \infty$, then $c_d \rightarrow c$, for some $0 < c \leq 1$. In order to explain the transitions in this process analytically, we define an indicator function χ_i for $i = 1, \dots, d$. For fixed d ,

$$\begin{aligned} \chi_i &= 1 && \text{if transition takes place in the } i^{th} \text{ co-ordinate} \\ &= 0 && \text{if no transition takes place in the } i^{th} \text{ co-ordinate.} \end{aligned} \quad (22)$$

Our assumptions imply that

$$P(\chi_i = 1) = c_d; \quad i = 1, \dots, d. \quad (23)$$

Then a feasible transition with respect to additive TMCMC can be analytically expressed as

$$(x_1, \dots, x_d) \rightarrow (x_1 + \chi_1 b_1 \epsilon, \dots, x_d + \chi_d b_d \epsilon), \quad (24)$$

where $\epsilon \equiv \frac{\ell}{\sqrt{d}} \epsilon^*$, where $\epsilon^* \sim N(0, 1)I_{\{\epsilon^* > 0\}}$. We then have the following theorem, the proof of which is presented in Section S-6.2 of the supplement.

Theorem 3.2. *Assume that f is positive with at least three continuous derivatives and that the fourth derivative exists almost everywhere. Also assume that $(\log f)'$ is Lipschitz continuous, and that (13) – (16) hold. Suppose also that the transition is given by (24) and that as $d \rightarrow \infty$, $c_d \rightarrow c$, for some $0 < c \leq 1$. Let $X_0^d \sim \pi$, that is, the d -dimensional additive TMCMC chain is started at stationarity. We then have*

$$\{U_t^d; t \geq 0\} \Rightarrow \{U_t; t \geq 0\},$$

where $U_0 \sim f$ and $\{U_t; t \geq 0\}$ satisfies the Langevin SDE

$$dU_t = g_c(\ell)^{1/2} dB_t + \frac{1}{2} g_c(\ell) (\log f(U_t))' dt, \quad (25)$$

where

$$g_c(\ell) = 4c\ell^2 \int_0^\infty u^2 \Phi\left(-\frac{u\ell\sqrt{c\mathbb{I}}}{2}\right) \phi(u) du, \quad (26)$$

and \mathbb{I} is given by (19).

Corollary 3.2. *The diffusion speed $g_c(\ell)$ is maximized by*

$$\ell_{opt} = \frac{2.426}{\sqrt{c\mathbb{I}}}, \quad (27)$$

and the optimal acceptance rate is given by

$$\alpha_{opt} = 4 \int_0^\infty \Phi\left(-\frac{u\ell_{opt}\sqrt{c\mathbb{I}}}{2}\right) \phi(u) du = 0.439 \quad (\text{up to three decimal places}). \quad (28)$$

4 Diffusion approximation for independent but non-identical random variables

So far we have considered only those target densities π which correspond to *iid* components of x . Now, we extend our investigation to those target densities that are associated with independent but not identically distributed random variables. That is, we now consider

$$\pi(x) = \prod_{i=1}^d f_i(x_i). \quad (29)$$

We concentrate on a particular form of the target density involving some scaling constant parameters, as considered in [Bedard \(2008b\)](#), [Bedard and Rosenthal \(2008\)](#).

$$\pi(x) = \prod_{j=1}^d \theta_j(d) f(\theta_j(d)x_j). \quad (30)$$

As before, we assume that f is twice continuously differentiable with existence of third derivative almost everywhere, and that $(\log f)'$ is Lipschitz continuous. We define $\Theta(d) = \{\theta_1(d), \theta_2(d), \dots, \theta_d(d)\}$ and we shall focus on the case where $d \rightarrow \infty$. Some of the scaling terms are allowed to appear multiple times. We assume that the first k terms of the parameter vector may or may not be identical, but the remaining $d - k$ terms can be split into m subgroups of independent scaling terms. In other words,

$$\Theta(d) = \left(\theta_1(d), \theta_2(d), \dots, \theta_k(d), \theta_{k+1}(d), \dots, \theta_{k+m}(d), \right. \\ \left. \underbrace{\theta_{k+1}(d), \dots, \theta_{k+1}(d)}_{r(1,d)-1}, \underbrace{\theta_{k+2}(d), \dots, \theta_{k+2}(d)}_{r(2,d)-1}, \dots, \underbrace{\theta_{k+m}(d), \dots, \theta_{k+m}(d)}_{r(m,d)-1} \right), \quad (31)$$

where $r(1, d), r(2, d), \dots, r(m, d)$ are the number of occurrences of the parameters in each of the m distinct classes. We assume that for any i ,

$$\lim_{d \rightarrow \infty} r(i, d) = \infty. \quad (32)$$

Also, we assume a particular form of each scaling parameter $\theta_i(d)$:

$$\frac{1}{\{\theta_i(d)\}^2} = \frac{K_i}{d^{\lambda_i}}; \quad i = 1, \dots, k, \quad \text{and} \quad \frac{1}{\{\theta_i(d)\}^2} = \frac{K_i}{d^{\gamma_i}}; \quad i = k+1, \dots, k+m. \quad (33)$$

Assume that $\theta_i^{-2}(d)$ are so arranged that γ_i are in a decreasing sequence for $i = k+1, \dots, k+m$ and also let λ_i form a decreasing sequence from $i = 1, \dots, k$. According to [Bedard \(2007\)](#), the optimal form of the scaling variance $\sigma^2(d)$ should be of the form $\sigma^2(d) = \frac{\ell^2}{d^\alpha}$, where ℓ^2 is some constant and α satisfies

$$\lim_{d \rightarrow \infty} \frac{d^{\lambda_1}}{d^\alpha} < \infty, \quad \text{and} \quad \lim_{d \rightarrow \infty} \frac{d^{\gamma_i} r(i, d)}{d^\alpha} < \infty; \quad i = 1, \dots, m. \quad (34)$$

Here, let U_t^d be the process at time t sped up by a factor of d^α . That is, $U_t^d = (X_1([d^\alpha t]), \dots, X_d([d^\alpha t]))$. We then have the following theorem, the proof of which is provided in Section S-6.3 of the supplement.

Theorem 4.1. *Assume that the target distribution is of the form (30), where f is positive with at least three continuous derivatives and that the fourth derivative exists almost everywhere. Also assume that $(\log f)'$ is Lipschitz continuous, and that (13) – (16), (31), (32), (33) and (34) hold. Let $X_0^d \sim \pi$, that is, the d -dimensional additive TMCMC chain is started at stationarity. Let the transition be given by $(x_1, \dots, x_d) \rightarrow (x_1 + b_1 \epsilon, \dots, x_d + b_d \epsilon)$, where, for $i = 1, \dots, d$, $b_i = \pm 1$ with equal probability and $\epsilon \equiv \frac{\ell}{\sqrt{2}} \epsilon^*$, with $\epsilon^* \sim N(0, 1)I_{\{\epsilon^* > 0\}}$. We then have*

$$\{U_t^d; t \geq 0\} \Rightarrow \{U_t; t \geq 0\},$$

where $U_0 \sim f$ and $\{U_t; t \geq 0\}$ satisfies the Langevin SDE

$$dU_t = g_\xi(\ell)^{1/2} dB_t + \frac{1}{2} g_\xi(\ell) (\log f(U_t))' dt, \quad (35)$$

where

$$g_\xi(\ell) = 4\ell^2 \int_0^\infty u^2 \Phi\left(-\frac{u\ell\xi\sqrt{\ell}}{2}\right) \phi(u) du. \quad (36)$$

Corollary 4.1. *The diffusion speed $g_c(\ell)$ is maximized by*

$$\ell_{opt} = \frac{2.426}{\xi\sqrt{\mathbb{I}}}, \quad (37)$$

and the optimal acceptance rate is given by

$$\alpha_{opt} = 4 \int_0^\infty \Phi\left(-\frac{u\ell_{opt}\xi\sqrt{\mathbb{I}}}{2}\right) \phi(u) du = 0.439 \quad (\text{up to three decimal places}). \quad (38)$$

4.1 TMCMC within Gibbs for independent but non-identical random variables

As in Section 3.1, here also we define transitions of the form (24), where χ_i , having the same definitions as (22) and (23), indicates whether or not the i -th co-ordinate x_i will be updated.

The rest of the proof is a simple modification of the proof for independent but non-identical random variables provided in Section S-6.3. There we must replace

$$\frac{1}{r(i, d)} \sum_{j=1}^{r(i, d)} \left(\frac{f'(u_j)}{f(u_j)} \right)^2 \rightarrow E \left[\left\{ \frac{f'(U)}{f(U)} \right\}^2 \right] = \mathbb{I}.$$

with

$$\frac{c_d}{c_d r(i, d)} \sum_{j=1}^{c_d r(i, d)} \left(\frac{f'(u_j)}{f(u_j)} \right)^2 \rightarrow c_d E \left[\left\{ \frac{f'(U)}{f(U)} \right\}^2 \right] = c\mathbb{I}. \quad (39)$$

With the above modification the diffusion speed can be calculated as

$$g_{c, \xi}(\ell) = 4c\ell^2 \int_0^\infty \left\{ u^2 \Phi\left(-\frac{u\ell\xi\sqrt{c\mathbb{I}}}{2}\right) \right\} \phi(u) du. \quad (40)$$

Formally, we have the following theorem:

Theorem 4.2. *Assume that the target distribution π is of the form (30), where f is positive with at least three continuous derivatives and that the fourth derivative exists almost everywhere. Also assume that $(\log f)'$ is Lipschitz continuous, and that (13) – (16), (31), (32), (33) and (34) hold. Let $X_0^d \sim \pi$, that is, the d -dimensional additive TMCMC chain is started at stationarity. Let the transition be $(x_1, \dots, x_d) \rightarrow (x_1 + \chi_1 b_1 \epsilon, \dots, x_d + \chi_d b_d \epsilon)$, where for $i = 1, \dots, d$, $P(\chi_i = 1) = c_d$, $b_i = \pm 1$ with equal probability, and $\epsilon \equiv \frac{\ell}{d^2} \epsilon^*$, with $\epsilon^* \sim N(0, 1)I_{\{\epsilon^* > 0\}}$. We then have*

$$\{U_t^d; t \geq 0\} \Rightarrow \{U_t; t \geq 0\},$$

where $U_0 \sim f$ and $\{U_t; t \geq 0\}$ satisfies the Langevin SDE

$$dU_t = g_{c, \xi}(\ell)^{1/2} dB_t + \frac{1}{2} g_{c, \xi}(\ell) (\log f(U_t))' dt, \quad (41)$$

where $g_{x, \xi}(\ell)$ is given by (40).

Corollary 4.2. *The diffusion speed $g_{c, \xi}(\ell)$ is maximized by*

$$\ell_{opt} = \frac{2.426}{\xi\sqrt{c\mathbb{I}}}, \quad (42)$$

and the optimal acceptance rate is given by

$$\alpha_{opt} = 4 \int_0^\infty \Phi \left(-\frac{u \ell_{opt} \xi \sqrt{c\mathbb{I}}}{2} \right) \phi(u) du = 0.439 \quad (\text{up to three decimal places}). \quad (43)$$

5 Diffusion approximation for a more general dependent family of distributions

So far, we assumed that the target density π is associated with either *iid* or mutually independent random variables, with a special structure. Now, we extend our notion to a much wider class of distributions where there is a particular form of dependence structure between the components of the distribution. In determining these non product measures, we adopted the framework of [Mattingly et al. \(2011\)](#), [Beskos et al. \(2009\)](#), [Beskos and Stuart \(2009\)](#), [Bedard \(2009\)](#). For clarity, we first discuss this in the case of finite dimension d , and then discuss the generalization in infinite dimensions.

Let $x^d \in \mathbb{R}^d$ denote the first d co-ordinates of $x \in \mathbb{R}^\infty$. Let us assume that the d -dimensional target density π^d satisfies

$$\frac{d\pi^d}{d\pi_0^d}(x^d) = M_{\Psi^d} \exp(-\Psi^d(x^d)), \quad (44)$$

where Ψ^d is measurable with respect to the Borel σ -field on \mathbb{R}^d , M_{Ψ^d} is an appropriate normalizing constant depending upon Ψ^d , and π^d has the density

$$\pi_0^d(x^d) = \prod_{j=1}^d \frac{1}{\lambda_j} \phi \left(\frac{x_j}{\lambda_j} \right) \quad (45)$$

with respect to the Lebesgue measure. In other words, under π_0^d , $x_j \sim N(0, \lambda_j^2)$; $j = 1, 2, \dots, d$.

Then, with respect to Lebesgue measure, π^d has the following density:

$$\pi^d(x^d) = M_{\Psi^d} \exp(-\Psi^d(x^d)) \prod_{i=1}^d \frac{1}{\lambda_i} \phi \left(\frac{x_i}{\lambda_i} \right). \quad (46)$$

The above finite dimensional structure can be represented in terms of projection onto the first d eigen functions of an appropriate covariance operator associated with a Hilbert space. Indeed, let $(\mathbb{H}, \langle \cdot, \cdot \rangle, \|\cdot\|)$ denote a real, separable Hilbert space. Consider a covariance operator $\Sigma : \mathbb{H} \rightarrow \mathbb{H}$, which is self-adjoint, positive, and trace class operator on \mathbb{H} with a complete orthonormal eigen basis $\{\lambda_j^2, \phi_j\}_{j=1}^\infty$ such that

$$\Sigma \phi_j = \lambda_j^2 \phi_j; \quad j = 1, 2, \dots \quad (47)$$

As in [Mattingly et al. \(2011\)](#) we assume that the eigenvalues are arranged in decreasing order and $\lambda_j > 0$.

Now note that any function x in \mathbb{R}^∞ can be uniquely represented as

$$x = \sum_{j=1}^\infty x_j \phi_j, \quad \text{where } x_j = \langle x, \phi_j \rangle. \quad (48)$$

The function x can be identified with its co-ordinates $\{x_j\}_{j=1}^\infty$ which belongs to the space of square-summable sequences. Note that Σ is diagonal with respect to the co-ordinates of this eigen basis, and if $x_j \sim N(0, \lambda_j^2)$; $j = 1, 2, \dots$ independently, then by the Karhunen-Loéve expansion (see, for example, [Prato and Zabczyk \(1992\)](#)), x follows the Gaussian measure π_0 ,

which is an infinite dimensional generalization of (45). In particular, we assume that π_0 is a Gaussian measure with mean 0 and covariance Σ .

Now, let $\Psi^d(\cdot) = \Psi(P^d \cdot)$, where P^d denotes projection (in \mathbb{H}) onto the first d eigen functions of Σ , and Ψ is a real π_0 -measurable function on \mathbb{R}^∞ . Then $\pi^d(x^d)$ given by (46) can be represented as

$$\pi^d(x) = M_{\Psi^d} \exp \left(-\Psi^d(x) - \frac{1}{2} \langle x, (\Sigma^d)^{-1} x \rangle \right), \quad (49)$$

where $\Sigma^d = P^d \Sigma P^d$. As $d \rightarrow \infty$, (49) approximates the target density $\pi(x)$, where the Radon Nikodym derivative of the target π with respect to the Gaussian measure π_0 is given by

$$\frac{d\pi}{d\pi_0}(x) = M_\Psi \exp(-\Psi(x)). \quad (50)$$

Hence, for our purpose we shall work with the finite-dimensional approximation (49); as $d \rightarrow \infty$, the appropriate piecewise linear, continuous interpolant (to be defined subsequently in Section 5.2) that is described by our additive TMCMC algorithm and associated with π^d will converge to the correct diffusion equation associated with the infinite dimensional distribution π represented by (50).

5.1 Representation of the additive TMCMC algorithm in the dependent set-up

Under the TMCMC set up, the move at the $(k+1)$ -th time point can be explicitly stated in terms of the position at k -th time point as follows

$$x^{k+1} = \gamma^{k+1} y^{k+1} + (1 - \gamma^{k+1}) x^k, \quad (51)$$

where

$$\gamma^{k+1} \sim \text{Bernoulli} \left(\min \left\{ 1, \frac{\pi^d(y^{k+1})}{\pi^d(x^k)} \right\} \right).$$

We define the move y^{k+1} as

$$y^{k+1} = x^k + \sqrt{\frac{2\ell^2}{d}} \Sigma^{\frac{1}{2}} \xi^{k+1}, \quad (52)$$

where $\xi^{k+1} = (b_1^{k+1} \epsilon^{k+1}, \dots, b_d^{k+1} \epsilon^{k+1})$ with $b_i = \pm 1$ with probability 1/2 each, and $\epsilon \sim N(0, 1)_{I_{\{\epsilon > 0\}}}$. From (49) it follows that $\min \left\{ 1, \frac{\pi^d(y^{k+1})}{\pi^d(x^k)} \right\}$ can be written as $\min \left\{ 1, e^{\mathbb{Q}(x^k, \xi^{k+1})} \right\}$ where $\mathbb{Q}(x, \xi)$ is given by

$$\mathbb{Q}(x, \xi) = \frac{1}{2} \left\| \Sigma^{-\frac{1}{2}} (P^d x) \right\|^2 - \frac{1}{2} \left\| \Sigma^{-\frac{1}{2}} (P^d y) \right\|^2 + \Psi^d(x) - \Psi^d(y). \quad (53)$$

Using (52), one obtains

$$\mathbb{Q}(x, \xi) = -\sqrt{\frac{2\ell^2}{d}} \langle \eta, \xi \rangle - \frac{\ell^2}{d} \|\xi\|^2 - r(x, \xi), \quad (54)$$

where

$$\eta = \Sigma^{-\frac{1}{2}} (P^d x) + \Sigma^{\frac{1}{2}} \nabla \Psi^d(x), \quad (55)$$

and

$$r(x, \xi) = \Psi^d(y) - \Psi^d(x) - \langle \nabla \Psi^d(x), P^d y - P^d x \rangle. \quad (56)$$

We further define

$$R(x, \xi) = -\sqrt{\frac{2\ell^2}{d}} \sum_{j=1}^d \eta_j \xi_j - \frac{\ell^2}{d} \sum_{j=1}^d \xi_j^2, \quad (57)$$

and

$$R_i(x, \xi) = -\sqrt{\frac{2\ell^2}{d}} \sum_{j=1, j \neq i}^d \eta_j \xi_j - \frac{\ell^2}{d} \sum_{j=1, j \neq i}^d \xi_j^2 \quad (58)$$

Using Lemma 5.5 of [Mattingly et al. \(2011\)](#), for large d one can show that

$$\mathbb{Q}(x, \xi) = R(x, \xi) - r(x, \xi) \approx R_i(x, \xi) - \sqrt{\frac{2\ell^2}{d}} \eta_i \xi_i. \quad (59)$$

Using (57) and (59) it can be seen that $\mathbb{Q}(x, \xi)$ is approximately equal to $R(x, \xi)$ as d goes to ∞ , where $R(x, \xi)$ in our case is given by

$$R(x, \xi) = -\epsilon \sqrt{\frac{2\ell^2}{d}} \sum_{j=1}^d \eta_j b_j - \ell^2 \epsilon^2. \quad (60)$$

Note that in the case of [Mattingly et al. \(2011\)](#), conditional on x , $R_i(x, \xi)$ was independent of ξ_i , which enabled them to compute $E_0(\min\{1, e^{\mathbb{Q}(x, \xi)}\} \xi_i)$ by first computing it over ξ_i and then over $\xi \setminus \xi_i$. However, such independence does not hold in our case since all the components of ξ involve ϵ .

To obtain $E_0(\min\{1, e^{\mathbb{Q}(x, \xi)}\} \xi_i)$ in our case, we need to obtain the asymptotic distribution of $\mathbb{Q}(x, \xi)$ for large d . Since our TMCMC based proposal is not *iid*, we verify Lyapunov's central limit theorem; see Section S-7.1. For obtaining the diffusion approximation in this dependent set-up we need to obtain the expected drift and the expected diffusion coefficient. In Section S-7.2 we calculate the expected drift and in Section S-7.3, we obtain the expected diffusion coefficient.

5.2 Formal statement of our main result in the general dependent set-up

Before formally stating our result in the dependent set-up, we need to provide the explicit form of a continuous interpolant which converges to the solution of the appropriate SDE.

Note that we can construct, following [Mattingly et al. \(2011\)](#), the following continuous interpolant

$$z^d(t) = (dt - k)x^{k+1} + (k + 1 - dt)x^k, \quad k \leq dt < k + 1. \quad (61)$$

Observe that $z^d(t)$ admits the following representation

$$z^d(t) = z^0 + \int_0^t \vartheta^d(\bar{z}^d(s)) ds + \sqrt{2g(\ell)} W^d(t), \quad (62)$$

where $z^0 \sim \pi$, $g(\ell) = \ell^2 \beta$, $\vartheta^d(x) = dE_0(x^1 - x)$, $\bar{z}^d(t) = x^k$; $t \in [t^k, t^{k+1}]$ is a piecewise constant interpolant of x^k , where

$$t^k = k\Delta t, \quad \eta^{k,d} = \sqrt{\Delta t} \sum_{j=1}^k \Gamma^{j,d}, \quad (63)$$

$$W^d(t) = \eta^{[dt],d} + \frac{dt - [dt]}{\sqrt{d}} \Gamma^{[dt]+1,d}; \quad t \in [0, T], \quad (64)$$

where $T > 0$ is fixed.

In fact as $d \rightarrow \infty$, there exists $\widehat{W}^d \Rightarrow W$ such that $z^d(t)$ admits the following representation:

$$z^d(t) = z^0 - g(\ell) \int_0^t \left(z^d(s) + \Sigma \nabla \Psi \left(z^d(s) \right) \right) ds + \sqrt{2g(\ell)} \widehat{W}^d(t). \quad (65)$$

It can be shown, proceeding in the same way, and using the same assumptions on the covariance operator and Ψ as Mattingly *et al.* (2011), that $z^d(t)$ converges weakly to z (see Mattingly *et al.* (2011) for the rigorous definition), where z satisfies the SDE given by

$$\frac{dz}{dt} = -g(\ell) (z + \Sigma \nabla \Psi(z)) + \sqrt{2g(\ell)} \frac{dW}{dt}, \quad z(0) = z^0, \quad (66)$$

where $z^0 \sim \pi$, W is a Brownian motion in a relevant Hilbert space with covariance operator Σ , and

$$g(\ell) = \ell^2 \beta, \quad (67)$$

is the diffusion speed.

Our result, which we state as Theorem 5.1, requires the same assumptions on the decay of eigen values λ_j^2 of Σ and properties of Ψ that were also required by Mattingly *et al.* (2011). For the sake of completeness we present these assumptions below. But before that we need to define some new notation, as follows.

Using the expansion (48), following Mattingly *et al.* (2011) we define the Sobolev spaces \mathbb{H}^r ; $r \in \mathbb{R}$, where the inner products and norms are defined by

$$\langle x, y \rangle_r = \sum_{j=1}^{\infty} j^{2r} x_j y_j, \quad \|x\|_r^2 = \sum_{j=1}^{\infty} j^{2r} x_j^2.$$

For an operator $L : \mathbb{H}^r \rightarrow \mathbb{H}^l$, we denote, following Mattingly *et al.* (2011), the operator norm on \mathbb{H} by $\|L\|_{\mathcal{L}(\mathbb{H}^r, \mathbb{H}^l)}$ defined by

$$\|L\|_{\mathcal{L}(\mathbb{H}^r, \mathbb{H}^l)} = \sup_{\|x\|_r=1} \|Lx\|_l.$$

5.2.1 Assumptions

(1) *Decay of eigen values λ_j^2 of Σ* : There exist $M_-, M_+ \in (0, \infty)$ and $\kappa > \frac{1}{2}$ such that

$$M_- \leq j^\kappa \lambda_j \leq M_+, \quad \forall j \in \mathbb{Z}_+ = \{1, 2, 3, \dots\}. \quad (68)$$

(2) *Assumptions on Ψ* : There exist constants $M_i \in \mathbb{R}$, $i \leq 4$ and $s \in [0, \kappa - \frac{1}{2})$ such that

$$M_1 \leq \Psi(x) \leq M_2 (1 + \|x\|_s^2) \quad \forall x \in \mathbb{H}^s \quad (69)$$

$$\|\nabla \Psi(x)\|_{-s} \leq M_3 (1 + \|x\|_s) \quad \forall x \in \mathbb{H}^s \quad (70)$$

$$\|\partial^2 \Psi(x)\|_{\mathcal{L}(\mathbb{H}^r, \mathbb{H}^l)} \leq M_4 \quad \forall x \in \mathbb{H}^s. \quad (71)$$

(3) *Assumptions on Ψ^d* : The functions Ψ^d satisfy the same conditions imposed on Ψ given by (69), (70) and (71) with the same constants uniformly across d .

Theorem 5.1. *Let assumptions (1) – (3), as stated in Section 5.2.1, hold. Let $x^0 \sim \pi^d$, where π^d is given by (49) and let $z^d(t)$ be given by (61). Then z^d converges weakly to the diffusion process z given by (66) with $z(0) \sim \pi$.*

Corollary 5.1. *The diffusion speed $g(\ell)$ is maximized by*

$$\ell_{opt} = \frac{2.426}{\sqrt{2}} = 1.715, \quad (72)$$

and the optimal acceptance rate is given by

$$\alpha_{opt} = 4 \int_0^\infty \Phi\left(-\frac{\ell_{opt}u}{\sqrt{2}}\right) \phi(u)du = 0.439 \quad (\text{up to three decimal places}). \quad (73)$$

5.3 TMCMC within Gibbs for the dependent family of distributions

As before, here we define transitions of the form (24), where the random variable χ_i ; $i = 1, \dots, d$ indicates whether or not the i -th co-ordinate of x will be updated. Formally,

$$x^{k+1} = \gamma^{k+1}y^{k+1} + (1 - \gamma^{k+1})x^k, \quad (74)$$

where

$$\gamma^{k+1} \sim \text{Bernoulli}\left(\min\left\{1, \frac{\pi^d(y^{k+1})}{\pi^d(x^k)}\right\}\right).$$

We define the new move y^{k+1} of the same form as (52), but with the indicator variables χ_i incorporated appropriately. In other words,

$$y^{k+1} = x^k + \sqrt{\frac{2\ell^2}{d}}\Sigma^{\frac{1}{2}}\xi^{k+1}, \quad (75)$$

where $\xi^{k+1} = (\chi_1^{k+1}b_1^{k+1}\epsilon^{k+1}, \dots, \chi_d^{k+1}b_d^{k+1}\epsilon^{k+1})$; $b_i = \pm 1$ with probability 1/2 each, $\epsilon \sim N(0, 1)I_{\{\epsilon > 0\}}$, and for any $k > 0$ and for $i = 1, \dots, d$, $P(\chi_i^{k+1} = 1) = c_d$. As before, we assume that $c_d \rightarrow c$ as $d \rightarrow \infty$, where $0 < c \leq 1$.

The proof again required only minor modification to the above proof provided in the case of this dependent family of distributions. Here, additionally, we only need to take expectations with respect to χ_i^{k+1} ; $i = 1, \dots, d$, so that we now have

$$[\mathbb{Q}(x, \xi)|b_i, \epsilon] \approx d \left(-\ell^2\epsilon^2 - c\epsilon\sqrt{\frac{2\ell^2}{d}}\eta_i b_i, 2\ell^2\epsilon^2 c^2 \right).$$

Proceeding in the same manner as in the above proof, we obtain a stochastic differential equation of the same form as (66), but with $g(\ell)$ replaced with

$$g_c(\ell) = c\ell^2\beta_c, \quad (76)$$

where

$$\beta_c = 4 \int_0^\infty u^2 \Phi\left(-\frac{\ell u}{c\sqrt{2}}\right) \phi(u)du.$$

The result can be stated formally as follows:

Theorem 5.2. *Let assumptions (1) – (3), as stated in Section 5.2.1, hold. Let $x^0 \sim \pi^d$, where π^d is given by (49) and let $z^d(t)$ be given by (61), where $z^d(t)$ depends upon x^k and x^{k+1} through $\xi^{k+1} = (\chi_1^{k+1}b_1^{k+1}\epsilon^{k+1}, \dots, \chi_d^{k+1}b_d^{k+1}\epsilon^{k+1})$, where for any $k > 0$ and for $i = 1, \dots, d$, $P(\chi_i^{k+1} = 1) = c_d$, other definitions remaining the same as before. Then z^d converges weakly to the diffusion process z having the same form as (66), but $g(\ell)$ replaced with $g_c(\ell)$ given by (76), and as before, $z(0) \sim \pi$.*

Corollary 5.2. *The diffusion speed $g_c(\ell)$ is maximized by*

$$\ell_{opt} = \frac{2.426c}{\sqrt{2}} = 1.715c, \quad (77)$$

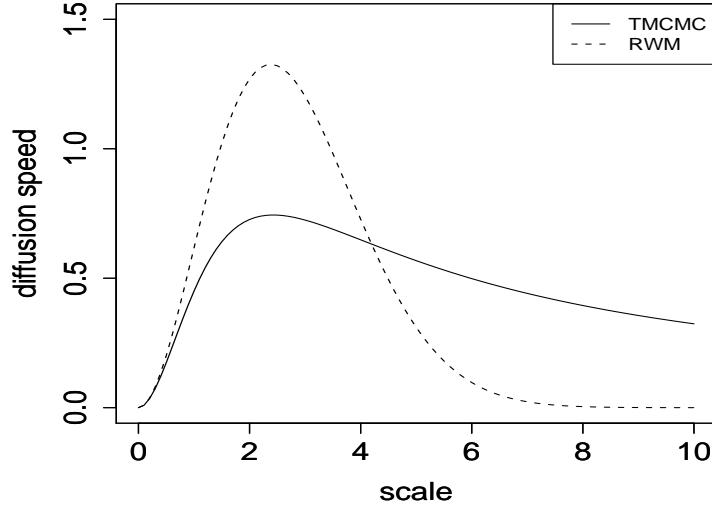


Figure 1: Comparison of diffusion speeds of TCMC and RWM in the *iid* case.

and the optimal acceptance rate is given by

$$\alpha_{opt} = 4 \int_0^\infty \Phi\left(-\frac{\ell_{opt}u}{c\sqrt{2}}\right) \phi(u)du = 0.439 \quad (\text{up to three decimal places}). \quad (78)$$

6 Comparison with RWM

6.1 Comparison in the *iid* set-up

Note that for both the standard RWM algorithm and our additive TCMC algorithm, the diffusion process reduces to the Langevin diffusion having the same form, but different diffusion speeds. For the RWM algorithm, the diffusion speed $h(\ell)$ is given by $h(\ell) = 2\ell^2\Phi\left(-\frac{\ell\sqrt{\mathbb{I}}}{2}\right)$, and the optimal acceptance rate is $2\Phi\left(-\frac{\ell_{opt}\sqrt{\mathbb{I}}}{2}\right)$, where ℓ_{opt} maximizes $h(\ell)$. A comparison between (18) and the above diffusion speed reveals that if, instead of the standard normal distribution, z_1^* associated with equation (13) of the supplement, corresponding to the proof of Theorem 3.1, had a distribution that assigned probability 1/2 to each of +1 and -1, then the additive TCMC-based diffusion speed would reduce to the RWM-based diffusion speed.

Note that the optimum value of ℓ in RWM is $\ell_{opt} = \frac{2.381}{\sqrt{\mathbb{I}}}$ and the corresponding expected acceptance rate is 0.234. However, in TCMC it is observed on maximizing (18) that $\ell_{opt} = \frac{2.426}{\sqrt{\mathbb{I}}}$ and the corresponding expected acceptance rate is 0.439; see Corollary 3.1. Hence, although the values of the optimizer ℓ_{opt} are close for RWMH and additive TCMC, the optimal acceptance rate of the latter is significantly higher. This much higher acceptance rate for TCMC is to be expected because effectively just a one-dimensional proposal distribution is used to update the entire high-dimensional random vector x .

Figure 1 compares the diffusion speeds of TCMC and RWM in the *iid* case. Observe that the maximum diffusion speed for RWM is greater than that of TCMC. However, the graph for RWM falls much more steeply compared to TCMC for large ℓ , showing that the diffusion speed is quite sensitive towards mis-specification of the scaling constant, and that scaling constants other than the maximizer can substantially decrease the diffusion speed. On the other hand, the graph for TCMC is much more flat, indicating relatively more robustness with respect to the choice of ℓ .

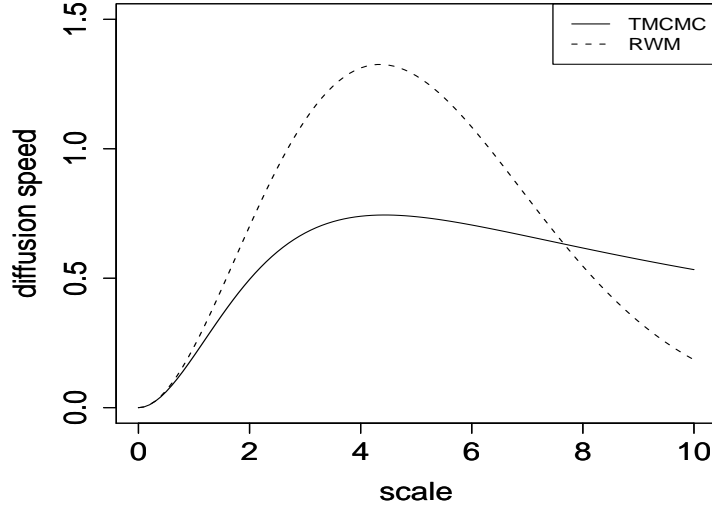


Figure 2: Comparison of diffusion speeds of TCMC within Gibbs and RWM within Gibbs in the *iid* case, with $c = 0.3$.

As we will see, the same phenomenon holds for all the other set-ups, such as the target distributions with non-identical and dependent components. This is an important issue in practice for general high-dimensional target distributions, particularly with non-identical and dependent components since, as discussed in Sections S-3 and S-4, in practice, tuning the scaling constants of the proposal distributions to approximately achieve the optimal acceptance rate is generally infeasible in high dimensions, which in turn makes the maximum diffusion speed infeasible to achieve. For the RWM algorithm any such mis-specification entails a sharp fall in the diffusion speed. Since in high dimensions mis-specifications are very much likely, RWM is quite generally prone to sub-optimal performances. From the discussion presented in Section S-5 it can be anticipated that in very high dimensions, it may not be practically feasible to achieve the optimal acceptance rate using adaptive algorithms based on RWM. On the other hand, additive TCMC remains far more robust even in the face of such mis-specifications, thus significantly cutting down the risk of poor performance in high dimensions. Adaptive algorithms based on additive TCMC are also demonstrated by [Dey and Bhattacharya \(2015a\)](#) to be much more efficient compared to the adaptive RWM algorithms.

6.1.1 Within Gibbs comparison in the *iid* set-up

Now we compare TCMC within Gibbs based diffusion speed and optimal acceptance rate given by

$$g_c(\ell) = 4c\ell^2 \int_0^\infty u^2 \Phi\left(-\frac{u\ell\sqrt{c\ell}}{2}\right) \phi(u) du. \quad (79)$$

(see (26) of the supplement, Section S-6.2) and (28) with those of RWM within Gibbs. The diffusion speed for the RWM within Gibbs algorithm is $h_c(\ell) = 2c\ell^2 \Phi\left(-\frac{\ell\sqrt{c\ell}}{2}\right)$, and the optimal acceptance rate is $2\Phi\left(-\frac{\ell_{opt}\sqrt{c\ell}}{2}\right)$, where ℓ_{opt} maximizes $h_c(\ell)$; see [Neal and Roberts \(2006\)](#). It turns out that ℓ_{opt} for RWM within Gibbs is given by $\frac{2.381}{\sqrt{c\ell}}$, and the optimal acceptance rate is 0.234, as before. Figure 2 compares the diffusion speeds associated with TCMC within Gibbs and RWM within Gibbs, with $c = 0.3$. Once again, we observe that the diffusion speed of TCMC within Gibbs is more robust with respect to mis-specification of the scale.

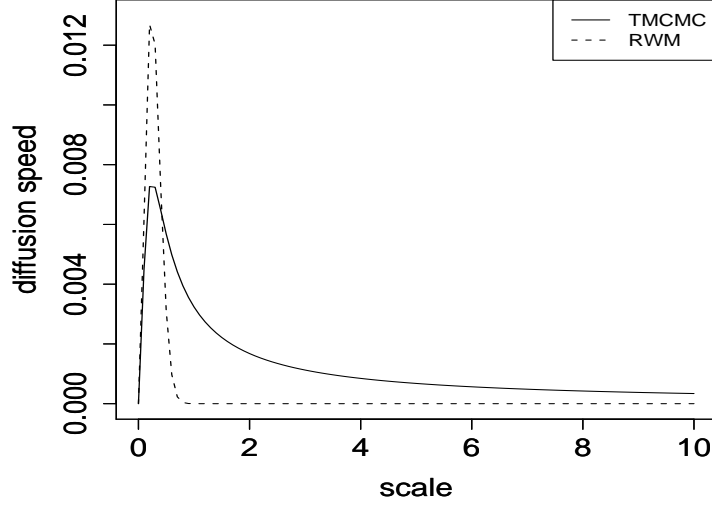


Figure 3: Comparison of diffusion speeds of TMCMC within Gibbs and RWM within Gibbs in the independent but non-identical case, with $\xi = 10$.

6.2 Comparison in the independent but non-identical set-up

The equations

$$g_{\xi}(\ell) = 4\ell^2 \int_0^{\infty} \left\{ u^2 \Phi \left(-\frac{u\ell\xi\sqrt{\mathbb{I}}}{2} \right) \right\} \phi(u) du. \quad (80)$$

(see also (39) of the supplement) and (38) provide the diffusion speed and the optimal acceptance rate for TMCMC in the independent but non-identical set-up. The corresponding quantities for RWM are given by $2\ell^2\Phi\left(-\frac{\ell\xi\sqrt{\mathbb{I}}}{2}\right)$ and $2\Phi\left(-\frac{\ell_{opt}\xi\sqrt{\mathbb{I}}}{2}\right)$, respectively. As before, the optimal acceptance rates remain 0.234 and 0.439 for RWM and TMCMC, respectively. Figure 3 compares the diffusion speeds associated with TMCMC and RWM, with $\xi = 10$. Here both the graphs are steep, but that for RWM is much more steeper, leading to the same observations regarding robustness with respect to mis-specification of scale.

6.2.1 Within Gibbs comparison in the independent but non-identical set-up

It can be easily shown that the RWM-based diffusion speed and the acceptance rate in the independent but non-identical set-up are $2c\ell^2\Phi\left(-\frac{\ell\xi\sqrt{c\mathbb{I}}}{2}\right)$ and $2\Phi\left(-\frac{\ell_{opt}\xi\sqrt{c\mathbb{I}}}{2}\right)$, respectively. These are to be compared with the TMCMC-based quantities given by (40) and (43). The optimal acceptance rates for TMCMC and RWM, as before, are 0.234 and 0.439. Conclusions similar as before are reached on observing Figure 4 that compares the diffusion speeds of TMCMC and RWM in this case.

6.3 Dependent case

In the dependent case, the diffusion speed and the optimal acceptance rate of additive TMCMC are of the forms (67) and (73), respectively. As usual, the TMCMC-based optimal acceptance rate turns out to be 0.439. The corresponding RWM-based optimal acceptance rate, having the form $2\Phi\left(-\frac{\ell_{opt}}{\sqrt{2}}\right)$, turns out to be 0.234 as before, where ℓ_{opt} maximizes the corresponding diffusion speed $2\ell^2\Phi\left(-\frac{\ell}{\sqrt{2}}\right)$. Similar information as before are provided by Figure 5.

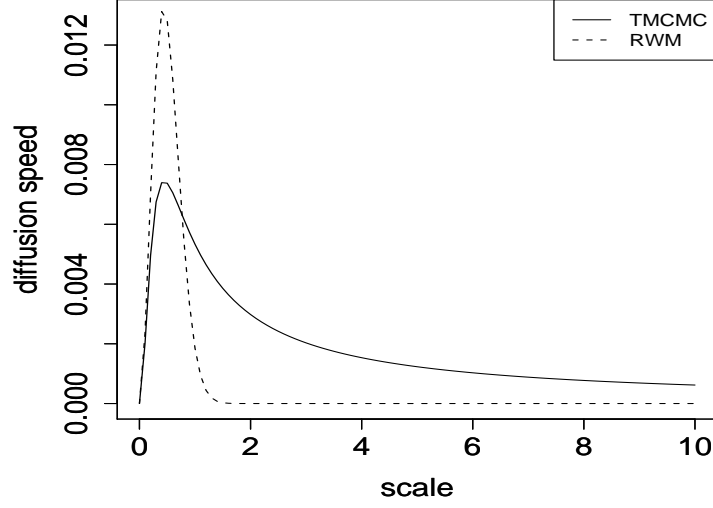


Figure 4: Comparison of diffusion speeds of TCMC within Gibbs and RWM within Gibbs in the independent but non-identical case, with $\xi = 10$, $c = 0.3$.

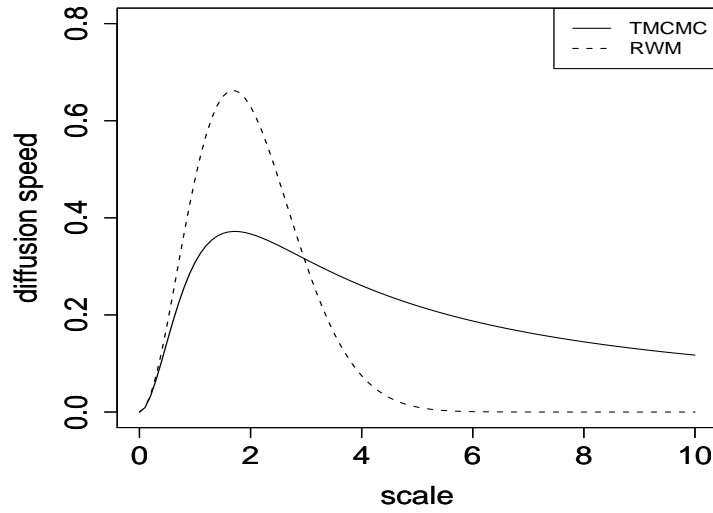


Figure 5: Comparison of diffusion speeds of TCMC and RWM in the dependent case.

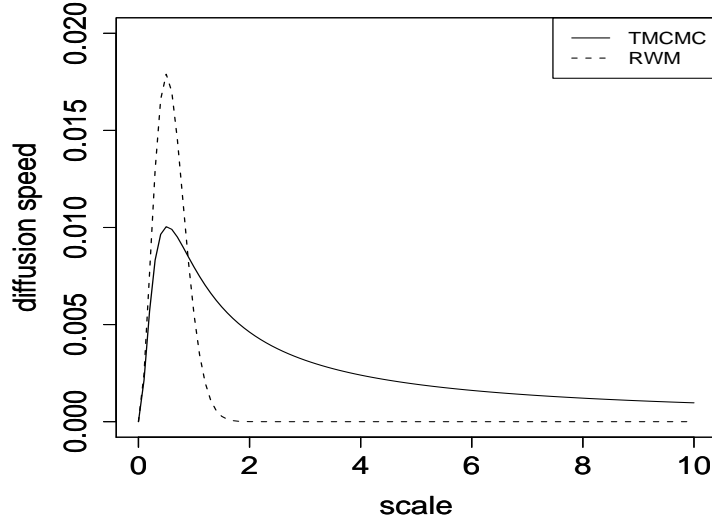


Figure 6: Comparison of diffusion speeds of TCMC within Gibbs and RWM within Gibbs in the dependent case, with $c = 0.3$.

6.3.1 Within Gibbs comparison in the dependent set-up

In the dependent case, it is easily shown that the RWM-based diffusion speed and the acceptance rate are, respectively, $2c\ell^2\Phi\left(-\frac{\ell}{c\sqrt{2}}\right)$ and $2\Phi\left(-\frac{\ell_{opt}}{c\sqrt{2}}\right)$. The corresponding TCMC-based quantities are (76) and (78). The optimal acceptance rates remain 0.234 and 0.439 for RWM and TCMC. Figure 6, comparing the diffusion speeds of TCMC within Gibbs and RWM within Gibbs in the dependent set-up, lead to similar observations as before.

7 Simulation Experiments

So far, we have invested most of our efforts in the theoretical development of optimal scaling mechanism in the additive TCMC case. Now, we shall consider some simulation experiments to illustrate the performance of our method with respect to the standard RWM methodology, under the *iid*, independent but non-identical, and dependent set-ups.

7.1 Comparison of additive TCMC and RWM in the *iid* case

We compare the performance of RWM and TCMC corresponding to three different choices of the proposal variance, with scalings ℓ being 2.4 (approximately optimal for both RWM and additive TCMC) and 6 (sub-optimal for both RWM and additive TCMC) respectively. We consider target densities of dimensions ranging from 2 to 200. For our purpose we consider the target density π to be the multivariate normal distribution with mean vector zero and covariance matrix I , the identity matrix. The starting point x_0 is randomly generated from $U(-2, 2)$, the uniform distribution on $(-2, 2)$. The univariate density of ϵ for TCMC was taken to be a left-truncated normal having mean 0 and variance $\frac{\ell^2}{d}$ for each co-ordinate, where ℓ is the value of the scaling constant. For RWM, each co-ordinate of the d dimensional proposal density was assumed to have the above distribution, but without the truncation.

In each run, the chain was observed up to 100,000 trials (including the rejected moves). The choice of burn-in was made somewhat subjectively, removing one fourth of the total number of iterates initially. This choice was actually a bit conservative as both RWM and TCMC were

found to be sufficiently close to the target density well ahead of the chosen point. We measured the efficiency of the TMCMC chain with respect to the RWM chain using certain performance evaluation measures – *Acceptance rate*, *Average Jump Size* (AJS), *Integrated Auto-Correlation Time* (IACT) and *Integrated Partial Auto-Correlation Time* (IPACT) (see [Roberts and Rosenthal \(2009\)](#)). All calculations of AJS, IACT, IPACT were done corresponding to the process after burn-in in order to ensure stationarity. In calculating the integrated autocorrelation time, we considered 25 lags of ACF. IPACT was similarly computed. The first eight columns of Table 1 compare the performances of TMCMC and RWM with respect to these measures.

7.1.1 Average Kolmogorov-Smirnov distance for comparing convergence of TMCMC and RWM

The measures acceptance rate, IACT, IPACT and AJS do not explicitly measure how close the MCMC-based empirical distribution is to the target distribution. For this we also considered the Kolmogorov-Smirnov (K-S) distance to evaluate the performances of the MCMC algorithms. We ran 100 copies of the RWM and TMCMC chains starting from the same initial point and with the same target density π and observed how well the empirical distribution corresponding to these 100 copies, after discarding the burn-in period, fits the true density by evaluating the K-S distance ([Smirnov \(1948\)](#)) at each time point for both the chains. As an overall measure we take the average of the K-S distances over all the time points. This averaging over the time points makes sense since the chains are assumed to be in stationarity after the burn-in period, and hence every time point must yield the same (stationary) distribution. Our average K-S distance can be viewed as quantifying how well the MCMC algorithm explores the stationary distribution after convergence is attained. The average K-S distances for RWM and TMCMC are shown in the last two columns of Table 1.

7.1.2 Observations regarding the results presented in Table 1

As evident from Table 1, TMCMC seems to have a uniformly better acceptance rate than RWM for all dimensions and all choices of proposal variances. There is sufficient gain in acceptance rate over RWM even for 2 dimensions and the difference increases once we move to higher dimensions or consider larger proposal variances. That large proposal variance would affect the performance of RWM is intuitively clear, because in this case getting an outlying observation in any of the d co-ordinates becomes more likely.

An interesting observation from Table 1 is that even for 2 dimensions, our acceptance ratio corresponding to the optimal scaling of 2.4 is very close to 0.44 and it remains close to the optimal value for all the dimensions considered. It is interesting to note that 0.44 is also the (non-asymptotic) optimal acceptance rate of RWM for one-dimensional proposals in certain settings obtained by minimizing the first order auto-correlation of the RWM algorithm; see [Roberts and Rosenthal \(2001\)](#), [Roberts and Rosenthal \(2009\)](#). Since in one dimension additive TMCMC is equivalent to RWM and because the former is effectively a one-dimensional algorithm irrespective of the actual dimensionality, this perhaps intuitively suggests that for TMCMC, the optimal acceptance rate will remain very close to 0.44 irrespective of dimensionality. For RWM however, the optimal acceptance rate is quite far from 0.234 for smaller dimensions. From the asymptotics perspective (setting aside the above argument regarding TMCMC being effectively one-dimensional for any actual dimension), this demonstrates that convergence to the diffusion equation occurs at a much faster rate in TMCMC as compared to RWM. Hence, even in smaller dimensions a TMCMC user can tune the proposal to achieve approximately 44% acceptance rate. Indeed, in low dimensions the tuning exercise is far more easier than in higher dimensions.

When the scale is changed from the optimum value 2.4 to the sub-optimal value 6, we witness very significant drop in the acceptance rates of RWM. Particularly for dimensions $d = 100$ and $d = 200$ the acceptance rate of RWM falls off very sharply and becomes almost negligible. In

keeping with the discussion presented in Sections S-3 and S-4 of the supplement this indicates how difficult it can be in the case of general, high-dimensional target distributions, to adjust the RWM proposal to achieve the acceptance rates between 15% and 50%, as suggested by [Roberts and Rosenthal \(2001\)](#). On the other hand, for any dimension, the acceptance rate of TMCMC remains more than 20%, indicating it is a lot more easier and safer to tune the TMCMC proposal.

The measure IACT is uniformly higher for TMCMC for all dimensions when the optimal scale is considered. This is to be expected since the maximum diffusion speed is higher for RWM, and IACT decreases as diffusion speed increases. However, when the scale is sub-optimal, IACT of TMCMC is uniformly lower than that of RWM in all dimensions. This is in accordance with the discussion on the lack of robustness of RWM and the relative robust behaviour of the diffusion speed of TMCMC with respect to scale changes, presented in Sections S-3 and S-4 of the supplement. Indeed, the sub-optimal scale choice causes the diffusion speed of RWM to drop sharply, increasing the integrated autocorrelation in the process. On the other hand, the diffusion speed of TMCMC remains relatively more stable, thus not allowing IACT to increase significantly.

Although in the lower dimensions IPACT is slightly higher for TMCMC than for RWM, in dimensions 10, 100 and 200, it is slightly lesser for TMCMC when the scale is suboptimal (for $d = 200$ IPACT is almost the same for both the algorithms in the sub-optimal case).

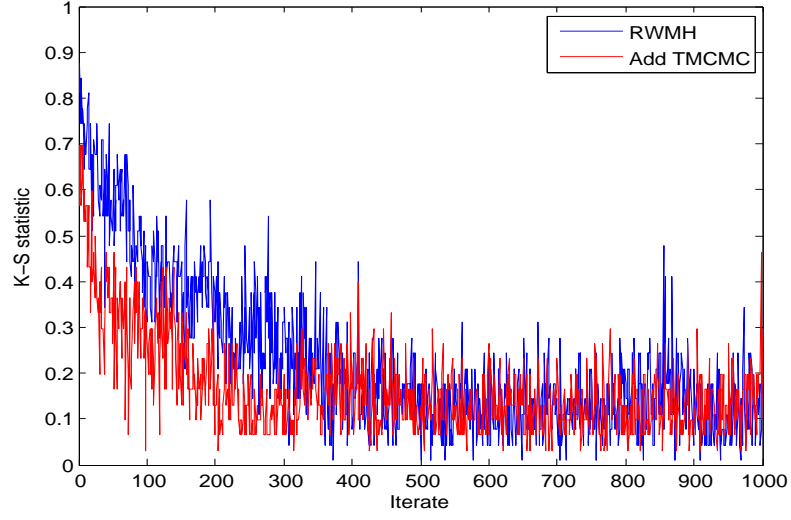
The average jump size, AJS, is uniformly somewhat larger for RWM compared to TMCMC when the scale is optimally chosen. However, for the sub-optimal scaling, AJS for TMCMC is significantly larger than those for RWM for dimensions $d = 5, 10, 100, 200$. Since in general sub-optimal scaling is to be expected, as per the discussions in Sections S-3 and S-4 of the supplement, one can expect better exploration (in terms of AJS) of the general, high-dimensional target density, by additive TMCMC.

For dimensions $d = 100$ and $d = 200$, the average K-S distance is smaller for TMCMC with respect to both optimal and sub-optimal scales. Moreover, for the sub-optimal scale, the K-S distance is uniformly smaller for TMCMC for all the dimensions considered. Furthermore, note that for the sub-optimal scale, as the dimension increases, the difference between the average K-S distances of RWM and TMCMC also increases. This suggests that at least when the scale is sub-optimal, TMCMC performs increasingly better than RWM in terms of better exploration of the target density, as dimension increases.

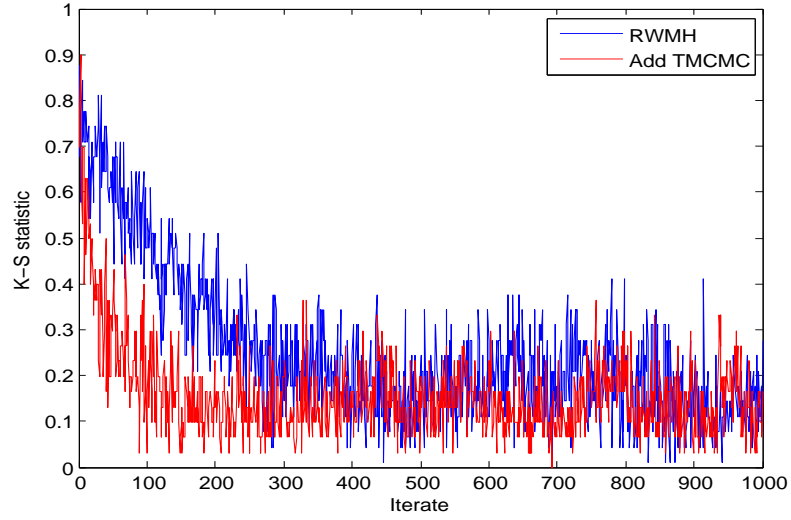
7.1.3 Visualizing the rate of convergence of TMCMC and RWM to the stationary distribution using Kolmogorov-Smirnov distance

Apart from measuring the performance of the chains after stationarity, one might be interested in visualizing how fast the chains converge to the target density starting from an initial value. In other words, it is of interest to know which of these chains have a steeper downward trend with respect to the other, when the respective optimal scales are used for both the algorithms. To investigate this empirically, we again use the K-S distance, plotting the distances with respect to the iteration number (time). Thus, while the average K-S distance, calculated after the burn-in, provides an overall measure of how well an MCMC algorithm explores the stationary distribution after convergence, a simple plot of the K-S distances with respect to time can help visualize the rate of convergence of the MCMC algorithm to stationarity.

For smaller dimensions like 2 and 10, we did not perceive much difference between the two chains in terms of the plots of the K-S distance. But for higher dimensions, we observed a significant improvement in convergence for our TMCMC method in comparison with that of RWM. Two instances, for dimensions $d = 30$ and $d = 100$, are presented in Figures 7 and 8, respectively.

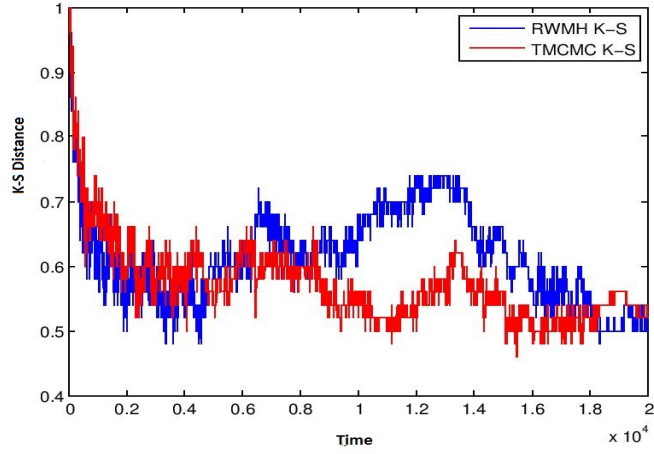


(a) $d = 30, \ell = 2.4$.

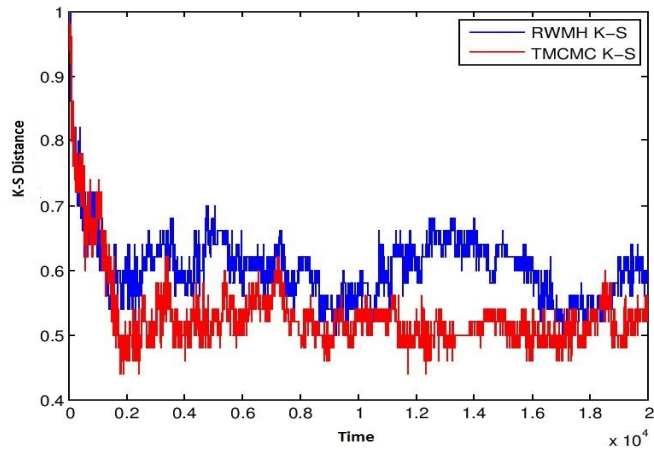


(b) $d = 30, \ell = 6$.

Figure 7: K-S distance comparison before burn-in between the RWM and the TCMC chains for dimension $d = 30$.



(a) $d = 100$, $\ell = 2.4$.



(b) $d = 100$, $\ell = 6$.

Figure 8: K-S distance comparison before burn-in between the RWM and the TMCMC chains for dimension $d = 100$.

7.2 Comparisons between additive TMCMC and RWM in the independent, but non-identical set-up

We now compare additive TMCMC with RWM under an instance of independent, but non-identical situation provided in [Bedard \(2008a\)](#). In particular, we assume the target distribution to have independent normal components with all the means zero, and variances given by $\theta^{-2}(d) = (d^{-1/5}, d^{-1/5}, 3, d^{-0.5}, 3, d^{-0.5}, \dots, 3, d^{-0.5})$. For our purpose, we set $d = 50$ and implement 30 chains each for additive TMCMC and RWM, each chain run for 10,000 iterations. For any given iteration, and for both TMCMC and RWM, we then compute the K-S distances based on the 30 chains, which are then compared.

Note that $\theta^{-2}(d)$ consists of three forms of co-ordinates, namely, $\theta^{-2}(d) = 3$, $\theta^{-2}(d) = d^{-0.5}$, and $\theta^{-2}(d) = d^{-1/5}$. These are associated with three distinct marginal target densities. In the figures below, for these three distinct marginals, we separately compare TMCMC and RWM using K-S distances. That is, Figures 9, 10 and 11 compare TMCMC and RWM when $\theta^{-2}(d) = 3$, $\theta^{-2}(d) = d^{-0.5}$, and $\theta^{-2}(d) = d^{-1/5}$, respectively.

All the three instances, Figures 9, 10 and 11, clearly demonstrate the superiority of additive TMCMC over RWM.

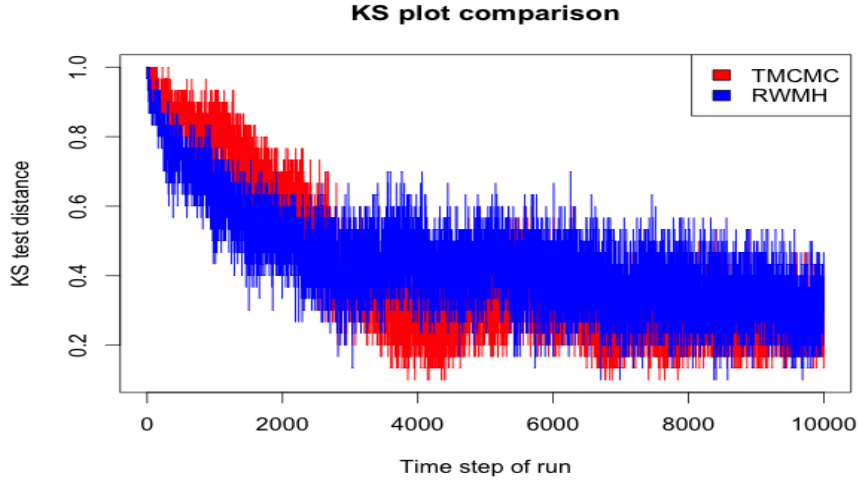


Figure 9: Independent but non-identical case: K-S comparisons between additive TMCMC and RWM for $\theta^{-2}(d) = 3$.

7.3 Comparisons between additive TMCMC and RWM in the dependent set-up

We now compare additive TMCMC and RWM in the dependent set-up, as (46). That is, here we consider target densities of the type

$$\pi_d(x_d) = \exp(-x_d^T M_d x_d) \prod_{i=1}^d \frac{1}{\lambda_i} \phi\left(\frac{x_i}{\lambda_i}\right).$$

For our purpose, we consider the following forms of $\lambda = (\lambda_1, \dots, \lambda_d)$ and M_d :

$$\lambda = \alpha \left(1, \frac{1}{d}, \frac{1}{d^2}, \dots, \frac{1}{d^d}\right),$$

and

$$M_d = \gamma(1 - \rho)\mathbf{I}_d + \rho \mathbf{1}_d \mathbf{1}_d^T,$$

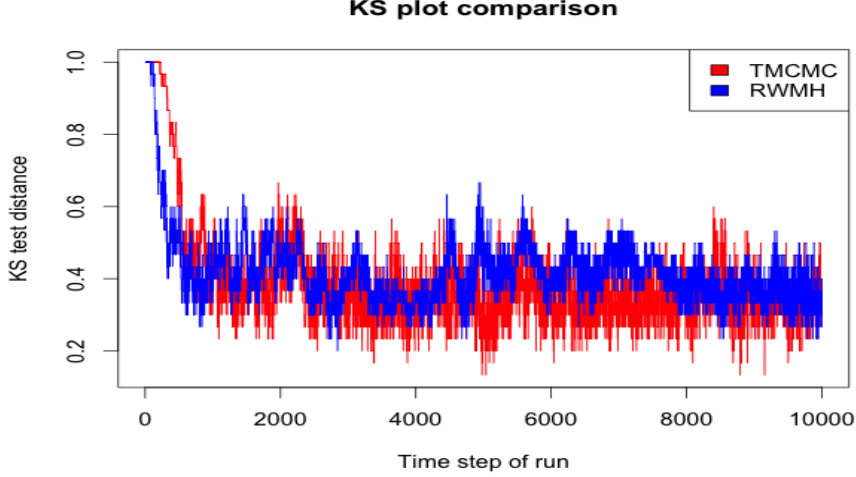


Figure 10: Independent but non-identical case: K-S comparisons between additive TMCMC and RWM for $\theta^{-2}(d) = d^{-0.5}$.

where \mathbf{I}_d is the identity matrix of order d and $\mathbf{1}_d$ is the d -component vector with all elements 1. We report the results of our experiments with three set-ups: (a) $\rho = 0.3$, $\alpha = 0.1$, $\gamma = 100$; (b) $\rho = 0.3$, $\alpha = 0.01$, $\gamma = 100$, and (c) $\rho = 0.3$, $\alpha = 0.01$, $\gamma = 1000$. The corresponding K-S based comparisons are provided in Figures 12, 13 and 14. In all the three experiments TMCMC very convincingly outperforms RWM. With various other choices of ρ , α and γ we observed similar results (not reported due to lack of space).

7.4 Discussion on simulation studies with multivariate Cauchy and multivariate t as target densities

We have so far restricted ourselves to comparisons between TMCMC and RWM when the target distribution is Gaussian (*iid*, independent but non-identical, and dependent). However, Dey and Bhattacharya (2015b) conduct comparative studies between the two algorithms when the targets are multivariate Cauchy and multivariate t . Briefly, they compare the algorithms with respect to K-S distance, when the location vectors and scale matrices are $\boldsymbol{\mu} = \mathbf{0}_d$ and $\boldsymbol{\Sigma} = \text{diag}\{0.71'_d\} + 0.31_d \mathbf{1}'_d$, respectively, where $\mathbf{0}_d$ is a d -dimensional vector with all elements 0. For multivariate t , they choose $\nu = 10$ degrees of freedom. For both RWMH and additive TMCMC they consider the scale of the proposal distribution to be 2.4, and illustrate the methods for dimension $d = 50$.

In fact, they compare the performances of RWM and additive TMCMC by two methods. In one method, since the above-mentioned target densities are not in the super-exponential family (see Dey and Bhattacharya (2015b) and the references therein), they transform them to superexponential distributions using a diffeomorphism proposed by Johnson and Geyer (2012), obtain samples from the transformed target densities using RWM and TMCMC, and then give inverse transformations to the simulated values so that they finally represent the original multivariate Cauchy and multivariate t . The other method is direct application of the algorithms to the original targets. In other words, Dey and Bhattacharya (2015b) also apply RWM and TMCMC directly to multivariate Cauchy and multivariate t , without resorting to diffeomorphism, and compare their performances. However, they also note that there are substantial gains with respect to mixing properties in the diffeomorphism based approach.

In either case, Dey and Bhattacharya (2015b) demonstrate that additive TMCMC outperforms RWM quite significantly in the case of the dependent, high-dimensional target densities. They even compare their performances in the case of *iid* Cauchy and t (with $\nu = 10$ degrees of

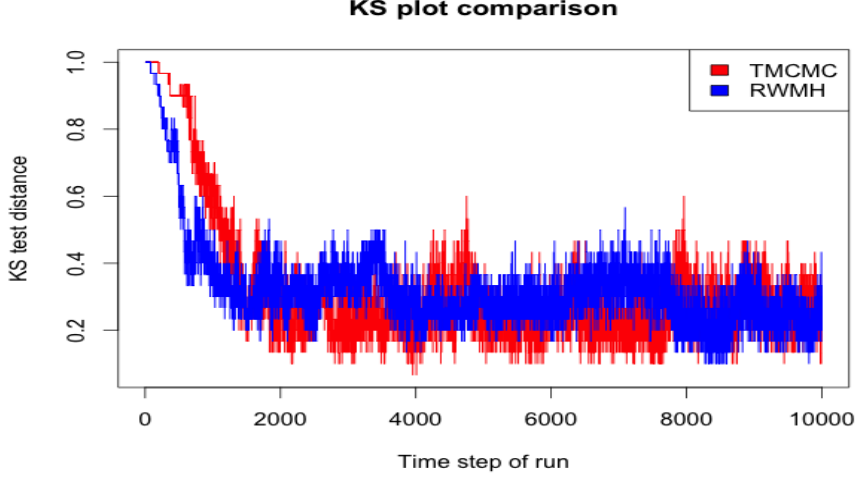


Figure 11: Independent but non-identical case: K-S comparisons between additive TCMC and RWM for $\theta^{-2}(d) = d^{-\frac{1}{5}}$.

freedom) distributions and reach the same conclusions.

8 Comparison of additive TCMC and RWM in the case of a real, spatial data set

We now compare additive TCMC and RWM with respect to a real, spatial dataset on radionuclide count data on Rongelap Island, analysed by [Diggle *et al.* \(1998\)](#) using a Bayesian hierarchical spatial model. This dataset and the model has been used subsequently by [Christensen \(2006\)](#) and [Dutta and Bhattacharya \(2014\)](#), to evaluate performances of Metropolis-Hastings and TCMC algorithms, respectively.

8.1 Model and prior specification

For $i = 1, \dots, 157$, [Diggle *et al.* \(1998\)](#) model the radionuclide count data as

$$Y_i \sim \text{Poisson}(M_i),$$

where

$$M_i = t_i \exp\{\beta + S(\mathbf{x}_i)\};$$

t_i is the duration of observation at location \mathbf{x}_i , β is an unknown parameter and $S(\cdot)$ is a zero-mean Gaussian process with isotropic covariance function of the form

$$\text{Cov}(S(\mathbf{z}_1), S(\mathbf{z}_2)) = \sigma^2 \exp\{-(\alpha \|\mathbf{z}_1 - \mathbf{z}_2\|)^\delta\}$$

for any two locations $\mathbf{z}_1, \mathbf{z}_2$. In the above, $\|\cdot\|$ denotes the Euclidean distance between two locations, and $(\sigma^2, \alpha, \delta)$ are unknown parameters. Following [Christensen \(2006\)](#) we set $\delta = 1$, and assume uniform priors on the entire parameter space corresponding to $(\beta, \log(\sigma^2), \log(\alpha))$. Thus, there are 160 parameters to be updated in each iteration of additive TCMC and RWM.

8.2 Optimal scaling

Note that the likelihood times the prior in this case can be approximately expressed as (46), that is, although the Poisson likelihood is expressible in the form $\exp(-\Psi^d(x^d))$, the Gaussian

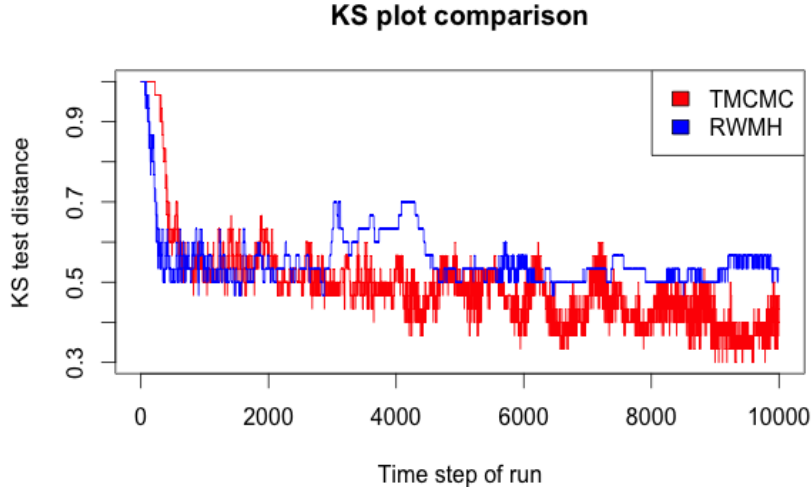


Figure 12: Dependent case: K-S comparisons between additive TCMC and RWM for $\rho = 0.3$, $\alpha = 0.1$, $\gamma = 100$.

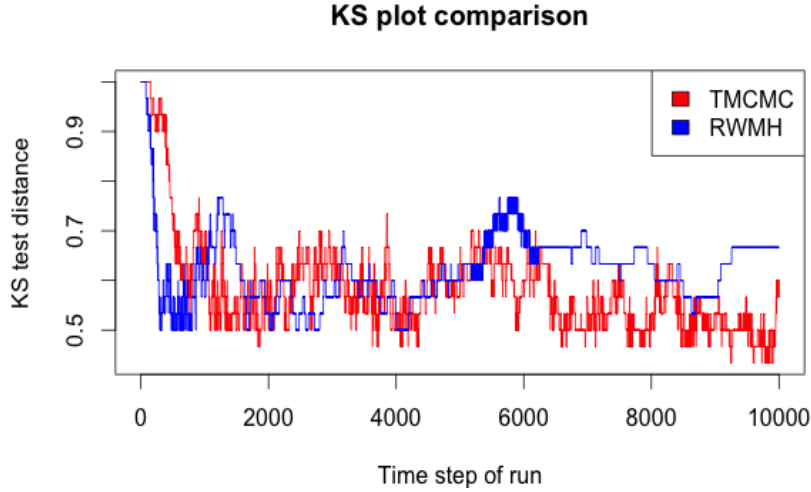


Figure 13: Dependent case: K-S comparisons between additive TCMC and RWM for $\rho = 0.3$, $\alpha = 0.01$, $\gamma = 100$.

process prior for $S(\cdot)$ does not of course admit the form $\prod_{i=1}^d \frac{1}{\lambda_i} \phi\left(\frac{x_i}{\lambda_i}\right)$ because of its dependence structure. Hence, this is an instance of a target density which does not fall within the class of densities for which optimal scaling theory has been developed. As is recommended in general cases, one may attempt tuning the parameters to approximately achieve the optimal acceptance rate. But this is a difficult task because of the large dimensionality, as already discussed. A far more important cause for concern is that, even if one succeeds in approximating the optimal acceptance rate, the corresponding scales will generally still be sub-optimal, because of the existence of many solutions such that the optimal acceptance rate holds. Indeed, we devise a method for approximately obtaining the optimal acceptance rates, but show that the corresponding scales lead to really poor performance of RWM, while thanks to the robustness property of additive TCMC, the latter yields much reasonable performance. Details follow.

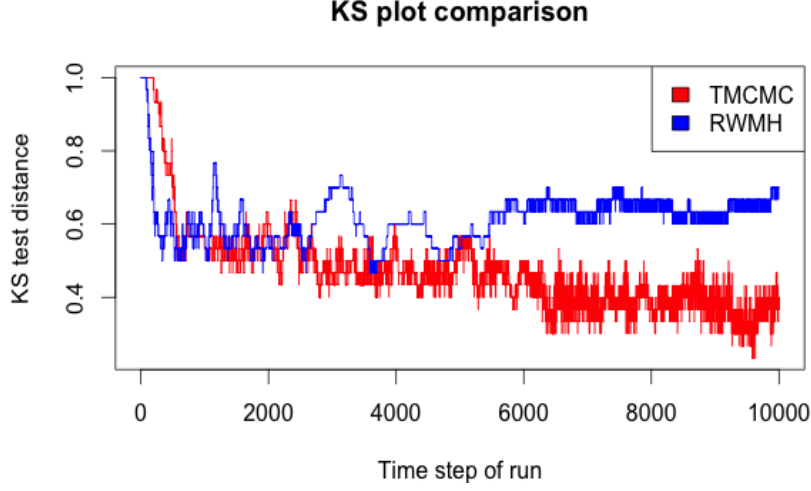


Figure 14: Dependent case: K-S comparisons between additive TCMC and RWM for $\rho = 0.3$, $\alpha = 0.01$, $\gamma = 1000$.

8.2.1 Pilot TCMC for facilitating approximate optimal scaling

We first consider a pilot TCMC run consisting of 11×10^6 iterations, with the same TCMC algorithm used by [Dutta and Bhattacharya \(2014\)](#). In other words, for the pilot run we draw $\epsilon \sim N(0, 1)\mathbb{I}(\epsilon > 0)$, and consider the following additive transformations:

$$\begin{aligned} T(\beta, \epsilon) &= \beta \pm 2\epsilon, \\ T(\log(\sigma^2), \epsilon) &= \log(\sigma^2) \pm 5\epsilon, \\ T(\log(\alpha), \epsilon) &= \log(\alpha) \pm 5\epsilon, \\ T(S(\mathbf{x}_i), \epsilon) &= S(\mathbf{x}_i) \pm 2\epsilon; \text{ for } i = 1, \dots, 157, \end{aligned}$$

where “+” and “−” occur with probability 1/2 each.

After discarding the first 10^6 iterations as burn-in, we then store one TCMC sample in every 100 iterations to yield 10^5 thinned TCMC realizations. With these stored realizations, we then obtain the empirical variance-covariance matrix of the 160 unknowns and store the 160 eigenvalues of the matrix.

8.2.2 Approximately optimal acceptance rates of additive TCMC and RWM using the stored eigenvalues

For $i = 1, \dots, 160$, letting θ_i denote the unknowns, and λ_i , the corresponding eigenvalues, we then consider the following additive transformations for TCMC:

$$T(\theta_i, \epsilon) = \theta_i \pm c_{TCMC} \sqrt{\frac{2\lambda_i \ell_{opt, TCMC}^2}{d}} \epsilon,$$

where $\epsilon \sim N(0, 1)\mathbb{I}(\epsilon > 0)$, “+” and “−” occur with probability 1/2 each, $\ell_{opt, TCMC} = 1.715$ (see (72)), and c_{TCMC} is a tuning parameter for adjusting the acceptance rate to about 44%. It turned out, after setting $c_{TCMC} = 0.16$, that the empirical acceptance rate obtained from a TCMC run of length 6×10^7 , after discarding the first 10^7 iterations as burn-in, is approximately 0.435. Implementing this TCMC algorithm, we store one in every 100 realizations after the burn-in to obtain 5×10^5 thinned additive TCMC realizations from the posterior distribution.

For RWM, we consider the following proposal:

$$T(\theta_i, \epsilon_i) = \theta_i + c_{RWM} \sqrt{\frac{2\lambda_i \ell_{opt,RWM}^2}{d}} \epsilon_i,$$

where $\epsilon \stackrel{iid}{\sim} N(0, 1)$, $\ell_{opt,RWM} = 1.715$, and $c_{RWM} = 0.3$. We obtain the empirical acceptance rate from a RWM run of length 6×10^7 , after discarding the first 10^7 iterations as burn-in, as approximately 0.227. We implement this RWM algorithm, storing one in every 100 realizations after the burn-in to obtain 5×10^5 thinned RWM realizations from the posterior.

8.3 Results of comparison

Figures 15 and 16 show the trace plots of the stored realizations obtained by TMCMC and RWM, respectively, after a further thinning of size 50 (note that we apply this thinning only to reduce the sizes of the figure files). It is quite interesting to observe that the TMCMC-based trace plots do not show evidence of non-convergence, while the RWM-based trace plots seem to exhibit severe non-convergence problems. The visual evidences remain intact for the trace plots obtained for 5×10^5 stored samples. It is clear that, unlike TMCMC, an extremely large sample size is required for RWM to attain proper convergence.

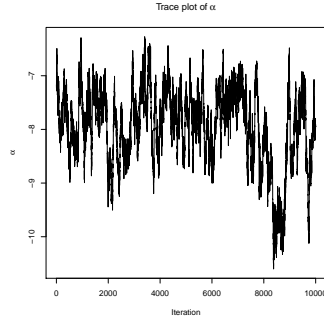
Figure 17 compares the autocorrelations of the stored 5×10^5 realizations generated by TMCMC and RWM. Panels (b), (d), (e) and (f), but particularly panels (d) and (e), show that the TMCMC based autocorrelations are very significantly smaller compared to those based on RWM, demonstrating much faster mixing of TMCMC for these parameters. Since scaling is directly related to autocorrelation (see Sections S-3 and S-4 of the supplement), it is clear that poor scaling of RWM in comparison with additive TMCMC is the reason for the relatively poor performance of the former. Indeed, even though we could approximately achieve the desired acceptance rates, there are many solutions for the scales, given the same acceptance rate; in fact, selecting reasonable scales gets increasingly difficult with increasing dimensions. Thus, it is highly unlikely that the chosen scales are even reasonable in this high-dimensional example, for either TMCMC or RWM. As a result it makes sense to conclude with respect to the autocorrelations that, in this real data study, sensitivity of RWM with respect to optimal scales is the reason for its poor performance, while robustness of TMCMC in this regard is the reason for its quite reasonable performance.

For the other panels of Figure 17, although TMCMC does not seem to outperform in terms of autocorrelations, the trace plots of Figures 15 and 16 hold out a much clearer picture, showing that even though the autocorrelations are comparable, TMCMC marches off to convergence much faster than RWM, exploiting its more localized move types thanks to a single ϵ . Indeed, unlike TMCMC, RWM, composed of 160 ϵ_i 's in this example, is prone to require many more iterations to return to any given set with positive posterior probability, once it leaves it.

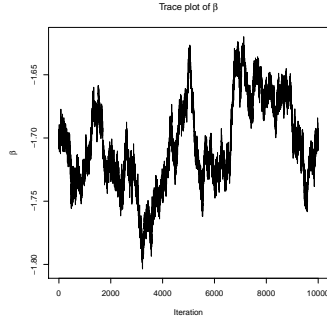
Thus, in this real data example, additive TMCMC very clearly and very convincingly outperforms RWM.

9 Conclusion

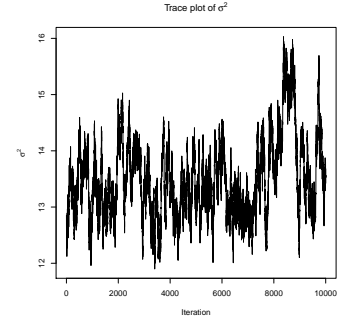
Overall, our assessment is that TMCMC is clearly advantageous compared to RWM from various perspectives. It has significantly less computational complexity and the acceptance rate corresponding to the optimal scaling for TMCMC (0.439) is almost twice that of RWM (0.234). Although the maximum diffusion speed of RWM is somewhat higher than that of additive TMCMC, the latter is much more robust with respect to mis-specifications of the scales. The advantages of such robustness are spelt out in the discussions in Sections S-3 and



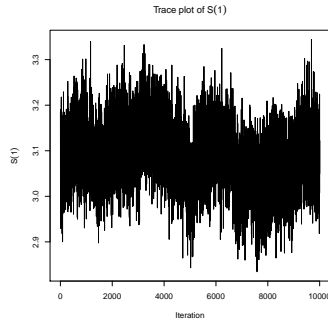
(a) Trace plot of α .



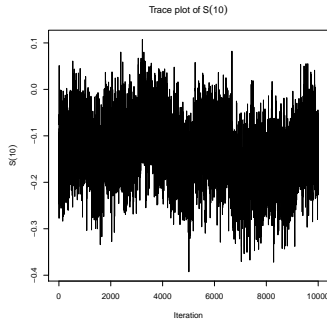
(b) Trace plot of β .



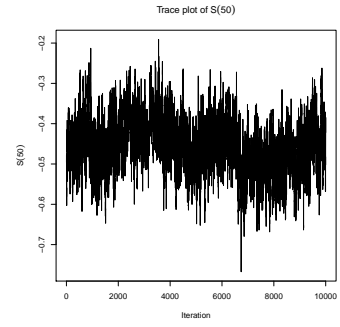
(c) Trace plot of σ^2 .



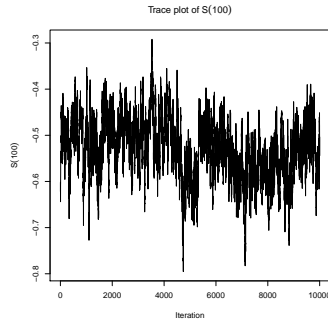
(d) Trace plot of $S(\mathbf{x}_1)$.



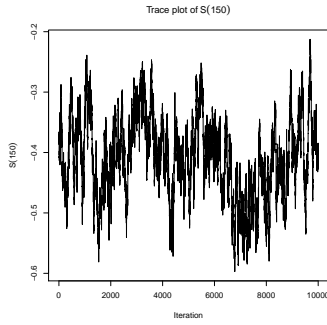
(e) Trace plot of $S(\mathbf{x}_{10})$.



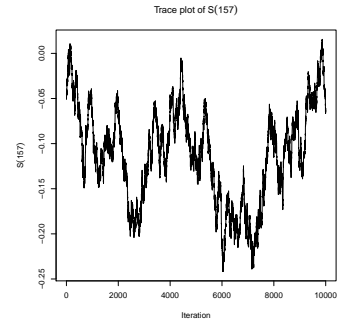
(f) Trace plot of $S(\mathbf{x}_{50})$.



(g) Trace plot of $S(\mathbf{x}_{100})$.

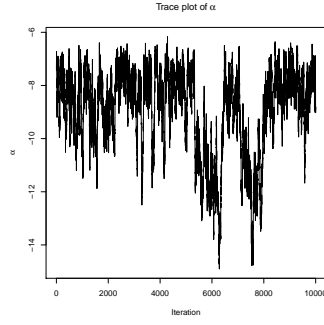


(h) Trace plot of $S(\mathbf{x}_{150})$.

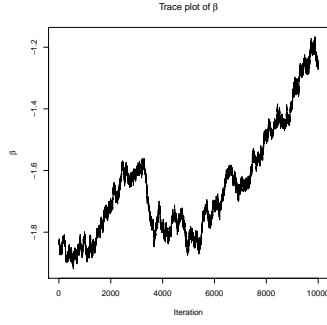


(i) Trace plot of $S(\mathbf{x}_{157})$.

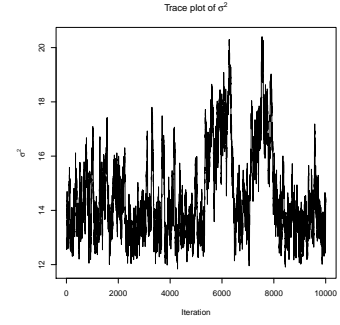
Figure 15: Rongelap island data: TMCMC based trace plots.



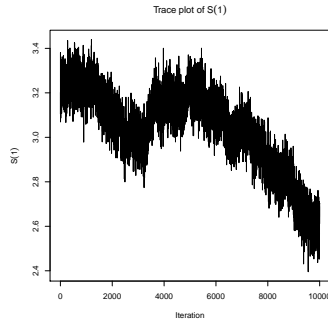
(a) Trace plot of α .



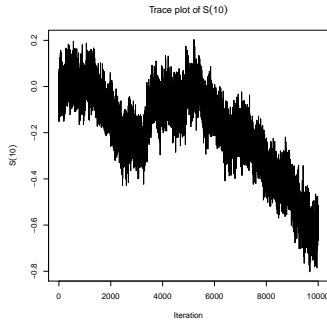
(b) Trace plot of β .



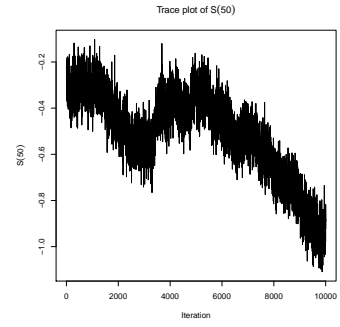
(c) Trace plot of σ^2 .



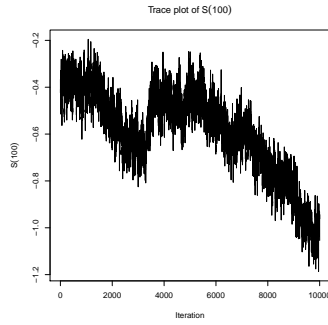
(d) Trace plot of $S(\mathbf{x}_1)$.



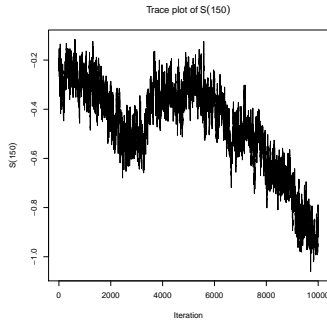
(e) Trace plot of $S(\mathbf{x}_{10})$.



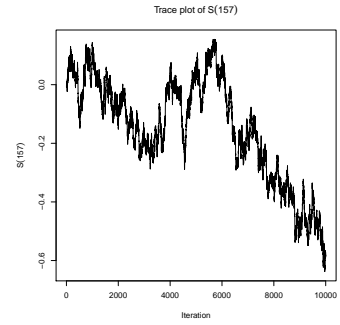
(f) Trace plot of $S(\mathbf{x}_{50})$.



(g) Trace plot of $S(\mathbf{x}_{100})$.

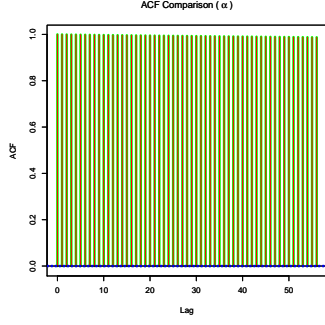


(h) Trace plot of $S(\mathbf{x}_{150})$.

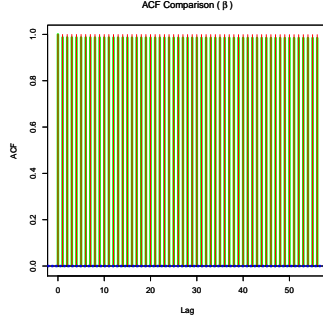


(i) Trace plot of $S(\mathbf{x}_{157})$.

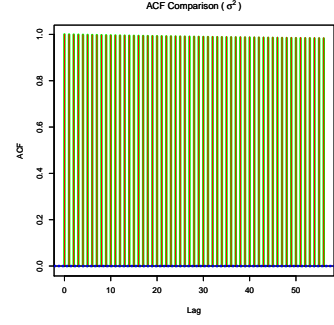
Figure 16: Rongelap island data: RWM based trace plots.



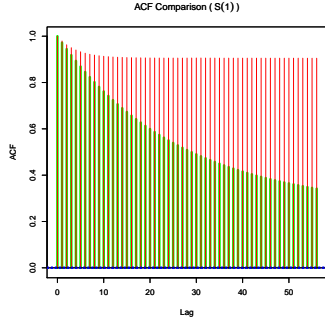
(a) ACF comparison for α .



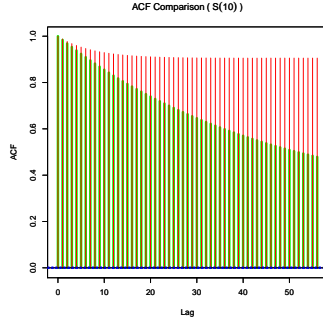
(b) ACF comparison for β .



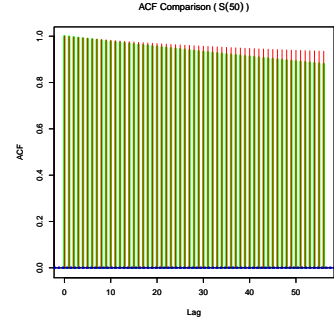
(c) ACF comparison for σ^2 .



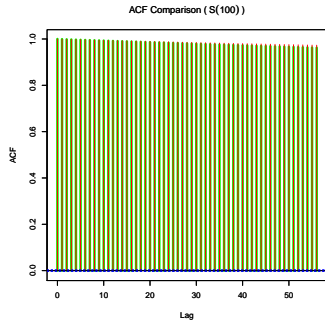
(d) ACF comparison for $S(\mathbf{x}_1)$.



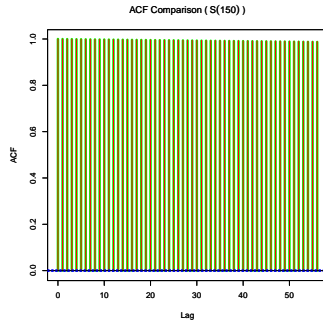
(e) ACF comparison for $S(\mathbf{x}_{10})$.



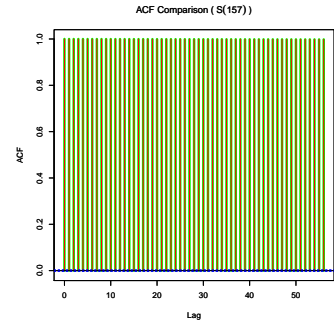
(f) ACF comparison for $S(\mathbf{x}_{50})$.



(g) ACF comparison for $S(\mathbf{x}_{100})$.



(h) ACF comparison for $S(\mathbf{x}_{150})$.



(i) ACF comparison for $S(\mathbf{x}_{157})$.

Figure 17: Rongelap island data: Comparisons of the ACF's based on TMCMC and RWM. The TMCMC-based ACF's are depicted by the green colour and the red colour is associated with RWM-based ACF's.

S-4 of the supplement. Our simulation studies reported in Section 7 and Table 1, and the real data analysis in Section 8, clearly vindicate these discussions.

Related to the discussions on robustness and the difficulty of choosing proper scalings in high dimensions is also the issue of increasing computational complexity, particularly in the Bayesian paradigm. Note that complex, high-dimensional posteriors routinely arise in Bayesian applications. It is extremely uncommon among MCMC practitioners to use the RWM algorithm for updating all the parameters in a single block associated with any significantly high-dimensional posterior arising from any complex Bayesian application. We presume that the extreme difficulty of determining proper scalings in practice prevent the researchers from using the RWM as an algorithm for updating all the parameters in a single block. Indeed, as we demonstrated with our simulation study reported in Table 1, mis-specification even in the case of the simple target distribution being a product of *iid* normal densities, leads to acceptance rates that are almost zero. In the context of the real data study in Section 8 we proposed a method for approximately obtaining the presumed optimal acceptance rates, and which appears to be generally applicable, but as we demonstrated, RWM failed to exhibit even reasonable performance. Adaptive strategies may be thought of as alternative methods, but these are yet to gain enough popularity among applied MCMC practitioners; moreover, as we mention in Section S-5 of the supplement, extremely long runs may be necessary to reach adequate acceptance rates for adaptive RWM, which may be prohibitive in very high dimensions, for example, when the acceptance ratio involves high-dimensional matrix inversions at every iteration, such as in our spatial example.

The aforementioned difficulties force the researchers to use RWM to *sequentially* update the parameters, either singly, or in small blocks. Since one (or just a few) parameters are updated at a time by RWM, the acceptance rate can be controlled at each stage of the sequential updating procedure. However, this sequential procedure also requires computation of the acceptance ratio as many times as every small block is updated in a sequence. If each parameter is updated singly (that is, each small block consists of only one element), then the computational complexity increases d -folds compared to the procedure where all the d parameters are updated in a single block. Thus, when d is large, the computation can become prohibitively slow.

On the other hand, TCMCMC is designed to update all the parameters in a single block in such a way that the acceptance rate remains reasonable in spite of the high dimensionality and complexity of the target distribution. Our simulation studies and real data example in Section 8 show that mis-specification of the scales do not have drastic effect on the efficiency of additive TCMCMC, thanks to its robustness property. As a result, with much less effort compared to that required for RWM, we can achieve reasonable scalings that ensure adequate performance of additive TCMCMC, so that resorting to sequential updating will not be necessary.

This also implies that unlike RWM, additive TCMCMC can save enormous computational effort when the dimension d is large. Finally, adaptive TCMCMC may be of much value in very high dimensions because of its quick convergence to the correct optimal acceptance rate, and for ensuring good performance. The details will be covered in [Dey and Bhattacharya \(2015a\)](#).

Our empirical findings reported in this article with respect to the simulation studies pertaining to *iid*, independent but non-identical, as well as dependent cases clearly point towards supremacy of TCMCMC over RWM. Quite importantly, in the real, spatial data example, TCMCMC outperformed RWM very significantly. Indeed, even though we could tune the scales so as to achieve approximately the respective optimal acceptance rates, the chosen scales need not be actually optimal, for either of TCMCMC and RWM. Here RWM performs miserably because of its non-robustness with respect to the scales, while TCMCMC sails through thanks to its remarkably robust nature with respect to the choice of scales. Thus, all our experiments, particularly, the challenging real data example, lead us to clearly recommend TCMCMC in general situations.

Given the importance of the general TCMCMC idea, we have decided to create a software

for its general usage. In this regard, we have now made available an R package **tmcmcR** for implementing TMCMC along with its adaptive versions at the Github page

<https://github.com/kkdey/tmcmcR>.

The software will be continuously updated in accordance with further developments of TMCMC; moreover, TTMCMC, the variable-dimensional version of TMCMC, will also be incorporated, and kept updated.

Acknowledgment

We are sincerely grateful to the two reviewers for very encouraging and constructive comments which helped substantially improve the quality of our manuscript.

Supplementary Material

Throughout, we refer to our main manuscript [Dey and Bhattacharya \(2015c\)](#) as DB.

S-1 Computational efficiency of TMCMC

It may seem that TMCMC is computationally more expensive because we are randomly generating $d + 1$ many values $(\epsilon, b_1, b_2, \dots, b_d)$ whereas in RWM, we are generating d many random variables $(\epsilon_1, \epsilon_2, \dots, \epsilon_d)$ where $\epsilon \sim N(0, \frac{\ell^2}{d})I_{\{\epsilon > 0\}}$ and $\epsilon_i \sim N(0, \frac{\ell^2}{d}) \forall i = 1, 2, \dots, d$. However generating b_i is equivalent to simple tosses of a fair coin which is a much easier exercise compared to drawing a set of independent normal random variables required by RWM. As a vindication of this, we obtain the average computation time (in seconds) of 100,00,00 iterations with RWM and TMCMC algorithms across dimensions 2 to 100, averaged over 100 replications of 100,00,00 iterations for each dimension, when the d -dimensional target density is a product of d standard normals. The codes are written in C and implemented in an ordinary 32-bit laptop. The results of our experiment are displayed in Figure S-1. Figure S-2 displays the computation times of RWM and TMCMC with respect to a single replication of the 100,00,00 iterations. In both the diagrams, TMCMC is seen to take significantly less computational time compared to the RWM algorithm, particularly in higher dimensions. Much longer runs, particularly in very high dimensions, would see TMCMC saving very substantial amount of computational time in comparison with RWM. For further discussion on computational gains of TMCMC over RWM, see Section 9 of DB.

It must be emphasized that the proposal density for ϵ in TMCMC can be any distribution on the positive support. Similarly, the RWM algorithm also does not require the proposal to be normal. However, the optimal scaling results for RWM inherently assume normality and for the sake of comparison, we have also restricted our focus on $\epsilon \sim N(0, \frac{\ell^2}{d})I_{\{\epsilon > 0\}}$ in the subsequent sections.

S-2 Details on the need for optimal scaling of additive TMCMC

We first try to impress the fact that too small or too large values of ℓ can both lead to poor performance of the chain and it is this trade-off that draws our interest in finding an optimal value of ℓ . If the value of ℓ or equivalently, the proposal variance, is large, then the probability of a move falling in low density regions (with respect to the target density) of the space increases as the moves $(x_1 + b_1\epsilon, \dots, x_d + b_d\epsilon)$ are likely to be quite far apart from (x_1, \dots, x_d) . This leads to smaller values of the ratio $\frac{\pi(x_1 + b_1\epsilon, \dots, x_d + b_d\epsilon)}{\pi(x_1, \dots, x_d)}$ and thus lower acceptance rates. In fact, for high dimensions, this acceptance rate can be quite low for even moderately large values of

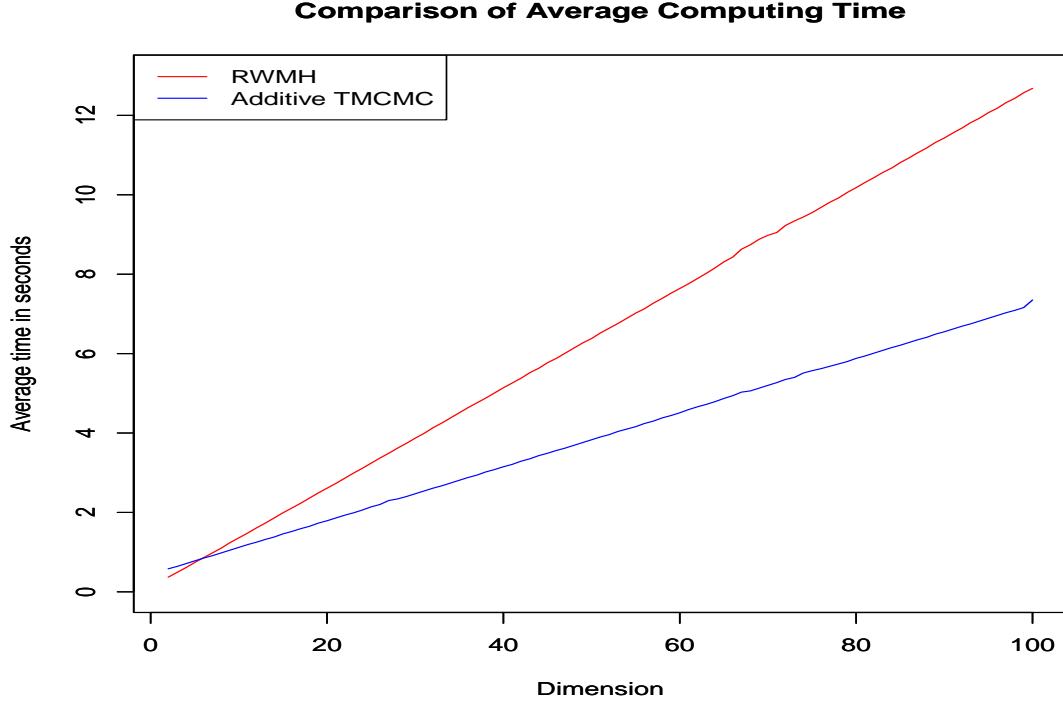


Figure S-1: Average computation time (in seconds) of 100,00,00 iterations with RWM and TMCMC algorithms corresponding to dimensions varying from 2 to 100. TMCMC takes significantly less computation time compared to RWM, particularly in higher dimensions. The codes are written in C and implemented on an ordinary 32-bit laptop.

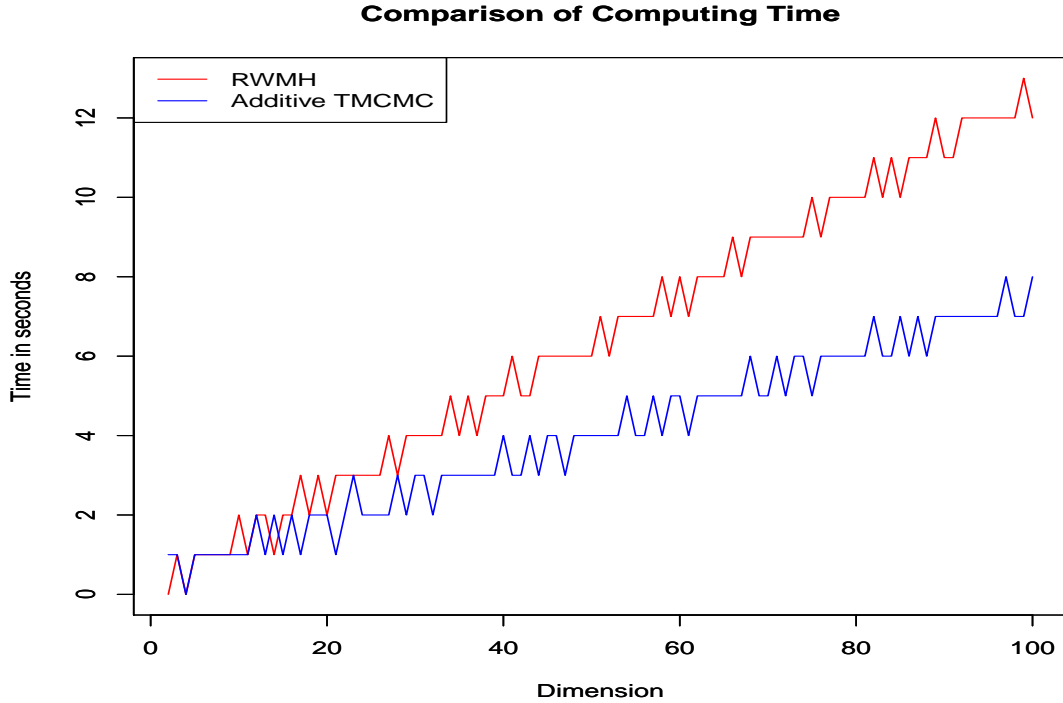
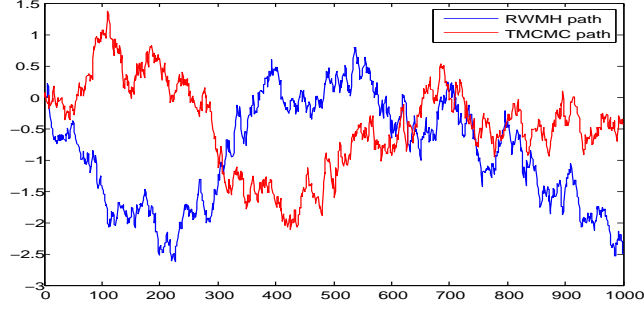
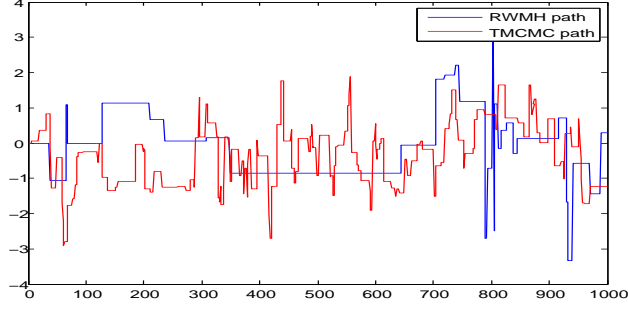


Figure S-2: Computation time (in seconds) of 100,00,00 iterations with RWM and TMCMC algorithms corresponding to dimensions varying from 2 to 100. TMCMC takes significantly less computation time compared to RWM, particularly in higher dimensions. The codes are written in C and implemented on an ordinary 32-bit laptop.



(a) Sample paths of RWM and additive TCMC for small proposal variance.



(b) Sample paths of RWM and additive TCMC for large proposal variance.

Figure S-3: Comparison of RWM and additive TCMC sample paths for small and large values of the proposal variance. The target density is $N(0,1)$, the standard normal distribution.

ℓ . On the other hand, if the value of ℓ is too small, then the acceptance rate will be higher but we then have to compromise in terms of exploration of the space. Much of our moves will lie very close to the initial point and as a result, the chain will move very slowly. An instance of the movement of the RWM and additive TCMC chain for significantly small and large values of ℓ are depicted in Figure S-3 assuming that the target distribution is standard normal. For small values of ℓ , the fact that the chain moves slowly gets reflected in the autocorrelation factor (ACF) of the chain, which would be on the higher side (Figure S-4). All these motivate us to find an optimal value of ℓ that would take care of these problems. Our approach would be to derive the diffusion process approximation of the additive TCMC process in the limit as $d \rightarrow \infty$ and then we maximize the diffusion speed or the rate of change of variance of the chain in the limit. Intuitively, if the scale factor ℓ is small, then starting from a point X_t at time t , the moves corresponding to adjacent time points X_{t+h} are quite close and so the limiting change of variation is quite small for the corresponding diffusion process. If on the other hand the scale factor ℓ is large, the chain hardly moves, and hence X_{t+h} for sufficiently small h are often same as X_t , thereby leading to lower value of diffusion speed. On optimizing the diffusion speed for the TCMC chain, we obtain the optimal value of the acceptance rate to be 0.439. Panels (a), (b) and (c) of Figure S-5 depict the path of the TCMC chain for various choices of proposal variance, ranging from too small through the optimal value to quite large. Note that the target density is best approximated by the chain at optimal scaling. A better understanding of this is achieved by perceiving how well the histogram of observations obtained after running a chain up to a certain length of time, approximates the true density (panels (c), (d), (e) of Figure S-5).

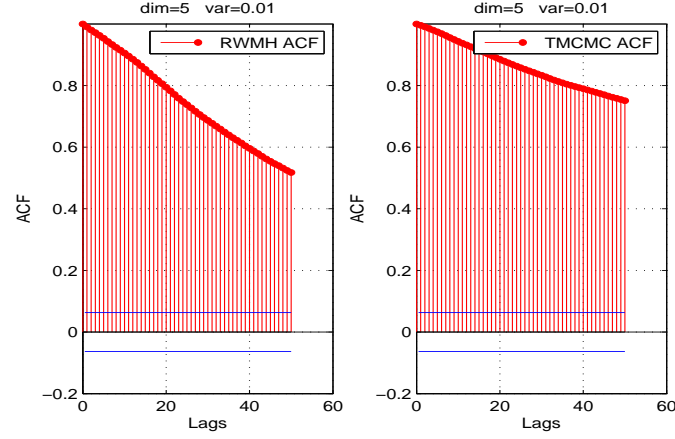


Figure S-4: ACFs of RWM and additive TMCMC for small proposal variance. The target density is $N(0, 1)$, the standard normal distribution.

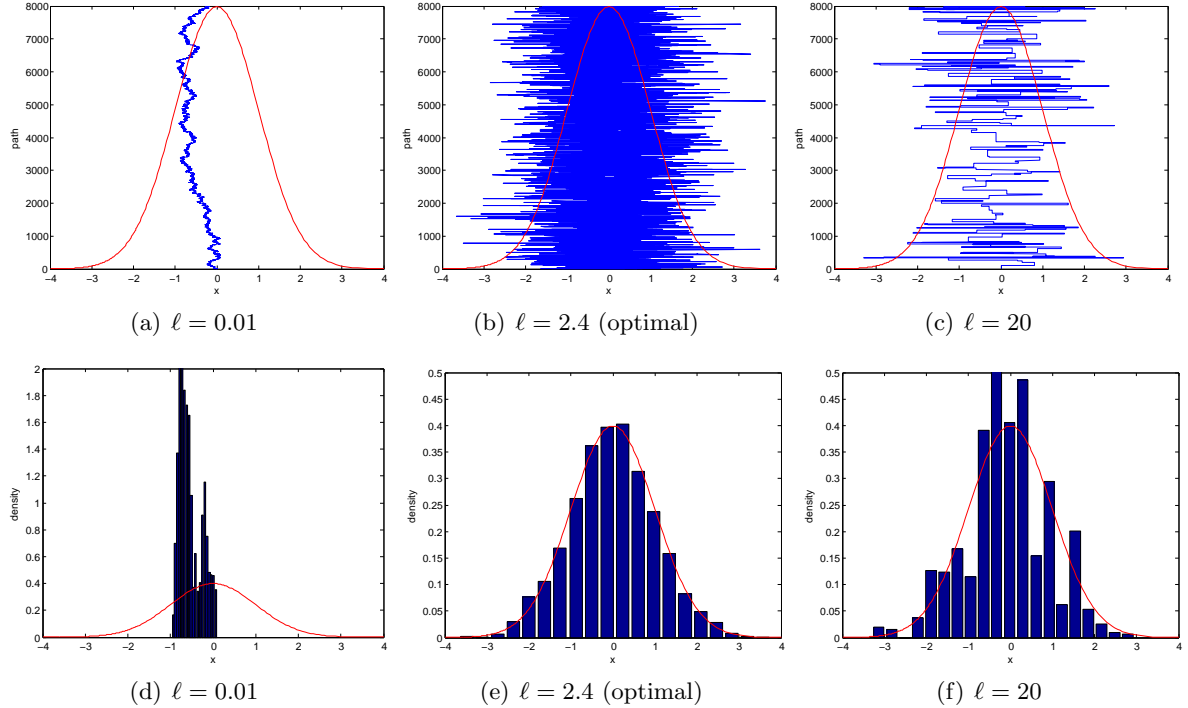


Figure S-5: The upper panels (a), (b) and (c) show the paths of TCMC chain for three various choices of scalings together with the target density $N(0, 1)$ plot. These highlight how well the paths explore the given target density. The lower panels (c), (d) and (e) display the histograms of the sample observations obtained from TCMC for these choices of scalings together with the target density $N(0, 1)$. These highlight how well the histograms approximate the target density for the given run of TCMC.

S-3 Discussion on consequences of non-robustness of RWM with respect to scale choices

For general, d -dimensional target distributions, RWM entails the proposal with transitions of the form $(x_1, \dots, x_d) \rightarrow (x_1 + \frac{\ell_1}{\sqrt{d}}\epsilon_1, \dots, x_d + \frac{\ell_d}{\sqrt{d}}\epsilon_d)$, where, for $i = 1, \dots, d$, $\epsilon_i \sim N(0, 1)$, and ℓ_i are constants to be chosen appropriately. Often ℓ_i may be of the form ℓa_i , where a_i may be needed to determine appropriately in addition to ℓ . As instance of this form occurs in the dependent set-up of [Mattingly et al. \(2011\)](#), but a_i in that set-up are the square roots of the eigenvalues of the Gaussian measure with independent components that is assumed to dominate the target density. However, in practice such assumption of independent Gaussian components will generally not hold, and hence it is far from straightforward to determine a_i appropriately in realistic cases.

Since all the set-ups considered so far yield the optimal acceptance rate 0.234 for RWM, it may be anticipated that the result holds quite generally, and applied MCMC practitioners may be advised to tune (ℓ_1, \dots, ℓ_d) such that the acceptance rate is close to 0.234. In fact, using a measure of efficiency which is the reciprocal of integrated autocorrelation time, [Roberts and Rosenthal \(2001\)](#) demonstrate that the RWM proposal may be tuned to achieve an acceptance rate between 0.15 to 0.5, which would make the algorithm around 80% efficient. However, for large dimension d , appropriate tuning of so many scale parameters seems to be an extremely arduous task. In our simulations presented in Section 8 of DB we observe that even in the simple situation where the target density is an *iid* product of normal densities, when the dimension increases, particularly when $d = 100$ and $d = 200$, departure from the optimal scale results in drastic fall in acceptance rates, far below what is prescribed by [Roberts and Rosenthal \(2001\)](#); see Table 1 of DB. The diffusion speeds under such mis-specifications tend to be quite low because of non-robustness with respect to scale choice (see Figures 1 – 6 of DB). Since low diffusion speed is equivalent to high autocorrelation (see equation (18) of [Roberts and Rosenthal \(2001\)](#)), the efficiency measures of [Roberts and Rosenthal \(2001\)](#) that use integrated autocorrelation, are also expected to indicate less efficiency. Thus, in summary manually tuning the RWM proposals appropriately in more general and complicated situations and in high dimensions seems to be a very daunting task. There are methods for automatically and adaptively tuning the scales to progress towards the desired optimal acceptance rate as number of iterations increases, but as we discuss in Section S-5 computationally this can be a very costly exercise in high dimensions.

S-4 Discussion on possible advantages of additive TMCMC for relatively more robust behaviour with respect to scale choices

Our results on optimal scaling offers the following general thumb rule to the users of additive TMCMC: tune the additive TMCMC proposal to achieve approximately 44% acceptance rate. Note that even though the optimal acceptance rate of additive TMCMC is significantly higher than that of RWM, both the algorithms have approximately the same optimal scalings that maximize the diffusion speeds (see Figures 1 – 6).

The results of our simulation studies reported in Table 1 of DB demonstrate that even in dimension as low as $d = 2$, our optimal acceptance rate 0.439 is remarkably accurate. The table further demonstrates that even if the scale of additive TMCMC is sub-optimally chosen, the acceptance rates remain higher than 20% for all dimensions, whereas for the same sub-optimal scale choice the acceptance rate of RWM falls to about 0.33% in high dimensions. Figures 1 – 6 show that around the optimal scale, the diffusion speeds of additive TMCMC under various set-ups do not change significantly. Using the relationship between diffusion speed and the measure of efficiency proposed by [Roberts and Rosenthal \(2001\)](#) one can conclude that unlike RWM,

the efficiency of additive TMCMC is not substantially affected by sub-optimal scale choices. Hence, tuning the additive TMCMC proposal is a far more safe and easy exercise compared to that of RWM. It seems to us that this is quite an advantage of additive TMCMC over RWM in general, high-dimensional set-ups. As we discuss in Section S-5 adaptive methods can be employed to approach the exact optimal acceptance rate 0.439 in substantially less number of iterations compared to adaptive RWM, facilitating huge computational gain over the latter.

S-5 Discussion on adaptive versions of RWM and additive TMCMC for enforcing optimal acceptance rates in complex, high-dimensional problems

Adaptive MCMC methods (see, for example, Roberts and Rosenthal (2009) and the references therein) are designed to combat the difficulty of determining appropriate proposal scalings. In the context of RWM, various adaptive strategies are presented in Roberts and Rosenthal (2009) to choose the scalings in an adaptive manner so that the optimal acceptance rate 0.234 is achieved in the long run. Dey and Bhattacharya (2015a) adopted the strategies in the case of additive TMCMC and made a detailed comparison with the corresponding adaptive RWM methods. In particular, they found that even after a very large number of iterations most of the the adaptive methods related to RWM yielded acceptance rates which are significantly different from 0.234, while the adaptive TMCMC algorithms very quickly yielded acceptance rates reasonably close 0.439, even in dimensions as low as $d = 2$. This implies quite substantial savings of TMCMC in terms of computation time in comparison with RWM. Performance wise as well, the results of Dey and Bhattacharya (2015a) favour adaptive TMCMC over adaptive RWM in high dimensions, with respect to the various measures which we also employ in this current work.

S-6 Proofs of optimal scaling results of additive TMCMC

S-6.1 Proof of Theorem 3.1 of DB

Proof. For our purpose, we define the discrete time generator of the TMCMC approach, as

$$G_d V(x) = \frac{d}{2^d} \sum_{\left\{ \begin{array}{l} b_i \in \{-1, +1\} \\ \forall i = 1, \dots, d \end{array} \right\}} \int_0^\infty \left[\left(V(x_1 + b_1\epsilon, \dots, x_d + b_d\epsilon) - V(x_1, \dots, x_d) \right) \times \left(\min \left\{ 1, \frac{\pi(x_1 + b_1\epsilon, \dots, x_d + b_d\epsilon)}{\pi(x_1, x_2, \dots, x_d)} \right\} \right) \right] q(\epsilon) d\epsilon. \quad (81)$$

Since by our assumption $(\log f)'$ is Lipschitz, in the above equation we may assume that V belongs to the space of infinitely differentiable functions with compact support (see, for example, Bedard (2007) for further details).

The Skorohod topology allows us to treat G_d as a continuous time generator that has jumps at the rate d^{-1} . Given our restricted focus on a one dimensional component of the actual process, we assume V to be a function of the first co-ordinate only. Under this assumption, the generator defined in (81) is a function of only ϵ and b_1 , and can be rephrased as

$$\begin{aligned}
G_d V(x) &= \frac{d}{2} \int_0^\infty \sum_{b_1 \in \{-1, +1\}} \left[\left(V(x_1 + b_1 \epsilon) - V(x_1) \right) \right. \\
&\quad \left. \times E_{b_2, \dots, b_d} \left(\min \left\{ 1, \frac{\pi(x_1 + b_1 \epsilon, \dots, x_d + b_d \epsilon)}{\pi(x_1, \dots, x_d)} \right\} \right) \right] q(\epsilon) d\epsilon,
\end{aligned} \tag{82}$$

where E_{b_2, \dots, b_d} is the expectation taken conditional on b_1 and ϵ .

First we show that the quantity $G_d V(x)$ is a bounded quantity.

$$\begin{aligned}
G_d V(x) &\leq d E_{\{b_1, \epsilon\}} [V(x_1 + b_1 \epsilon) - V(x_1)] \\
&= d V'(x_1) E_{\{b_1, \epsilon\}}(b_1 \epsilon) + \frac{d}{2} V''(x_1^*) E_{\{b_1, \epsilon\}}(\epsilon^2) \\
&\leq \ell^2 K,
\end{aligned} \tag{83}$$

where x_1^* lies between x_1 and $x_1 + b_1 \epsilon$ and K is the maximum value of V'' .

Note that

$$\begin{aligned}
&E_{b_2, \dots, b_d} \left[\min \left\{ 1, \frac{\pi(x_1 + b_1 \epsilon, \dots, x_d + b_d \epsilon)}{\pi(x_1, \dots, x_d)} \right\} \right] \\
&= E_{b_2, \dots, b_d} \left[\min \left\{ 1, \exp \left(\log(f(x_1 + b_1 \epsilon)) - \log(f(x_1)) \right) \right. \right. \\
&\quad \left. \left. + \sum_{j=2}^d \left\{ b_j \epsilon \{\log(f(x_j))\}' + \frac{\epsilon^2}{2!} \{\log(f(x_j))\}'' + \frac{b_j \epsilon^3}{3!} \{\log(f(x_j))\}''' + \frac{\epsilon^4}{4!} \{\log(f(x_j))\}'''' \right\} \right\} \right] \Bigg],
\end{aligned} \tag{84}$$

where E_{b_2, \dots, b_d} denotes expectation with respect to b_2, \dots, b_d , holding ϵ, b_1, x_1, x_j and z_j ($j = 2, \dots, d$) fixed; and for $j = 2, \dots, d$, z_j lies between x_j and $x_j + b_j \epsilon$. Since $b_j; j = 2, \dots, d$ are *iid*, as $d \rightarrow \infty$, conditional on ϵ, b_1, x_1, x_j and z_j ($j = 2, \dots, d$) one can apply Lyapunov's central limit theorem.

Writing $\zeta_j = b_j \left[\epsilon \{\log(f(x_j))\}' + \frac{\epsilon^3}{6} \{\log(f(x_j))\}''' \right]$, we note that conditional on ϵ and x_j , $E_{b_j}(\zeta_j) = 0$ and $Var_{b_j}(\zeta_j) = \left[\epsilon \{\log(f(x_j))\}' + \frac{\epsilon^3}{6} \{\log(f(x_j))\}''' \right]^2$. Viewing $b_j \epsilon$ as $b_j \epsilon^* \frac{\ell}{\sqrt{d}}$, where $\epsilon^* \sim N(0, 1) I_{\{\epsilon^* > 0\}}$, we next show that, almost surely with respect to π ,

$$\frac{\sum_{j=2}^d E_{b_j}(|\zeta_j|^\delta)}{\left\{ \sqrt{\sum_{j=2}^d Var_{b_j}(\zeta_j)} \right\}^\delta} \rightarrow 0,$$

for $\delta = 4$.

First note that $\epsilon \equiv \epsilon^* \frac{\ell}{\sqrt{d}}$, where $\epsilon^* \sim N(0, 1) I_{\{\epsilon^* > 0\}}$, and so, for any $\zeta > 0$,

$$\sum_{d=1}^\infty P \left(\epsilon^* \frac{\ell}{\sqrt{d}} > \zeta \right) < \left(\frac{\ell}{\zeta} \right)^4 E \left(\epsilon^{*4} \right) \sum_{d=1}^\infty \frac{1}{d^2} < \infty. \tag{85}$$

That is, $\epsilon \equiv \epsilon^* \frac{\ell}{\sqrt{d}} \xrightarrow{a.s.} 0$, *a.s.* denoting “almost surely”. Thus, there exists a null set \mathcal{N}_ϵ

(with respect to the distribution of ϵ^*) such that for all $\omega_\epsilon \in \mathcal{N}_\epsilon^c$, $\epsilon \equiv \epsilon^*(\omega_\epsilon) \frac{\ell}{\sqrt{d}} \rightarrow 0$, as $d \rightarrow \infty$. Now observe that, for any given $\omega_\epsilon \in \mathcal{N}_\epsilon^c$, as $d \rightarrow \infty$, $\frac{1}{d-1} \sum_{j=2}^d E_{b_j}(|\zeta_j|^\delta) = \frac{1}{d-1} \sum_{j=2}^d \left[\epsilon \{\log(f(x_j))\}' + \frac{\epsilon^3}{6} \{\log(f(x_j))\}''' \right]^4 \xrightarrow{a.s.} E_{x_2} \left[\epsilon \{\log(f(x_2))\}' + \frac{\epsilon^3}{6} \{\log(f(x_2))\}''' \right]^4$, by the strong law of large numbers (SLLN). The expectation, which is with respect to x_2 , is clearly finite, due to the assumptions (13), (14), (15) of DB and the Cauchy-Schwartz inequality. In other words, given $\omega_\epsilon \in \mathcal{N}_\epsilon^c$, there exists a null set \mathcal{N}_1 (with respect to f) such that for all $\omega \in \mathcal{N}_1^c$, the convergence takes place deterministically. Also,

$$\begin{aligned} \frac{1}{d-1} \sum_{j=2}^d \text{Var}_{b_j}(\zeta_j) &= \frac{1}{d-1} \sum_{j=2}^d \left[\epsilon \{\log(f(x_j))\}' + \frac{\epsilon^3}{6} \{\log(f(x_j))\}''' \right]^2 \\ &\xrightarrow{a.s.} E_{x_2} \left[\epsilon \{\log(f(x_2))\}' + \frac{\epsilon^3}{6} \{\log(f(x_2))\}''' \right]^2, \end{aligned}$$

which is again finite, thanks to (13), (14) and (15) of DB, and the Cauchy-Schwartz inequality. Let \mathcal{N}_2 denote the null set (with respect to f) such that deterministic convergence takes place for all $\omega \in \mathcal{N}_2^c$. Let $\mathbb{N}_1 = \mathcal{N}_\epsilon \otimes \mathcal{N}_1 \cup \mathcal{N}_\epsilon \otimes \mathcal{N}_2$, where \otimes denotes cartesian product. Then \mathbb{N}_1 is a null set with respect to the distribution of ϵ and f . For $\omega \in \mathbb{N}_1^c$, we have, for $\delta = 4$, $\sum_{j=2}^d E_{b_j}(|\zeta_j|^\delta) = O(d)$, and $\sum_{j=2}^d \text{Var}_{b_j}(\zeta_j) = O(d)$. Hence, for $\delta = 4$, and for $\omega \in \mathbb{N}_1^c$, we have,

$$\frac{\sum_{j=2}^d E_{b_j}(|\zeta_j|^\delta)}{\left\{ \sqrt{\sum_{j=2}^d \text{Var}_{b_j}(\zeta_j)} \right\}^\delta} = O(d^{-1}) \rightarrow 0.$$

Thus, Lyapunov's central limit theorem applies, and we have the following:

$$\frac{\sum_{j=2}^d b_j \left[\epsilon \{\log(f(x_j))\}' + \frac{\epsilon^3}{6} \{\log(f(x_j))\}''' \right]}{\sqrt{\sum_{j=2}^d \left[\epsilon \{\log(f(x_j))\}' + \frac{\epsilon^3}{6} \{\log(f(x_j))\}''' \right]^2}} \xrightarrow{\mathcal{L}} N(0, 1), \quad (86)$$

for almost all ϵ and x_2, \dots, x_d . Also note that, the square of the denominator of (86) is given by

$$\sum_{j=2}^d \left[\epsilon \{\log(f(x_j))\}' + \frac{\epsilon^3}{6} \{\log(f(x_j))\}''' \right]^2 = \epsilon^2 \sum_{j=2}^d \left[\{\log(f(x_j))\}' \right]^2 + \Delta, \quad (87)$$

where

$$\Delta = \frac{\epsilon^4}{6} \sum_{j=2}^d 2 \{\log(f(x_j))\}' \{\log(f(x_j))\}''' + \frac{\epsilon^6}{36} \sum_{j=2}^d \left[\{\log(f(x_j))\}''' \right]^2. \quad (88)$$

With the representation $\epsilon \equiv \epsilon^* \frac{\ell}{\sqrt{d}}$, where $\epsilon^* \sim N(0, 1)I_{\{\epsilon^* > 0\}}$, for $\omega_\epsilon \in \mathcal{N}_\epsilon^c$, the first term of (87) is given by $\epsilon^{*2} \frac{\ell^2}{d} \sum_{j=2}^d \left[\{\log(f(x_j))\}' \right]^2$. As $d \rightarrow \infty$, by SLLN, there exists a null set \mathcal{N}_3 with respect to f such that for all $\omega \in \mathcal{N}_3^c$,

$$\frac{1}{d-1} \sum_{j=2}^d \left[\{\log(f(x_j))\}' \right]^2 = -\frac{1}{d-1} \sum_{j=2}^d \{\log(f(x_j))\}'' \rightarrow \mathbb{I},$$

where \mathbb{I} is the information matrix corresponding to the density f .

Also,

$$\Delta = \frac{\epsilon^{*4}\ell^4}{6d} \frac{1}{d} \sum_{j=2}^d 2 \{\log(f(x_j))\}' \{\log(f(x_j))\}''' + \frac{\epsilon^{*6}\ell^6}{36d^2} \frac{1}{d} \sum_{j=2}^d \left[\{\log(f(x_j))\}''' \right]^2 \xrightarrow{a.s.} 0,$$

since

$$\frac{1}{d} \sum_{j=2}^d 2 \{\log(f(x_j))\}' \{\log(f(x_j))\}''' \xrightarrow{a.s.} E_f \left[2 \{\log(f(x_2))\}' \{\log(f(x_2))\}''' \right] < \infty,$$

$$\frac{1}{d} \sum_{j=2}^d \left[\{\log(f(x_j))\}''' \right]^2 \xrightarrow{a.s.} E_f \left[\{\log(f(x_2))\}''' \right]^2 < \infty,$$

$\frac{\epsilon^{*4}}{d} \xrightarrow{a.s.} 0$, and $\frac{\epsilon^{*6}}{d^2} \xrightarrow{a.s.} 0$. Hence, there exists a null set \mathcal{N}_4 (with respect to f) such that for all $\omega \in \mathcal{N}_4^c$, $\Delta(\omega) \rightarrow 0$ as $d \rightarrow \infty$.

We now deal with the last term of (84) given by $\sum_{j=2}^d \frac{\epsilon^4}{4!} \{\log(f(z_j))\}''''$. This tends to zero almost surely as $d \rightarrow \infty$ because $\epsilon^4 \equiv \epsilon^{*4} \frac{\ell^4}{d} \xrightarrow{a.s.} 0$, and

$$\frac{1}{d} \sum_{j=2}^d \{\log(f(z_j))\}'''' \xrightarrow{a.s.} E_f \left(\{\log(f(z_2))\}'''' \right) < \infty,$$

by (16) of DB. Let \mathcal{N}_5 denote the null set associated with the above almost sure convergence.

Let $\mathbb{N}_2 = \mathcal{N}_\epsilon \otimes \mathcal{N}_3 \cup \mathcal{N}_\epsilon \otimes \mathcal{N}_4 \cup \mathcal{N}_\epsilon \otimes \mathcal{N}_5$. Further, let $\mathbb{N} = \mathbb{N}_1 \cup \mathbb{N}_2$. Then \mathbb{N} is a null set with respect to the distribution of ϵ^* and f . Hence, given any $\omega \in \mathbb{N}^c$,

$$\left| E_{b_2, \dots, b_d} \left[\min \left\{ 1, \frac{\pi(x_1 + b_1\epsilon, \dots, x_d + b_d\epsilon)}{\pi(x_1, \dots, x_d)} \right\} \right] - E_{b_2, \dots, b_d} [\min \{1, e^X\}] \right| \rightarrow 0, \text{ as } d \rightarrow \infty,$$

where

$$X \sim N \left(\eta(x_1, b_1, \epsilon) - \frac{(d-1)\epsilon^2}{2} \mathbb{I}, (d-1)\epsilon^2 \mathbb{I} \right), \quad (89)$$

with

$$\eta(x_1, b_1, \epsilon) = \log(f(x_1 + b_1\epsilon)) - \log(f(x_1)). \quad (90)$$

We now recall the following result (Proposition 2.4 of [Roberts et al. \(1997\)](#)): if $X \sim N(\mu, \sigma^2)$, then

$$E [\min \{1, e^X\}] = \Phi \left(\frac{\mu}{\sigma} \right) + e^{\left\{ \mu + \frac{\sigma^2}{2} \right\}} \Phi \left(-\sigma - \frac{\mu}{\sigma} \right),$$

where Φ is the standard Gaussian cumulative distribution function (cdf). Applying this result to (84) we obtain

$$\begin{aligned} & E_{b_2, \dots, b_d} \left[\min \left\{ 1, \frac{\pi(x_1 + b_1\epsilon, \dots, x_d + b_d\epsilon)}{\pi(x_1, \dots, x_d)} \right\} \right] \\ &= \Phi \left(\frac{\eta(x_1, b_1, \epsilon) - \frac{(d-1)\epsilon^2}{2} \mathbb{I}}{\sqrt{(d-1)\epsilon^2 \mathbb{I}}} \right) + e^{\eta(x_1, b_1, \epsilon)} \Phi \left(-\sqrt{(d-1)\epsilon^2 \mathbb{I}} - \frac{\eta(x_1, b_1, \epsilon) - \frac{(d-1)\epsilon^2}{2} \mathbb{I}}{\sqrt{(d-1)\epsilon^2 \mathbb{I}}} \right) \\ &= \mathbb{W}(b_1, \epsilon, x_1). \end{aligned} \quad (91)$$

Note that using Taylor series expansion around x_1 , we can write (90) as

$$\eta(x_1, b_1, \epsilon) = b_1 \epsilon [\log f(x_1)]' + \frac{\epsilon^2}{2} [\log f(x_1)]'' + b_1 \frac{\epsilon^3}{3!} [\log f(\xi_1)]''' , \quad (92)$$

where ξ_1 lies between x_1 and $x_1 + b_1 \epsilon$. Re-writing $b_1 \epsilon$ as $\frac{\ell}{\sqrt{d}} z_1^*$, where z_1^* follows a $N(0, 1)$ distribution, η and \mathbb{W} can be expressed in terms of ℓ and z_1^* as

$$\eta(x_1, z_1^*, d) = \frac{\ell z_1^*}{\sqrt{d}} [\log f(x_1)]' + \frac{\ell^2 z_1^{*2}}{2!d} [\log f(x_1)]'' + \frac{\ell^3 z_1^{*3}}{3!d^{\frac{3}{2}}} [\log f(\xi_1)]''' \quad (93)$$

and

$$\mathbb{W}(x_1, z_1^*, d) = \Phi \left(\frac{\eta(x_1, z_1^*, d) - \frac{z_1^{*2} \ell^2}{2} \mathbb{I}}{\sqrt{z_1^{*2} \ell^2 \mathbb{I}}} \right) + e^{\eta(x_1, z_1^*, d)} \Phi \left(\frac{-\eta(x_1, z_1^*, d) - \frac{z_1^{*2} \ell^2 \mathbb{I}}{2}}{\sqrt{z_1^{*2} \ell^2 \mathbb{I}}} \right). \quad (94)$$

Now we consider the Taylor series expansion around x_1 of the term

$$\begin{aligned} & dE_{z_1^*} \left[\left(V \left(x_1 + \frac{z_1^* \ell}{\sqrt{d}} \right) - V(x_1) \right) \mathbb{W}(z_1^*, x_1, d) \right] \\ &= dE_{z_1^*} \left[\left\{ V'(x_1) \frac{z_1^* \ell}{\sqrt{d}} + \frac{1}{2} V''(x_1) \frac{z_1^{*2} \ell^2}{d} + \frac{1}{6} V'''(\xi_1) \frac{z_1^{*3} \ell^3}{d^{\frac{3}{2}}} \right\} \mathbb{W}(z_1^*, x_1, d) \right]. \end{aligned} \quad (95)$$

From (94) it is clear that $\mathbb{W}(z_1^*, x_1, d)$ is continuous but not differentiable at the point 0. So, this can not be expanded as a Taylor series around 0. Also, note that \mathbb{W} is an almost surely bounded function with respect to d . This follows from the fact that Φ is a bounded function and that $\eta(x_1, z_1^*, d) \xrightarrow{a.s.} 0$ as $d \rightarrow \infty$. The latter is easily proved by showing, as in (85), that each term of $\eta(x_1, z_1^*, d)$ tends to zero almost surely; here we need to use the facts that $E_f [\{\log(f(x_1))\}']^4 < \infty$, $E_f [\{\log(f(x_1))\}'']^2 < \infty$ and $E_f [\{\log(f(\xi_1))\}'''] < \infty$ which follow from assumptions (13), (14) and (15) of DB. By expanding the individual terms in the expression in (94) we obtain, for appropriate w_1, w_2, ξ_1 , the following:

$$\begin{aligned} \Phi \left(\frac{\eta(x_1, z_1^*, d) - \frac{z_1^{*2} \ell^2}{2} \mathbb{I}}{\sqrt{z_1^{*2} \ell^2 \mathbb{I}}} \right) &= \Phi \left(-\frac{\sqrt{z_1^{*2} \ell^2 \mathbb{I}}}{2} \right) + \frac{1}{\sqrt{d\mathbb{I}}} [\log f(x_1)]' \phi \left(-\frac{\sqrt{z_1^{*2} \ell^2 \mathbb{I}}}{2} \right) + \frac{1}{2d\mathbb{I}} \phi'(w_1), \\ \Phi \left(\frac{-\eta(x_1, z_1^*, d) - \frac{z_1^{*2} \ell^2}{2} \mathbb{I}}{\sqrt{z_1^{*2} \ell^2 \mathbb{I}}} \right) &= \Phi \left(-\frac{\sqrt{z_1^{*2} \ell^2 \mathbb{I}}}{2} \right) - \frac{1}{\sqrt{d\mathbb{I}}} [\log f(x_1)]' \phi \left(-\frac{\sqrt{z_1^{*2} \ell^2 \mathbb{I}}}{2} \right) + \frac{1}{2d\mathbb{I}} \phi'(w_2), \\ e^{\eta(x_1, z_1^*, d)} &= 1 + \frac{\ell z_1^*}{\sqrt{d}} [\log f(x_1)]' + \frac{\ell^2 z_1^{*2}}{2!d} [\log f(x_1)]'' + \frac{\ell^3 z_1^{*3}}{3!d^{\frac{3}{2}}} [\log f(\xi_1)]''' . \end{aligned} \quad (96)$$

Using these expanded forms and then simplifying the expression in (95), we obtain the following form of $G_d V(x)$:

$$G_d V(x) = V'(x_1) \frac{1}{2} \ell^2 (\log f(x_1))' E_{z_1^*} [z_1^{*2} \mathcal{H}(z_1^*)] + \frac{1}{2} V''(x_1) \ell^2 E_{z_1^*} [z_1^{*2} \mathcal{H}(z_1^*)] + O(d^{-\frac{1}{2}}),$$

where

$$\mathcal{H}(z_1^*) = 2\Phi\left(-\frac{|z_1^*|\ell\sqrt{\mathbb{I}}}{2}\right) = 2\left[1 - \Phi\left(\frac{|z_1^*|\ell\sqrt{\mathbb{I}}}{2}\right)\right]. \quad (97)$$

Hence, the limiting form of our generator is Langevin and is given by

$$GV(x) = \frac{1}{2}g(\ell)(\log f(x_1))'V'(x_1) + \frac{g(\ell)}{2}V''(x_1), \quad (98)$$

where $g(\ell)$ is given by (18) of DB. Since $G_dV(x)$ and $V''(x_1)$ are bounded, and $G_dV(x)$ converges pointwise to $GV(x)$, Dominated Convergence Theorem implies that

$$\lim_{d \rightarrow \infty} E |G_dV(x) - GV(x)| \rightarrow 0.$$

□

S-6.2 Proof of Theorem 3.2 of DB

Proof. We can write down the generator $G_dV(x)$ as follows:

$$G_dV(x) = \frac{d}{2^d}P(\chi_1 = 1) \int_0^\infty \sum_{b_1 \in \{-1, +1\}} \left[\left(V(x_1 + b_1\epsilon) - V(x_1) \right) \right. \\ \left. \times E \left\{ \begin{array}{c} b_2, b_3, \dots, b_d, \\ \chi_2, \chi_3, \dots, \chi_d \end{array} \right\} \left(\min \left\{ 1, \frac{\pi(x_1 + b_1\epsilon, \dots, x_d + \chi_d b_d\epsilon)}{\pi(x_1, \dots, x_d)} \right\} \right) \right] q(\epsilon) d\epsilon. \quad (99)$$

Note that since V is a function of x_1 only, if χ_1 is equal to 0, then no transition takes place and $V(x_1 + \chi_1 b_1\epsilon) - V(x_1) = 0$, so that the value of the generator is 0. In other words, the part of the generator associated with $P(\chi_1 = 0)$ is zero, and hence does not feature in (99).

Since b_j and χ_j always occur as products, we have

$$E \left\{ \begin{array}{c} b_2, b_3, \dots, b_d, \\ \chi_2, \chi_3, \dots, \chi_d \end{array} \right\} = E_{\{b_2\chi_2, b_3\chi_3, \dots, b_d\chi_d\}} \quad (100)$$

Our approach to obtaining the diffusion limit in this problem will be similar to that in the previous problem, where all the components of x are updated simultaneously at every iteration of TCMCMC. Here we leave $(1 - c_d)(d - 1)$ terms unchanged at each step and sum over $c_d d$ many terms inside the exponential. We make a very vital assumption that $c_d \rightarrow c$, which forces $c_d(d - 1)$ to go to ∞ as $d \rightarrow \infty$. We apply Lyapunov's central limit theorem as before (again the Lyapunov assumption holds good for $\delta = 4$), to obtain, given any $\omega \in \mathbb{N}^c$,

$$\left| E_{b_2\chi_2, \dots, b_d\chi_d} \left[\min \left\{ 1, \frac{\pi(x_1 + b_1\epsilon, \dots, x_d + \chi_d b_d\epsilon)}{\pi(x_1, \dots, x_d)} \right\} \right] - E_{b_2\chi_d, \dots, b_d\chi_d} [\min \{1, e^X\}] \right| \rightarrow 0, \text{ as } d \rightarrow \infty,$$

where, using Lyapunov's theorem and the same techniques as before, we obtain

$$X \sim N \left(\eta(x_1, b_1, \epsilon) - \frac{(c_d d - 1)\epsilon^2}{2} \mathbb{I}, (c_d d - 1)\epsilon^2 \mathbb{I} \right). \quad (101)$$

Analogously, we define $\mathbb{W}(x_1, z_1^*, c_d, d)$ as the following

$$\mathbb{W}(x_1, z_1^*, c_d, d) = \Phi \left(\frac{\eta(x_1, z_1^*) - \frac{z_1^{*2} \ell^2 c_d \mathbb{I}}{2}}{\sqrt{z_1^{*2} \ell^2 c_d \mathbb{I}}} \right) + e^{\eta(x_1, z_1^*)} \Phi \left(\frac{-\eta(x_1, z_1^*) - \frac{z_1^{*2} \ell^2 c_d \mathbb{I}}{2}}{\sqrt{z_1^{*2} \ell^2 c_d \mathbb{I}}} \right). \quad (102)$$

Proceeding in the same way as in the previous case, we obtain

$$G_d V(x) = V'(x_1) \frac{1}{2} c_d \ell^2 E_{z_1^*} \left[z_1^{*2} \mathcal{H}(z_1^*, x_1, c_d, d) \right] + \frac{1}{2} V''(x_1) c_d \ell^2 E_{z_1^*} \left[z_1^{*2} \mathcal{H}(z_1^*, x_1, c_d, d) \right] + O\left(d^{-\frac{1}{2}}\right), \quad (103)$$

where

$$\mathcal{H}(z_1^*, x_1, c_d) = 2\Phi \left(-\frac{|z_1^*| \ell \sqrt{c_d \mathbb{I}}}{2} \right) = 2 \left[1 - \Phi \left(\frac{|z_1^*| \ell \sqrt{c_d \mathbb{I}}}{2} \right) \right]. \quad (104)$$

Finally, the limiting form of the generator in this case of partial updating based additive TMCMC turns out to be analogous to the previous case where all the components of x are updated simultaneously at every step. This is given by

$$GV(x) = \frac{1}{2} g_c(\ell) (\log f(x_1))' V'(x_1) + \frac{g_c(\ell)}{2} V''(x_1), \quad (105)$$

where the diffusion speed $g_c(\ell)$ is given by

$$g_c(\ell) = 4c\ell^2 \int_0^\infty u^2 \Phi \left(-\frac{u\ell\sqrt{c\mathbb{I}}}{2} \right) \phi(u) du. \quad (106)$$

As before, the Dominated Convergence Theorem implies that

$$\lim_{d \rightarrow \infty} E |G_d V(x) - GV(x)| \rightarrow 0.$$

□

S-6.3 Proof of Theorem 4.1 of DB

Proof. The generator function of the process can be written as

$$\begin{aligned} G_d V(x) &= \frac{d^\alpha}{2^d} \int_0^\infty \sum_{b_1 \in \{-1, +1\}} \left[\left(V(x_1 + b_1 \epsilon) - V(x_1) \right) \right. \\ &\quad \left. \times E_{b_2, \dots, b_d} \left(\min \left\{ 1, \frac{\pi(x_1 + b_1 \epsilon, \dots, x_d + b_d \epsilon)}{\pi(x_1, \dots, x_d)} \right\} \right) \right] q(\epsilon) d\epsilon, \end{aligned} \quad (107)$$

where

$$\begin{aligned}
& E_{b_2, \dots, b_d} \left[\min \left\{ 1, \frac{\pi(x_1 + b_1 \epsilon, \dots, x_d + b_d \epsilon)}{\pi(x_1, \dots, x_d)} \right\} \right] \\
&= E_{b_2, \dots, b_d} \left[\min \left\{ 1, \exp \left(\log(f(x_1 + b_1 \epsilon)) - \log(f(x_1)) \right) \right. \right. \\
&\quad + \sum_{j=2}^k \left\{ b_j \epsilon \{ \log(f(\theta_j(d)x_j)) \}' + \frac{\epsilon^2}{2!} \{ \log(f(\theta_j(d)x_j)) \}'' + \frac{b_j \epsilon^3}{3!} \{ \log(f(\theta_j(d)x_j)) \}''' \right. \\
&\quad \left. \left. + \frac{\epsilon^4}{4!} \{ \log(f(\theta_j(d)x_j)) \}'''' \right\} \right. \\
&\quad \left. + \sum_{j=k+1}^d \left\{ b_j \epsilon \{ \log(f(\theta_j(d)x_j)) \}' + \frac{\epsilon^2}{2!} \{ \log(f(\theta_j(d)x_j)) \}'' + \frac{b_j \epsilon^3}{3!} \{ \log(f(\theta_j(d)x_j)) \}''' \right. \right. \\
&\quad \left. \left. + \frac{\epsilon^4}{4!} \{ \log(f(\theta_j(d)x_j)) \}'''' \right\} \right) \right] \quad (108)
\end{aligned}$$

Note that since ϵ can be represented, as before, as $\frac{\ell z_1^*}{d^{\frac{\alpha}{2}}}$ (where we assume that $\alpha > 0$), and, due to assumptions (13), (14), (15) and (34) of DB, and because k is finite, it is easy to see that the first sum in the expression in (108) goes to 0 almost surely. Then, we apply Lyapunov's central limit theorem on b_j for $j = k+1, \dots, d$, which deals with infinitely many random variables as $d \rightarrow \infty$, and we obtain, for every fixed $\omega \in \mathbb{N}^c$, where \mathbb{N} is an appropriate null set as before,

$$\frac{\sum_{j=k+1}^d b_j \left[\epsilon \{ \log(f(\theta_j(d)x_j)) \}' + \frac{\epsilon^3}{6} \{ \log(f(\theta_j(d)x_j)) \}''' \right]}{\sqrt{\sum_{j=k+1}^d [\epsilon \{ \log(f(\theta_j(d)x_j)) \}' + \frac{\epsilon^3}{6} \{ \log(f(\theta_j(d)x_j)) \}''']^2}} \xrightarrow{L} N(0, 1). \quad (109)$$

The square of the denominator of (109) can be written as $\epsilon^2 \sum_{j=k+1}^d \left[\{ \log(f(\theta_j(d)x_j)) \}' \right]^2 + \Delta$, where

$$\Delta = \frac{\epsilon^4}{6} \sum_{j=k+1}^d 2 \{ \log(f(\theta_j(d)x_j)) \}' \{ \log(f(\theta_j(d)x_j)) \}''' + \frac{\epsilon^6}{36} \sum_{j=k+1}^d \left[\{ \log(f(\theta_j(d)x_j)) \}''' \right]^2. \quad (110)$$

Representing ϵ as $\frac{\ell z_1^*}{d^{\frac{\alpha}{2}}}$, it can be seen as before that $\Delta \xrightarrow{a.s.} 0$ as $d \rightarrow \infty$. Writing $u_j = \theta_j(d)x_j$, we have

$$\begin{aligned}
\epsilon^2 \sum_{j=k+1}^d \left[\{ \log(f(\theta_j(d)x_j)) \}' \right]^2 &= \sum_{i=1}^m \frac{\ell^2 z_1^{*2}}{d^\alpha} \theta_j^2(d) r(i, d) \left\{ \frac{1}{r(i, d)} \sum_{j=1}^{r(i, d)} \left(\frac{f'(u_j)}{f(u_j)} \right)^2 \right\} \\
&= \sum_{i=1}^m \frac{\ell^2 z_1^{*2} d^{\gamma_i} r(i, d)}{K_{k+i} d^\alpha} r(i, d) \left\{ \frac{1}{r(i, d)} \sum_{j=1}^{r(i, d)} \left(\frac{f'(u_j)}{f(u_j)} \right)^2 \right\} \quad (111)
\end{aligned}$$

As $d \rightarrow \infty$, almost surely,

$$\frac{1}{r(i, d)} \sum_{j=1}^{r(i, d)} \left(\frac{f'(u_j)}{f(u_j)} \right)^2 \rightarrow E \left[\left\{ \frac{f'(U)}{f(U)} \right\}^2 \right] = \mathbb{I}. \quad (112)$$

Hence, as $d \rightarrow \infty$, almost surely,

$$\epsilon^2 \sum_{j=k+1}^d \left[\{\log(f(\theta_j(d)x_j))\}' \right]^2 \rightarrow \ell^2 z_1^{*2} \xi^2 \mathbb{I}, \quad (113)$$

where

$$\xi^2 = \lim_{d \rightarrow \infty} \sum_{i=1}^m \frac{d^{\gamma_i} r(i, d)}{K_{k+i} d^\alpha}$$

is finite due to (34) of DB and the fact that m is finite. Also, as before, the fourth order terms involved in (108) go to zero almost surely. Hence, given any $\omega \in \mathbb{N}^c$,

$$\left| E_{b_2, \dots, b_d} \left[\min \left\{ 1, \frac{\pi(x_1 + b_1 \epsilon, \dots, x_d + b_d \epsilon)}{\pi(x_1, \dots, x_d)} \right\} \right] - E_{b_2, \dots, b_d} [\min \{1, e^X\}] \right| \rightarrow 0, \text{ as } d \rightarrow \infty,$$

where

$$X \sim N \left(\eta(x_1, b_1, \epsilon) - \frac{(d-1)\epsilon^2}{2} \xi^2 \mathbb{I}, (d-1)\epsilon^2 \xi^2 \mathbb{I} \right). \quad (114)$$

We then follow a similar approach as in the previous two cases to obtain

$$\mathbb{W}(z_1^*, x_1, d, \xi) = \Phi \left(\frac{\eta(x_1, z_1^*, d) - \frac{z_1^{*2} \ell^2 \xi^2}{2} \mathbb{I}}{\sqrt{z_1^{*2} \ell^2 \xi^2 \mathbb{I}}} \right) + e^{\eta(x_1, z_1^*)} \Phi \left(\frac{-\eta(x_1, z_1^*, d) - \frac{z_1^{*2} \ell^2 \xi^2}{2} \mathbb{I}}{\sqrt{z_1^{*2} \ell^2 \xi^2 \mathbb{I}}} \right). \quad (115)$$

This expression when simplified yields the following expression for the generator term:

$$G_d V(x) = V'(x_1) \frac{1}{2} \ell^2 E_{z_1^*} \left[z_1^{*2} \mathcal{H}(z_1^*, x_1, \xi) \right] + \frac{1}{2} V''(x_1) \ell^2 E_{z_1^*} \left[z_1^{*2} \mathcal{H}(z_1^*, x_1, \xi) \right] + O(d^{-\frac{1}{2}}), \quad (116)$$

where

$$\mathcal{H}(z_1^*, x_1, \xi) = 2\Phi \left(-\frac{|z_1^*| \ell \xi \sqrt{\mathbb{I}}}{2} \right) = 2 \left[1 - \Phi \left(\frac{|z_1^*| \ell \xi \sqrt{\mathbb{I}}}{2} \right) \right]. \quad (117)$$

By the same arguments as in the previous cases, we have

$$\lim_{d \rightarrow \infty} E |G_d V(x) - G V(x)| \rightarrow 0,$$

where

$$G V(x) = \frac{1}{2} g_\xi(\ell) (\log f(x_1))' V'(x_1) + \frac{g_\xi(\ell)}{2} V''(x_1), \quad (118)$$

with

$$g_\xi(\ell) = 4\ell^2 \int_0^\infty \left\{ u^2 \Phi \left(-\frac{u \ell \xi \sqrt{\mathbb{I}}}{2} \right) \right\} \phi(u) du. \quad (119)$$

□

S-7 Calculations related to the dependent set-up

S-7.1 Verification of the conditions of Lyapunov's central limit theorem

To apply Lyapunov's central limit theorem we need to show the following: with probability 1 with respect to π ,

$$\frac{\sum_{j=1}^d E\left(\frac{b_j \eta_j}{\sqrt{d}}\right)^4}{\left(\sqrt{\sum_{j=1}^d \frac{\eta_j^2}{d}}\right)^4} = \frac{\sum_{j=1}^d \frac{\eta_j^4}{d^2}}{\left(\frac{\|\eta\|^2}{d}\right)^2} \rightarrow 0, \text{ as } d \rightarrow \infty. \quad (120)$$

By Lemma 5.2 of [Mattingly et al. \(2011\)](#), $\frac{\|\eta\|^2}{d} \rightarrow 1$ π -almost surely as $d \rightarrow \infty$. This implies that the denominator of the left hand side of (120) goes to 1 π -almost surely, as $d \rightarrow \infty$. Now, $\left(\frac{\|\eta\|^2}{d}\right)^2 = \sum_{j=1}^d \frac{\eta_j^4}{d^2} + \sum_{i=1}^d \frac{\eta_i^2}{d} \left(\sum_{j \neq i}^d \frac{\eta_j^2}{d}\right)$. Except on a π -null set \mathbb{N} , where $\sum_{j=1}^d \frac{\eta_j^2}{d}$ need not converge to 1, we have, for given $\zeta > 0$ and d_0 depending upon ζ , $1 - \zeta < \sum_{j \neq i}^d \frac{\eta_j^2}{d} < 1 + \zeta$ and $1 - \zeta < \sum_{i=1}^d \frac{\eta_i^2}{d} < 1 + \zeta$, for $d \geq d_0$. Hence, for $d \geq d_0$, $-\zeta^2 - 2\zeta < \zeta^2 - 2\zeta = (1 - \zeta)^2 - 1 < \sum_{i=1}^d \frac{\eta_i^2}{d} \left(\sum_{j \neq i}^d \frac{\eta_j^2}{d}\right) - 1 < (1 + \zeta)^2 - 1 = \zeta^2 + 2\zeta$, so that $\left|\sum_{i=1}^d \frac{\eta_i^2}{d} \left(\sum_{j \neq i}^d \frac{\eta_j^2}{d}\right) - 1\right| < \zeta^2 + 2\zeta$, showing that $\sum_{i=1}^d \frac{\eta_i^2}{d} \left(\sum_{j \neq i}^d \frac{\eta_j^2}{d}\right) \rightarrow 1$ on \mathbb{N}^c , the complement of \mathbb{N} . Since on \mathbb{N}^c , $\left(\frac{\|\eta\|^2}{d}\right)^2 \rightarrow 1$, we must have $\sum_{j=1}^d \frac{\eta_j^4}{d^2} \rightarrow 0$ on \mathbb{N}^c , showing that Lyapunov's condition (120) holds almost surely with respect to π .

Using Lyapunov's central limit theorem on b_j , and using the result that $\frac{\|\eta\|^2}{d} \rightarrow 1$ π -almost surely as $d \rightarrow \infty$, we obtain, for sufficiently large d ,

$$R(x, \xi) \sim AN(-\ell^2 \epsilon^2, 2\ell^2 \epsilon^2), \quad (121)$$

where "AN" stands for "asymptotic normal".

Now, (57) of DB and the fact that for large d , $\mathbb{Q}(x, \xi) \approx R(x, \xi)$, imply

$$\mathbb{Q}(x, \xi) \approx -\epsilon \sqrt{\frac{2\ell^2}{d}} \left(\eta_i b_i + \sum_{j=1, j \neq i}^d \eta_j b_j \right) - \ell^2 \epsilon^2, \quad (122)$$

so that

$$[\mathbb{Q}(x, \xi) | b_i, \epsilon] \sim AN\left(-\ell^2 \epsilon^2 - \epsilon \sqrt{\frac{2\ell^2}{d}} \eta_i b_i, 2\ell^2 \epsilon^2\right). \quad (123)$$

S-7.2 Expected drift

In order to obtain the diffusion approximation, we first obtain the expected drift conditions. In order to do that, we first define, as in [Mattingly et al. \(2011\)](#), \mathcal{F}_k to be the sigma algebra generated by $\{x^n, \xi^n, \gamma^k, n \leq k\}$, and denote the conditional expectations $E(\cdot | \mathcal{F}_k)$ by $E_k(\cdot)$. Following [Mattingly et al. \(2011\)](#) we let $x^0 = x$ and $\xi^1 = \xi$, and set $\xi^0 = 0$ and $\gamma^0 = 0$. We then

note that under stationarity, $E_k(x^{k+1} - x^k) = E_0(x^1 - x)$, and using (51) of DB we can write

$$\begin{aligned}
dE_0(x_i^1 - x_i) &= dE_0[\gamma^1(y_i^1 - x_i^1)] \\
&= dE_0\left[\alpha(x, \xi)\sqrt{\frac{2\ell^2}{d}}\left(\Sigma^{\frac{1}{2}}\xi\right)_i\right] \\
&= \frac{1}{\eta_i}\lambda_i\sqrt{2\ell^2d}E_0\left[\min\left\{1, e^{\mathbb{Q}(x, \xi)}\right\}\xi_i\right]\eta_i,
\end{aligned} \tag{124}$$

where $\alpha(x, \xi) = \min\left\{1, \frac{\pi(y_i^1)}{\pi(x_i^1)}\right\}$. The last step follows from (47) of DB, noting that $\xi = \sum_{i=1}^d \xi_i \phi_i$.

Noting that $\lambda_i \Sigma^{-\frac{1}{2}} \phi_i = \phi_i$, (55) and self-adjointness of $\Sigma^{-1/2}$ yields

$$\begin{aligned}
\lambda_i \eta_i &= \lambda_i \left\langle \Sigma^{-\frac{1}{2}}(P^d x) + \Sigma^{\frac{1}{2}} \nabla \Psi^d(x), \phi_i \right\rangle \\
&= \lambda_i \left\langle \Sigma^{-\frac{1}{2}}(P^d x) + \Sigma^{-\frac{1}{2}} \Sigma \nabla \Psi^d(x), \phi_i \right\rangle \\
&= \left\langle P^d x + \Sigma^d \nabla \Psi^d(x), \phi_i \right\rangle \\
&= \left(P^d x + \Sigma^d \nabla \Psi^d(x) \right)_i.
\end{aligned} \tag{125}$$

Thus, we can write

$$dE_0(x_i^1 - x_i) = \frac{1}{\eta_i} \left(P^d x + \Sigma^d \nabla \Psi^d(x) \right)_i \sqrt{2\ell^2 d} E_0 \left[\min \left\{ 1, e^{\mathbb{Q}(x, \xi)} \right\} \xi_i \right]. \tag{126}$$

Now, writing $\mu = -\ell^2 \epsilon^2 - \epsilon \sqrt{\frac{2\ell^2}{d}} \eta_i b_i$, $\sigma = \sqrt{2\ell} \epsilon$, using (123) and Proposition 2.4 of [Roberts et al. \(1997\)](#), it follows that

$$\begin{aligned}
&\sqrt{d} E_0 \left[\min \left\{ 1, e^{\mathbb{Q}(x, \xi)} \right\} \xi_i \right] \\
&= \sqrt{d} E_{b_i \epsilon} \left[b_i \epsilon E_0 \left\{ \min \left\{ 1, e^{\mathbb{Q}(x, \xi)} \right\} \middle| b_i, \epsilon \right\} \right] \\
&\approx \sqrt{d} E_{b_i \epsilon} \left[b_i \epsilon \left\{ \Phi \left(\frac{\mu}{\sigma} \right) + e^{\mu + \frac{\sigma^2}{2}} \Phi \left(-\sigma - \frac{\mu}{\sigma} \right) \right\} \right] \\
&= \sqrt{d} E_{b_i \epsilon} \left[b_i \epsilon \left\{ \Phi \left(-\frac{\ell \epsilon}{\sqrt{2}} - \frac{\eta_i b_i}{\sqrt{d}} \right) \right. \right. \\
&\quad \left. \left. + e^{-\epsilon \sqrt{\frac{2\ell^2}{d}} \eta_i b_i} \Phi \left(-\frac{\ell \epsilon}{\sqrt{2}} + \frac{\eta_i b_i}{\sqrt{d}} \right) \right\} \right].
\end{aligned} \tag{127}$$

Using the following Taylor's series expansions

$$\begin{aligned}
\Phi\left(-\frac{\ell\epsilon}{\sqrt{2}} - \frac{\eta_i b_i}{\sqrt{d}}\right) &= \Phi\left(-\frac{\ell\epsilon}{\sqrt{2}}\right) - \frac{\eta_i b_i}{\sqrt{d}} \phi\left(-\frac{\ell\epsilon}{\sqrt{2}}\right) + \frac{\eta_i^2}{2d} \phi'(w_1), \\
\Phi\left(-\frac{\ell\epsilon}{\sqrt{2}} + \frac{\eta_i b_i}{\sqrt{d}}\right) &= \Phi\left(-\frac{\ell\epsilon}{\sqrt{2}}\right) + \frac{\eta_i b_i}{\sqrt{d}} \phi\left(-\frac{\ell\epsilon}{\sqrt{2}}\right) + \frac{\eta_i^2}{2d} \phi'(w_2), \\
e^{-\epsilon\sqrt{\frac{2\ell^2}{d}}\eta_i b_i} &= 1 - \epsilon\sqrt{\frac{2\ell^2}{d}}\eta_i b_i + \frac{\ell^2\epsilon^2\eta_i^2}{d}e^{-w_3},
\end{aligned} \tag{128}$$

where w_1 lies between $-\frac{\ell\epsilon}{\sqrt{2}}$ and $-\frac{\ell\epsilon}{\sqrt{2}} - \frac{\eta_i b_i}{\sqrt{d}}$; w_2 lies between $-\frac{\ell\epsilon}{\sqrt{2}}$ and $-\frac{\ell\epsilon}{\sqrt{2}} + \frac{\eta_i b_i}{\sqrt{d}}$, and w_3 lies between 0 and $\epsilon\sqrt{\frac{2\ell^2}{d}}\eta_i b_i$, and noting that $E_{b_i\epsilon}\left[b_i\epsilon\Phi\left(-\frac{\ell\epsilon}{\sqrt{2}}\right)\right] = 0$, (127) can be easily seen to be of the form

$$\begin{aligned}
\sqrt{d}E_0\left[\min\left\{1, e^{\mathbb{Q}(x,\xi)}\right\}\xi_i\right] &\approx \sqrt{d}E_{b_i\epsilon}\left[b_i\epsilon\left\{\Phi\left(-\frac{\ell\epsilon}{\sqrt{2}} - \frac{\eta_i b_i}{\sqrt{d}}\right) \right. \right. \\
&\quad \left. \left. + e^{-\epsilon\sqrt{\frac{2\ell^2}{d}}\eta_i b_i}\Phi\left(-\frac{\ell\epsilon}{\sqrt{2}} + \frac{\eta_i b_i}{\sqrt{d}}\right)\right\}\right] \\
&= -\sqrt{2\ell^2}\eta_i \times 2 \int_0^\infty u^2 \Phi\left(-\frac{\ell u}{\sqrt{2}}\right) \phi(u) du + O\left(d^{-\frac{1}{2}}\right) \\
&\approx -\sqrt{\frac{\ell^2}{2}}\eta_i \beta,
\end{aligned} \tag{129}$$

where

$$\beta = 4 \int_0^\infty u^2 \Phi\left(-\frac{\ell u}{\sqrt{2}}\right) \phi(u) du. \tag{130}$$

Hence, we can re-write (126) as

$$\begin{aligned}
dE_0(x_i^1 - x_i) &= \frac{1}{\eta_i} \left(P^d x + \nabla \Psi^d(x)\right)_i \sqrt{2\ell^2 d} E_0\left[\min\left\{1, e^{\mathbb{Q}(x,\xi)}\right\}\xi_i\right] \\
&= -\ell^2 \beta \left(P^d x + \nabla \Psi^d(x)\right)_i.
\end{aligned} \tag{131}$$

S-7.3 Expected diffusion coefficient

Now we evaluate the expected diffusion coefficients involving the cross product terms. For $1 \leq i \neq j \leq d$, we have

$$dE_0[(x_i^1 - x_i)(x_j^1 - x_j)] = dE_0[\{\gamma^1(y_i^1 - x_i)\}\{\gamma^1(y_j^1 - x_j)\}]$$

Check that if $i \neq j$, then the above expectation is 0 using the fact that $b_i b_j \epsilon$ has 0 mean for $i \neq j$. However for $i = j$, using (125) again, we can reduce the above expectation to

$$\begin{aligned}
dE_0[(x_i^1 - x_i)(x_j^1 - x_j)] &= dE_0[(x_i^1 - x_i)^2] \\
&= dE_0[\alpha(x, \xi)(y_i^1 - x_i)^2] \\
&= 2\ell^2 \lambda_i^2 E_0\left[\xi_i^2 \min\left\{1, e^{\mathbb{Q}(x,\xi)}\right\}\right].
\end{aligned} \tag{132}$$

Using the same Taylor's series expansions (128) it is easily seen that

$$\begin{aligned} E_0 \left[\xi_i^2 \min \left\{ 1, e^{\mathbb{Q}(x, \xi)} \right\} \right] &\approx 4 \int_0^\infty u^2 \Phi \left(-\frac{\ell u}{\sqrt{2}} \right) \phi(u) du \\ &= \beta. \end{aligned} \quad (133)$$

Hence,

$$\begin{aligned} dE_0 \left[(x_i^1 - x_i) (x_j^1 - x_j) \right] &= 2\ell^2 \lambda_i^2 E_0 \left[\xi_i^2 \min \left\{ 1, e^{\mathbb{Q}(x, \xi)} \right\} \right] \\ &\approx 2\ell^2 \lambda_i^2 \beta \\ &= 2\ell^2 \beta \langle \phi_i, \Sigma \phi_i \rangle. \end{aligned} \quad (134)$$

It follows that

$$dE_0 \left[(x^1 - x) \otimes (x^1 - x) \right] \approx 2\ell^2 \beta \Sigma^d. \quad (135)$$

Note that, by definition,

$$x^{k+1} = x^k + E_k(x^{k+1} - x^k) + \sqrt{\frac{2\ell^2 \beta}{d}} \Gamma^{k+1, d},$$

where, for $k \geq 0$,

$$\Gamma^{k+1, d} = \sqrt{\frac{d}{2\ell^2 \beta}} \left(x^{k+1} - x^k - E_k(x^{k+1} - x^k) \right).$$

From (131), we have, for d large enough,

$$x^{k+1} \approx x^k - \frac{\ell^2 \beta}{d} m^d(x^k) + \sqrt{\frac{2\ell^2 \beta}{d}} \Gamma^{k+1, d}, \quad (136)$$

where

$$m^d(x) = P^d x + \Sigma^d \nabla \Psi^d(x). \quad (137)$$

From the definition of $\Gamma^{k, d}$ and (135) we have, as in Mattingly *et al.* (2011),

$$E_k \left(\Gamma^{k+1, d} \right) = 0 \quad \text{and} \quad E_k \left(\Gamma^{k+1, d} \otimes \Gamma^{k+1, d} \right) \approx \Sigma^d. \quad (138)$$

Thus, for large enough d , (136) can be viewed as the Euler scheme for simulating the finite dimensional approximation

$$x^{k+1} \approx x^k - g(\ell) m^d(x^k) \Delta t + \sqrt{2g(\ell) \Delta t} \Gamma^{k+1, d} \quad \text{where} \quad \Delta t = \frac{1}{d}, \quad (139)$$

(with drift function m^d and covariance operator Σ^d) of the SDE

$$\frac{dz}{dt} = -g(\ell) (z + \Sigma \nabla \Psi(z)) + \sqrt{2g(\ell)} \frac{dW}{dt}, \quad z(0) = z^0, \quad (140)$$

where $z^0 \sim \pi$, W is a Brownian motion in a relevant Hilbert space with covariance operator Σ , and

$$g(\ell) = \ell^2 \beta, \quad (141)$$

is the diffusion speed.

Bibliography

- Bedard, M. (2007). Weak Convergence of Metropolis Algorithms for Non-i.i.d. Target Distributions. *The Annals of Applied Probability*, **17**, 1222–1244.
- Bedard, M. (2008a). Efficient Sampling Using Metropolis Algorithms: Applications of Optimal Scaling Results. *Journal of Computational and Graphical Statistics*, **17**, 312–332.
- Bedard, M. (2008b). Optimal Acceptance Rates for Metropolis Algorithms: Moving Beyond 0.234. *Stochastic Processes and their Applications*, **118**, 2198–222.
- Bedard, M. (2009). On the Optimal Scaling Problem of Metropolis Algorithms for Hierarchical Target Distributions. Preprint.
- Bedard, M. and Rosenthal, J. S. (2008). Optimal Scaling of Metropolis Algorithms: Heading Toward General Target Distributions. *Canadian Journal of Statistics*, **36**, 483–503.
- Beskos, A. and Stuart, A. M. (2009). MCMC Methods for Sampling Function Space. In R. Jeltsch and G. Wanner, editors, *ICIAM07: 6th International Congress on Industrial and Applied Mathematics*. European Mathematical Society, pages 337–364.
- Beskos, A., Roberts, G. O., and Stuart, A. M. (2009). Optimal Scalings for Local Metropolis-Hastings Chains on Non-product Targets in High Dimensions. *The Annals of Applied Probability*, **19**, 863–898.
- Christensen, O. F. (2006). Robust Markov Chain Monte Carlo Methods for Spatial Generalized Linear Mixed Models. *Journal of Computational and Graphical Statistics*, **15**, 1–17.
- Das, M. and Bhattacharya, S. (2014). Transdimensional Transformation Based Markov Chain Monte Carlo. Available at <http://arxiv.org/pdf/1403.5207>.
- Dey, K. K. and Bhattacharya, S. (2015a). Adaptive Transformation based Markov Chain Monte Carlo. Manuscript under preparation.
- Dey, K. K. and Bhattacharya, S. (2015b). On Geometric Ergodicity of Additive and Multiplicative Transformation Based Markov Chain Monte Carlo in High Dimensions. *Brazilian Journal of Probability and Statistics*. To appear. Available at <http://arxiv.org/pdf/1312.0915v2.pdf>.
- Dey, K. K. and Bhattacharya, S. (2015c). On Optimal Scaling of Additive Transformation Based Markov Chain Monte Carlo. Submitted.
- Dey, K. K. and Bhattacharya, S. (2015d). Supplement to “On Optimal Scaling of Additive Transformation Based Markov Chain Monte Carlo”. Submitted.
- Diggle, P. J., Tawn, J. A., and Moyeed, R. A. (1998). Model-Based Geostatistics (with discussion). *Applied Statistics*, **47**, 299–350.
- Dutta, S. and Bhattacharya, S. (2014). Markov Chain Monte Carlo Based on Deterministic Transformations. *Statistical Methodology*, **16**, 100–116. Also available at <http://arxiv.org/abs/1106.5850>. Supplement available at <http://arxiv.org/abs/1306.6684>.
- Johnson, L. T. and Geyer (2012). Variable Transformation to Obtain Geometric Ergodicity in the Random-Walk Metropolis Algorithm. *The Annals of Statistics*, **40**, 3050–3076.
- Jourdain, B., Lelièvre, T., and Miasojedow, B. (2013). Optimal Scaling for the Transient Phase of the Random Walk Metropolis Algorithm: the Mean-Field Limit. Available at <http://arxiv.org/abs/1210.7639v2>.

- Koralov, L. B. and Sinai, Y. G. (2007). *Theory of Probability and Random Processes*. Springer, New York.
- Kou, S. C., Xie, X. S., and Liu, J. S. (2005). Bayesian Analysis of Single-Molecule Experimental Data. *Applied Statistics*, **54**, 469–506.
- Liu, J. S. and Sabatti, S. (2000). Generalized Gibbs Sampler and Multigrid Monte Carlo for Bayesian Computation. *Biometrika*, **87**, 353–369.
- Liu, J. S. and Yu, Y. N. (1999). Parameter Expansion for Data Augmentation. *Journal of the American Statistical Association*, **94**, 1264–1274.
- Mattingly, J. C., Pillai, N. S., and Stuart, A. M. (2011). Diffusion Limits of the Random Walk Metropolis Algorithm in High Dimensions. *The Annals of Applied Probability*, **22**, 881–930.
- Neal, P. and Roberts, G. O. (2006). Optimal Scaling for Partially Updating MCMC Algorithms. *The Annals of Applied Probability*, **16**, 475–515.
- Prato, G. D. and Zabczyk, J. (1992). Stochastic Equations in Infinite Dimensions. In *Encyclopedia of Mathematics and its Applications*, volume 44. Cambridge University Press, Cambridge.
- Roberts, G., Gelman, A., and Gilks, W. (1997). Weak Convergence and Optimal Scaling of Random Walk Metropolis Algorithms. *The Annals of Applied Probability*, **7**, 110–120.
- Roberts, G. O. and Rosenthal, J. S. (2001). Optimal Scaling for Various Metropolis-Hastings Algorithms. *Statistical Science*, **16**(4), 351–367.
- Roberts, G. O. and Rosenthal, R. S. (2009). Examples of Adaptive MCMC. *Journal of Computational and Graphical Statistics*, **18**, 349–367.
- Skorohod, A. V. (1956). Limit Theorems for Stochastic Processes. *Theory of Probability and its Applications*, **1**, 261–290.
- Smirnov, N. V. (1948). Tables for Estimating the Goodness of Fit of Empirical Distributions. *Annals of Mathematical Statistics*, **19**, 279.

Table 1: The performance evaluation of RWM and TCMC chains for different dimensions. It is assumed that proposal has independent normal components for RWM with same proposal variance along all co-ordinates. The proposal scales are 2.4 (optimal) and 6 (sub-optimal). All calculations done after burn in.

Dimension	Test		Acceptance Rate(%)		IACT		IPACT		AJS		Average K-S distance	
	Scaling		RWM	TCMC	RWM	TCMC	RWM	TCMC	RWM	TCMC	RWM	TCMC
2	2.4 (opt)		34.9	44.6	6.08	7.04	2.46	2.55	0.93	0.74	0.1651	0.1657
	6 (sub-opt)		18.66	29.15	7.08	8.08	2.52	2.56	0.79	0.62	0.1659	0.1655
5	2.4 (opt)		28.6	44.12	9.98	12.45	2.67	2.77	1.15	0.79	0.1659	0.1664
	6 (sub-opt)		2.77	20.20	15.6	14.11	2.77	2.81	0.39	0.48	0.1693	0.1674
10	2.4 (opt)		25.6	44.18	15.16	18.26	2.77	2.88	1.22	0.73	0.1667	0.1677
	6 (sub-opt)		1.37	20.34	17.55	16.31	2.91	2.86	0.25	0.49	0.1800	0.1688
100	2.4 (opt)		23.3	44.1	18.14	18.46	2.88	2.89	1.34	0.73	0.1794	0.1671
	6 (sub-opt)		0.32	20.6	18.62	18.25	2.89	2.88	0.26	0.69	0.1787	0.1684
200	2.4 (opt)		23.4	44.2	18.4	18.67	2.88	2.89	1.3	0.92	0.1813	0.1735
	6 (sub-opt)		0.33	20.7	18.86	18.74	2.89	2.89	0.09	0.54	0.1832	0.1755